The effect of macrophage polarisation on adipose tissue fibrosis in the context of hyperinsulinaemia

Submitted by Rebecca Symons to the University of Exeter as a dissertation for the degree of Masters by Research in Medical Studies

AUGUST 2019

I certify that all material in this document which is not my own work has been identified and that no material has previously been submitted for the award of a degree by this or any other university.

Signature:

Rebecca Symons

Abstract

In obesity, adipose tissue (AT) must remodel to accommodate adipocyte expansion. This remodelling is achieved through degradation and synthesis of extracellular matrix (ECM) components. Obese AT fibrosis, where excess fibrous ECM proteins accumulate, is thought to limit lipid storage capacity, leading to AT dysfunction and pathogenic ectopic lipid deposition. Dysfunctional AT is strongly associated with insulin resistance and characterised by low-level inflammation and increased macrophage infiltration. AT macrophages are classified as pro-inflammatory M1, or anti-inflammatory M2 (including M2a and M2c subtypes). M2 macrophage-secreted factors, as well as high levels of insulin, may induce AT fibrosis development thus increasing AT dysfunction. This study aimed to understand the role of polarised macrophage phenotypes and hyperinsulinaemia on the development of AT fibrosis.

THP-1 monocytes were differentiated and resulting macrophage phenotypes analysed by protein secretion and macrophage marker mRNA quantification. Macrophages were co-cultured with human omental AT explants (age: 49.5±7.83, BMI: 27.98±6.12) with vehicle-only, 1nM, 10nM or 100nM insulin for 48h before AT expression of fibrosis-associated genes was measured using qRT-PCR.

Macrophage characterisation suggested M (IFNγ+LPS) macrophages possessed a mixed M1/M2 phenotype, M (IL-4) macrophages were broadly M2-like, while M (IL-10) macrophages were considered not functionally differentiated. Co-culture

with M (IFNγ+LPS) macrophages significantly upregulated *FN1* (3.6±3.07 mean fold increase ±SD), and M (IL-4) macrophages upregulated molecular mediators of fibrosis *LOX* and *SPARC* (1.98±1.2 and 1.61±0.74) in AT. Under hyperinsulinaemic conditions (1nM or 10nM insulin) with M (IFNγ+LPS) macrophages, AT *COL4A1, COL5A3, TGFB1* and *FN1* were downregulated (0.78±0.13, 0.956±0.53, 1.00±0.34, 2.32±1.3 respectively) compared to the vehicle control.

Results suggest that mixed M1/M2 phenotype and M2-like macrophages may contribute to AT fibrosis, and hyperinsulinaemic conditions may moderate this effect. However, poor experimental design and inadequate optimisation prevented scientifically sound conclusions being drawn from this study. Further comprehensive work is required to determine the role of macrophages and hyperinsulinaemia in AT fibrosis.

List of Contents

ABSTRACT 2
LIST OF TABLES AND FIGURES 8
ACKNOWLEDGEMENTS 9
LIST OF ABBREVIATIONS 10
CHAPTER 1: INTRODUCTION 15

1.1 Adipose tissue 15
1.1.1 AT extracellular matrix 16
1.1.2 Fat storage function of AT 17
1.1.3 Endocrine function of AT 27
1.1.4 Paracrine/autocrine action of AT 29
1.1.5 AT expansion 30
1.1.6 ECM remodelling 31

1.2 Adipose tissue dysfunction 32
1.2.1 Obesity 32
1.2.2 Obese AT expansion 33
1.2.3 AT hypoxia 33
1.2.4 AT inflammation 34
1.2.5 AT fibrosis 41
1.2.6 Insulin resistance and fibrosis 48
1.2.7 Insulin resistance and T2DM 49
1.2.8 Inflammation and insulin resistance 51

1.3 Aims and objectives 52

CHAPTER 2: METHODS 54

2.1 THP-1 cell culture 54
2.2 Subject participation 56
2.2.1 Subject recruitment 56
2.2.2 Sample and data collection 57

2.3 Cell culture 57
2.3.1 THP-1 differentiation 57
2.3.2 THP-1/AT co-culture 59

2.4 Expression profiling 62
2.4.1 RNA extraction and purity 62
2.4.2 Sample selection 63
2.4.3 Reverse transcription 64
2.4.4 qRT-PCR 65
2.4.5 Enzyme-linked immunosorbent assay (ELISA) 70

2.5 Expression analysis 73
2.5.1 qRT-PCR plate calibrators 73
2.5.2 Quality control 73
2.5.3 Housekeeping gene selection 74
2.5.1 Housekeeping gene validation 75
2.5.1 Comparative $2^{-\Delta\Delta Ct}$ method 75
2.5.2 ELISA analysis 76
2.5.3 Statistical analysis 77
2.5.4 One-way ANOVA (Friedman non-parametric test) ... 77
2.5.5 Repeated measures two-way ANOVA 78
2.5.6 Kruskal Wallis test 78

CHAPTER 3: QUANTIFICATION OF MACROPHAGE DIFFERENTIATION 79

3.1 Introduction 79
3.2 Optimisation 80
3.3 Results 81
3.3.1 CD86 expression 83
3.3.2 CD206 expression 84
3.3.3 CD150 expression 84
3.3.4 CD163 expression 85
3.3.5 CD163 expression: second optimisation test 86
3.3.6 Secretory profile analysis 88
3.3.7 IL-1α secretion 89
3.3.8 IL-6 secretion 89
3.3.9 TNF-α secretion 90
3.3.10 OLR-1 secretion 90
3.3.11 IL-10 secretion 90
3.3.12 TGF-β secretion 91
3.4 Discussion 92
3.4.1 THP-1 monocytes retain a relatively 'undifferentiated' phenotype 92
3.4.2 IFNγ + LPS induces a mixed macrophage phenotype 93
3.4.3 M (IL-4) macrophages significantly upregulate CD206 97
3.4.4 M (IL-10) macrophages do not possess a distinct M2c phenotype 99
3.5 Summary 100

CHAPTER 4: THE INFLUENCE OF MACROPHAGES ON ADIPOSE TISSUE FIBROSIS 102

4.1 Introduction 102
4.2 Results 104
4.2.1 M (IFNγ + LPS) macrophages 107
4.2.2 M (IL-4) macrophages 107
4.2.3 M (IL-10) macrophages 107
4.2.4 THP-1 monocytes 108
4.3 Discussion 109
4.3.1 Co-culture with M (IL-10) macrophages did not upregulate expression of pro-fibrotic genes in OMAT 110
4.3.2 Co-culture with THP-1 monocytes influences AT expression of fibril-forming collagen I and TGFB1 .. 112
4.3.3 M (IFNγ + LPS) macrophages upregulate FN1 in AT 114
4.3.4 M (IL-4) macrophages upregulated expression of LOX and SPARC in AT 121
4.3.5 Limitations 123
4.4 Summary 125

CHAPTER 5: THE INFLUENCE OF INSULIN ON MACROPHAGE-MEDIATED AT FIBROSIS 126

5.1 Introduction 126
5.2 Results 127
5.2.1 ØM (no macrophages) 130
5.2.2 M (IFNγ + LPS) macrophages 131
5.2.3 M (IL-4) macrophages 131
5.2.4 M (IL-10) 131
5.2.5 THP-1 monocytes 132
5.3 Discussion 133
5.3.1 Insulin alone does not modulate expression of genes associated with fibrosis in OMAT explants 133
5.3.2 Insulin may modulate the pro-fibrotic effect of M (IFNγ + LPS) macrophages 135
5.3.3 The anti-fibrotic effect of insulin and M (IFNγ + LPS) macrophages is not concentration-dependent 136
5.3.4 Insulin and M (IL-4) macrophages do not significantly modulate pro-fibrotic gene expression 141

5.3.5 Insulin downregulates ELN expression in AT with undifferentiated THP-1 monocyte co-culture 142

5.4 Summary 143

CHAPTER 6: DISCUSSION 144

6.1 Main conclusions 144
6.2 Study strengths 146
6.2.1 AT explants 146

6.3 Study limitations 147
6.3.1 Participants 147
6.3.2 Use of THP-1 monocyte line 148
6.3.3 Optimisation experiments 150
6.3.4 Determination of macrophage phenotypes 151
6.3.5 OMAT and macrophage co-culture 152
6.3.6 RNA analysis of pro-fibrotic genes 155
6.3.7 Summary 157

6.4 Further work 158
6.4.1 Optimisation of macrophage differentiation and phenotypic classification 158
6.4.2 Optimisation of co-culture conditions 161
6.4.3 Effect of insulin on macrophage phenotype 162

6.5 Future perspectives 163
6.5.1 Macrophage classification 163

6.6 Final conclusions 164

APPENDIX 1 165

7.1 Optimisation experiments 165
7.1.1 THP-1 differentiation 165
7.1.1 AT/THP-1 co-culture 169
7.1.1 Housekeeping gene selection 172

APPENDIX 2 173

7.2 RNA concentration and quality in AT samples 173

REFERENCES 179

List of Tables and Figures

Figure 1: *Insulin action in adipocytes and muscle cells*.. 20
Figure 2: *Triglyceride composition*..... 21
Figure 3: *Lipogenesis and triglyceride synthesis*.. 23
Figure 4: *Lipolysis*..... 26
Figure 5: *Crown-like structure in obese adipose tissue.* 37
Figure 6: *Functional properties of classically and alternatively activated macrophages.*..... 39
Figure 7: *Schematic representation of hypothesised events leading to adipose tissue fibrosis.*..... 52
Figure 8: *Representation of co-culture setup, denoting the presence of AT, insulin concentration and macrophage differentiation.* 61
Figure 9: *Reverse transcription thermocycler programme* 65
Figure 10: *qPCR amplification of cDNA with FRET signalling.*. 68
Figure 11: *Biotin-streptavidin sandwich ELISA*. 72
Figure 12: *Relative mRNA expression of macrophage markers in differentiated THP-1 cells.*..... 82
Figure 13: *Relative expression of CD163 in cells from second optimisation test.*. 86
Figure 14: *Relative protein secretion from differentiated macrophages*. 88
Figure 15: *Relative expression of genes associated with fibrosis in AT after culture alone (ØM), or with M (IFNγ+LPS), M (IL-4), M (IL-10) and THP-1 cells.*. 105
Figure 16: *Effect of insulin on AT gene expression after co-culture with macrophages.*..... 128
Figure 17: *First optimisation test*..... 166
Figure 18: *Second optimisation test*.. 168
Figure 19: *Macrophage differentiation after pilot study.* 171
Figure 20: *Expression of housekeeping genes.*..... 172
Table 1: *Patient characteristics* 56
Table 2: *Composition of media for macrophage differentiation.* 59
Table 3: *Reverse transcription reaction mix.*..... 64
Table 4: *Composition of qPCR reaction mix* 66
Table 5: *qPCR run method* 69

Acknowledgements

This project would not have been completed without the help of many people. While it is not possible to thank everyone, I would like to acknowledge the contributions made by a selection of key people.

First, I would like to express gratitude to primary supervisor, Dr Katarina Kos, for helping me develop skills essential for a scientist and researcher.

I would like to thank my secondary supervisor, Professor Lorna Harries for her continued support, advice and infectious enthusiasm.

Special thanks go to Dr Emilie Pastel, whose technical support, knowledge and friendship has been invaluable over the course of my studies.

My appreciation is also extended to all the members of Team RNA, who provided motivational and technical support, with special thanks to Ben Lee.

Gratitude is extended to Dr Bea Knight and the patients who took part in the study, without whom the project would not have been possible, as well as the gynaecology surgeons and theatre staff who helped to provide tissue samples.

This project was funded by an NHS Small Grant, who are gratefully acknowledged.

List of Abbreviations

µl	Microlitre
µM	Micromole
aFABP	Adipose fatty acid-binding protein
AKT	Protein kinase B
ANOVA	Analysis of variance
AT	Adipose tissue
ATGL	Adipose triglyceride lipase
ATM	Adipose tissue macrophage
AU	Arbitrary units
BM	Basement membrane
BMI	Body mass index
cAMP	Cyclic adenosine monophosphate
CD	Cluster of differentiation
CDK2	Cyclin dependent kinase 2
cDNA	Complimentary deoxyribonucleic acid
COL1A1	Collagen I α1
COL3A1	Collagen III α1
COL4A1	Collagen IV α1
COL5A3	Collagen V α3
COL6A3	Collagen VI α3
C_t	Threshold cycle
CTGF	Connective tissue growth factor
DAG	Diacylglyceride

DMSO	Dimethyl sulphoxide
DNA	Deoxyribonucleic acid
dNTP	Deoxyribose nucleoside triphosphate
dsDNA	Double stranded DNA
EC	Endothelial cell
ECM	Extracellular matrix
ELISA	Enzyme-linked immunosorbent assay
ELN	Elastin
FA	Fatty acid
FACS	Fluorescence-activated cell sorting
FAS	Fatty acid synthase
FBS	Foetal bovine serum
FFA	Free fatty acid
FRET	Fluorescence resonance energy transfer
G-3-P	Glyceraldehyde-3-phosphate
GAPDH	Glyceraldehyde 3-phosphate dehydrogenase
GLUT	Glucose transporter
GM-CSF	Granulocyte macrophage-colony stimulating factor
GOI	Gene of interest
HBSS	Hanks' balanced salt solution
HFD	High fat diet
HIF1α	Hypoxia-inducible 1α
HSL	Hormone sensitive lipase
IFN-γ	Interferon gamma
iNOS	Inducible nitrogen oxide synthase

IL	Interleukin
IR	Insulin resistance
IRS	Insulin receptor subunit
JNK	c-Jun N-terminal kinase
KO	Knock-out
LOX	Lysyl oxidase
LPL	Lipoprotein lipase
LPS	Lipopolysaccharide
MAG	Monoacylglyceride
MAPK	Mitogen-activated protein kinase
MCP-1	Monocyte chemoattractant protein-1
M-CSF	Monocyte-colony stimulating factor
mg	Miligram
MGL	Monoglyceride lipase
ml	Millilitre
MMP	Matrix metalloproteinase
MRC1	Mannose receptor C-type 1
mRNA	Messenger ribonucleic acid
miRNA	Micro ribonucleic acid
n	Number
NFκB	Nuclear factor κB
NHS	National Health Service
nm	Nanometres
nM	Nanomolar
NO	Nitrogen oxide

NTC	No template control
OD	Optical density
OMAT	Omental adipose tissue
P	Pearson correlation coefficient
PAI-1	Plasminogen activator inhibitor 1
PBMC	Peripheral blood mononuclear cells
PI3K	Phosphatidyl inositol 3-kinase
PKA	Protein kinase A
POI	Protein of interest
PP1	Protein phosphatase 1
PPAR-γ	Peroxisome proliferator-activated receptor gamma
PPIA	Peptidyl-prolyl cis-trans isomerase A
PMA	Phorbol 12-myristate 13-acetate
P/S	Penicillin streptomycin
PTP1B	Protein tyrosine phosphatase 1B
qPCR	Quantitative polymerise chain reaction
RNA	Ribonucleic acid
RNase	Ribonuclease
rpm	Revolutions per minute
RPMI	Roswell Park Memorial Institute
RT	Reverse transcription
S	Svedberg units
SCAT	Subcutaneous adipose tissue
SD	Standard deviation
SEM	Standard error of the mean

SPARC	Secreted protein, acidic and rich in cysteine
ssDNA	Single stranded DNA
SVF	Stromal vascular fraction
T2DM	Type 2 diabetes mellitus
TAG	Triacylglyceride
TB	Tissue Bank
TCA	Tricarboxylic acid cycle
TG	Triglycerol
TGF-β	Transforming growth factor beta
THP-1	Tohoku Hospital Paediatrics-1
TIMP	Tissue inhibitor of metalloproteinases
TLR	Toll-like receptor
TNF-α	Tumour necrosis factor alpha
UNG	Uracil-DNA glycosylase
VAT	Visceral adipose tissue
VEGF	Vascular endothelial growth factor
VLCD	Very low calorie diet
VLDL	Very low density lipoprotein
WAT	White adipose tissue
WT	Wild type

Chapter 1: Introduction

The following chapter briefly introduces the structure and primary metabolic functions of adipose tissue, and will establish the main mechanisms and consequences of its dysfunction in the context of obesity. The pathophysiological importance of adipose tissue inflammation, fibrosis and insulin resistance will also be discussed.

1.1 Adipose tissue

Adipose tissue is a loose connective tissue where the body stores energy in the form of lipids. The main parenchymal cell of adipose tissue is the adipocyte, where lipids are stored as triglycerides and various important metabolic processes take place, as detailed in this chapter. The other cells of the tissue are referred to as the stromal vascular fraction (SVF), and include endothelial cells, fibroblast-like pre-adipocytes and immune cells such as macrophages[1]. These cells are surrounded by extracellular matrix (ECM), principally composed of a fibrous network of collagens and fibronectin[2].

In mammals, both brown and white adipose tissue is present. Brown adipose tissue (BAT) is predominantly found in newborn babies, with decreased prevalence in adults[3]. Its main function is thermogenesis, as brown adipocytes produce heat by oxidising free fatty acids at their mitochondria, whereas adipocytes of white adipose tissue (WAT) release free fatty acids (FFAs) into the bloodstream for oxidation by other organs[3]. BAT contains very high numbers of

mitochondria and is densely vascularised, giving its characteristic 'brown' appearance[4].

Until relatively recently, WAT (hereby referred to as AT) was considered solely a fat storage organ, providing additional insulation and cushioning internal organs[4]. It is now known to be a highly active endocrine organ essential for maintenance of metabolic homeostasis[5], with AT dysfunction heavily implicated in the development of type 2 diabetes mellitus (T2DM)[5]. AT is distributed throughout the body in distinct regional depots, either subcutaneously (under the skin) or viscerally (surrounding internal organs)[6]. Subcutaneous and visceral AT differ in their observable morphology, i.e. cell size and tissue structure, and are thought to have subtle differences in biological function[7]. Visceral adipose tissue (VAT) is categorised as omental, mesenteric, retroperitoneal, gonadal or pericardial dependent on its deposition[6].

1.1.1 *AT extracellular matrix*

The extracellular matrix (ECM) provides a physical scaffold for cell adhesion and migration and is essential for tissue homeostasis[8]. Its composition determines the elasticity and tensile strength of a tissue, and therefore reflects tissue-specific requirements[9]. Additionally, the ECM directs cell differentiation and organisation during tissue development through the interaction of ECM components with cell-surface receptors, stimulating specific cell-signalling pathways responsible for regulating gene expression[9].

ECM components are categorised into two groups of macromolecules: proteoglycans and fibrous proteins. Proteoglycans are composed of short carbohydrate chains (glycosaminoglycans) bound to a protein 'backbone', e.g. aggrecan and perlecan[10,11]. The fibrous proteins of the ECM are collagen, fibronectin, elastin and laminin[9]. Of these, collagens are the most abundant[9]. Collagens are triple helical proteins composed of three polypeptide α-chains, bound by hydrogen bonds, and are categorised into one of 28 types according to their arrangement, localisation, and function[9]. Fibril-forming collagens, such as types I, II, III and V, are initially synthesised by fibroblast-like cells in the form of soluble procollagen and after much post-translational processing provide tensile strength to the tissue[12]. Network-forming collagens, such as collagen IV, are prominent in the basement membrane of AT and surround adipocytes[13,14]. Collagen VI helices associate into tetramers, before assembling into microfibrils as pericellular 'beaded-filaments'[15], which reportedly play a role in the regulation of adipogenesis and adipocyte size[16]. The pathophysiological roles of ECM collagens are further discussed in section 1.2.5.

1.1.2 *Fat storage function of AT*

Insulin action and glucose homeostasis

The effects of insulin are twofold: the anabolic hormone is responsible for controlling metabolism at low concentrations, and promoting growth when at higher concentrations for a period of hours or days[17]. Insulin is secreted by glucose-sensitive β-cells within the islets of the pancreas, in response to increased glucose metabolism after a carbohydrate meal[18]. It functions as a

major regulator of circulating glucose concentration, and facilitates the uptake of glucose from the blood into muscle, liver and adipocytes, providing energy[17].

Insulin-sensitive cells present a glycoprotein transmembrane cell surface receptor with four subunits: two α-subunits and two β-subunits, joined together by disulphide bonds[17,19]. The α-subunits protrude from the cell surface and provide a binding site for insulin, whereas β-subunits span the lipid membrane and expose a tyrosine kinase domain on the cytoplasmic side[17,19]. While dormant, the α-subunits act to inhibit the tyrosine kinase activity of the β-subunits, but binding of insulin molecules to the α-subunits derepresses this kinase activity (as shown in Figure 1). This allows for β-subunit phosphorylation which induces a conformational change within the insulin receptor, increasing kinase activity further[19].

Insulin receptor activation can induce signalling via both the phosphatidyl inositol 3-kinase (PI3K) pathway[20] and the mitogen-activated protein kinase (MAPK) pathway[21,22]. The MAPK pathway, which involves activation of Ras, Raf, MEK and ERK, is thought to directly influence preadipocyte growth and differentiation[23–25] and regulate gene expression in the nucleus[22]. PI3K pathway activation, via insulin receptor subunit (IRS) and protein kinase B (AKT) activation, is reported to play a role in regulation of glucose uptake via GLUT4 translocation (Figure 1), the cellular differentiation of human preadipocytes into mature adipocytes[26], cytokine production, and insulin-mediated inhibition of lipolysis[27,28].

Insulin signalling is tightly controlled by a plethora of molecular mechanisms. Suppressor of cytokine signalling (SOCS) proteins, for example, negatively regulate insulin signalling[29–32]. SOCS-3 is upregulated by insulin and TNF-α, and competitively inhibits Stat5B-mediated binding and activation of the insulin receptor[29]. SOCS-3 also prevents interactions between IRS-1/2 and the insulin receptor[30]. SOCS-1 and SOCS-3 induce ubiquitin-mediated degradation of IRS-1/2[31], and SOCS-1 and SOCS-6 reduce IRS-1 tyrosine phosphorylation by inhibiting insulin receptor kinase activity[32]. Protein tyrosine phosphatase 1B (PTP1B) is a ubiquitous cytoplasmic phosphatase which dephosphorylates tyrosine residues of the insulin receptor, inhibiting downstream PI3K activity[33], and as such is implicated in the development of insulin resistance.

Insulin receptor internalisation and cycling is a well-established regulatory mechanism of insulin-signalling[34,35]. Upon ligand binding and insulin receptor autophosphorylation, the complex is endocytosed via clathrin and caveolae-mediated pathways[36] and trafficked to acidic lysosomes where insulin dissociates and is degraded, and the insulin receptor is recycled to the cell surface[37].

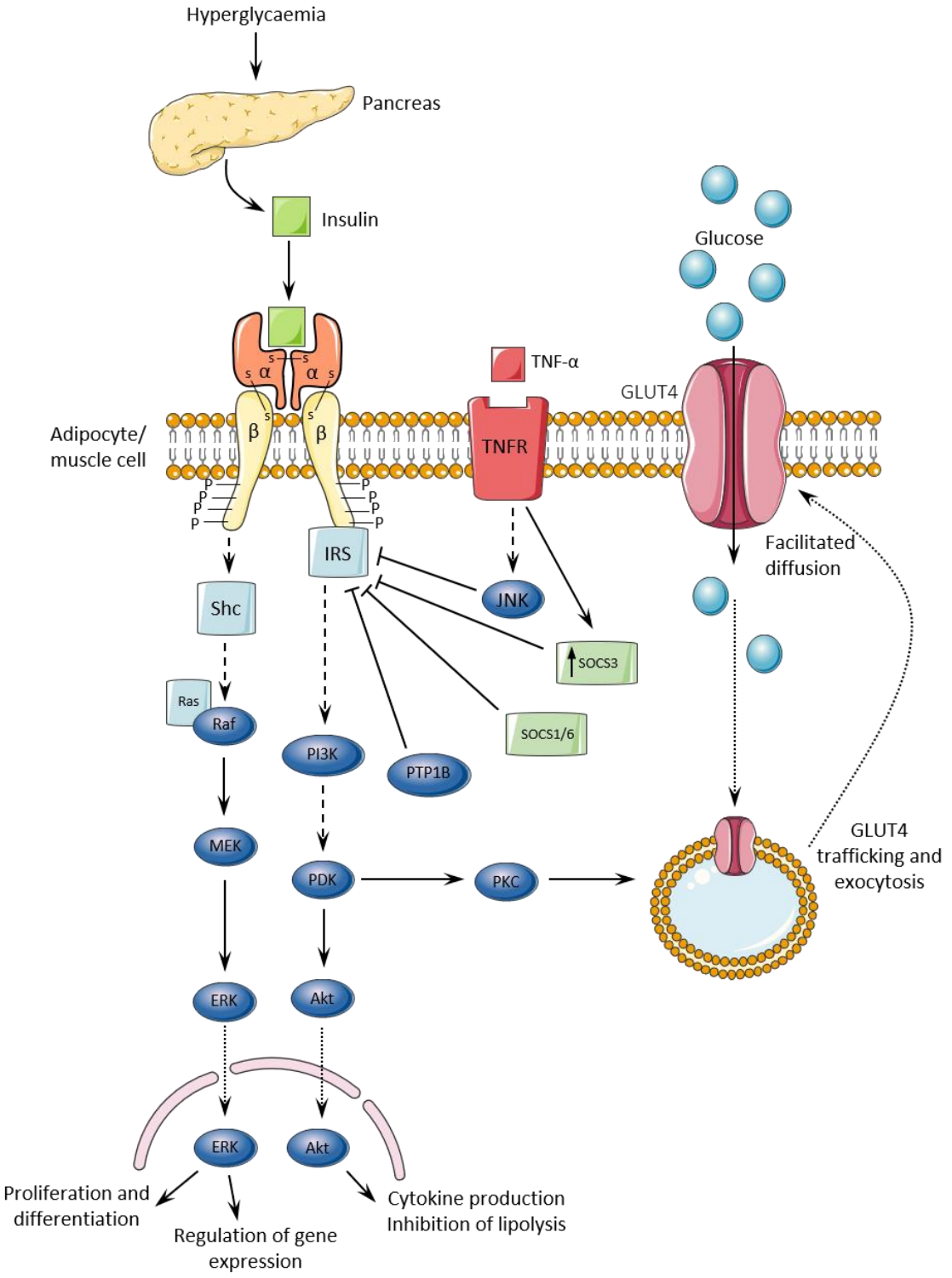

Figure 1: *Insulin action in adipocytes and muscle cells.* Adapted from Saltiel et al (2001)[19] and Godsland (2010)[307]. Insulin secreted from the pancreas stimulates its receptor to facilitate the uptake of glucose into fat or muscle cells. The tyrosine kinase domain of the β subunit of the insulin receptor is autophosphorylated by insulin binding to the α subunit. A conformational change catalyses activation of MAPK and PI3K pathways, resulting in the trafficking and exocytosis of the GLUT4 transporter and subsequent facilitated diffusion of glucose molecules into the cell. Insulin signalling is negatively regulated by TNF-α signalling, SOCS family molecules and PTP1B. Dashed arrows indicate a multi-step process.

The primary glucose transporter present in muscle and adipocytes is GLUT4. Under conditions of low insulin, the GLUT4 transporter is sequestered within intracellular vesicles, and is transported to the plasma membrane of the cell through a currently undefined mechanism, thought to involve the actin cytoskeleton[19]. Vesicles dock before undergoing exocytosis, exposing the transporter on the surface of the cell (Figure 1). Once the GLUT4 transporter is in place, glucose can enter the cell from the bloodstream via facilitated diffusion[19]. When the insulin signal is removed, the GLUT4 transporter is conserved and endocytosed back into the cytoplasm for future re-use[38].

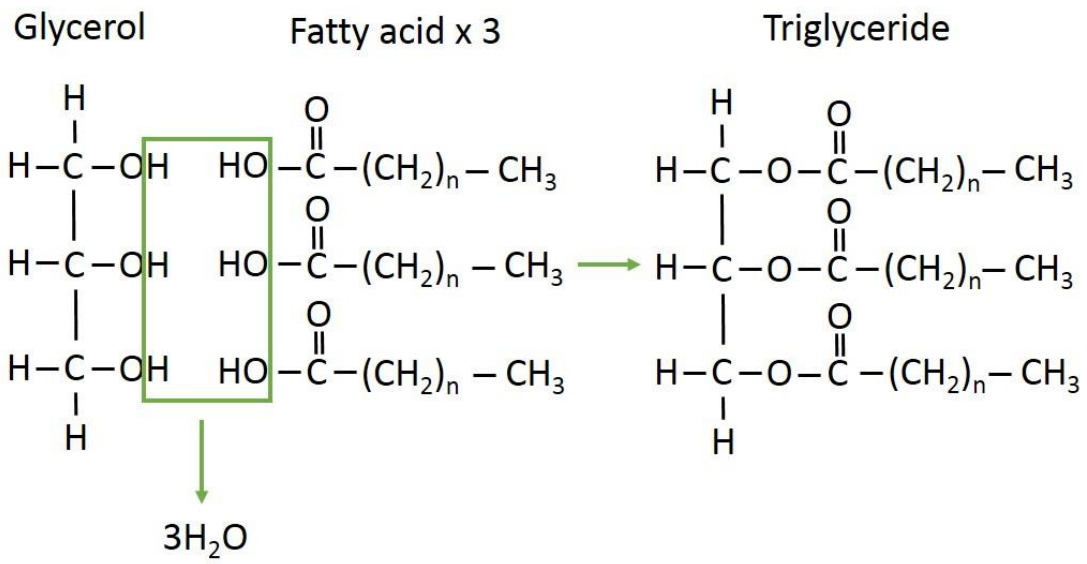

Figure 2: *Triglyceride composition*

Triglyceride molecules are synthesised from a single glucose-derived glycerol molecule, via glycerol-3-phosphate. Through a condensation reaction, three fatty acid molecules bind to the glycerol ‘backbone’ to form a single triglyceride molecule.

Lipogenesis and triglyceride synthesis

A key function of AT is the 'buffering' of lipid, which enables excess energy to be stored in the form of triglycerides during periods of calorie surplus, before being released for oxidation in an energy deficit[39]. During *de novo* lipogenesis (Figure 3) fatty acids are synthesised from glucose, obtained from dietary carbohydrates, via acetyl-CoA[40]. The process of glycolysis converts glucose into pyruvate (via glyceraldehyde-3-phosphate) which, after taking part in the tricarboxylic acid cycle (TCA) at the cell mitochondria, is converted into fatty acids[40]. One of the key enzymes involved in this process is fatty acid synthase (FAS)[41]. Three fatty acid molecules are required to build a single triglyceride molecule, in combination with glycerol-3-phosphate, which provides the backbone[42]. Glucose within the cell is converted to glycerol, and then glycerol-3-phosphate. After synthesis (mechanism detailed in Figure 2), triglycerides are deposited into the lipid droplet organelle within the adipocyte[43,44].

The process of lipogenesis has been shown to be positively regulated by insulin[45], which alongside facilitating the uptake of glucose, has been implicated in the regulation of genes controlling lipogenesis[46], primarily the expression of lipogenic enzymes FAS and acetyl CoA carboxylase[47].

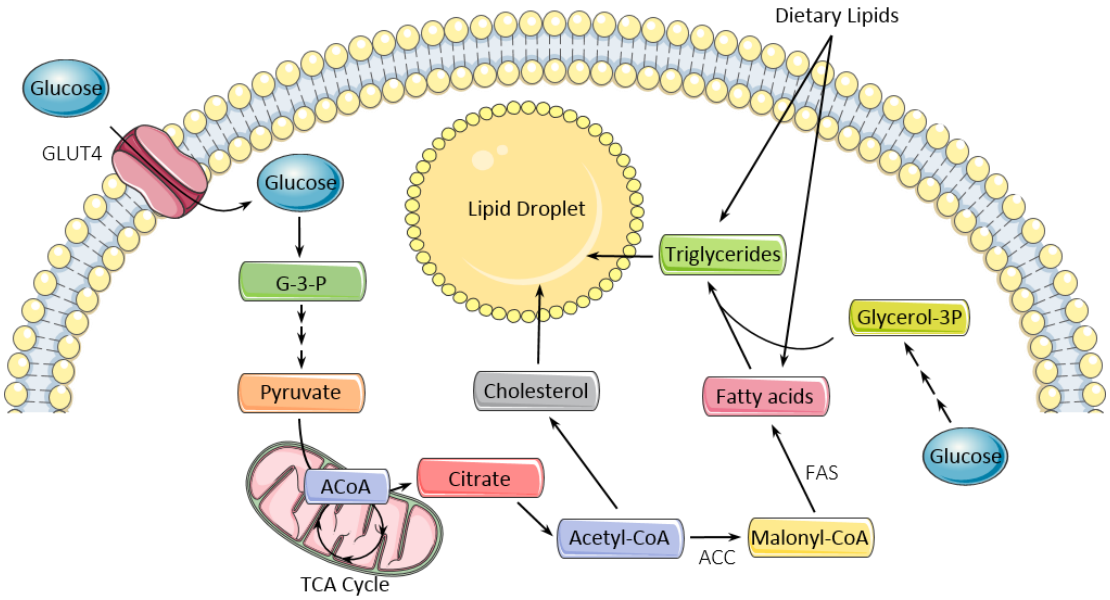

Figure 3: *Lipogenesis and triglyceride synthesis*. Adapted from Junjie *et al* (2014).

Glucose enters the cell via the GLUT4 transmembrane transporter where it is converted to glyceraldehyde-3-phosphate (G-3-P). Via a multistep process, G-3-P is converted to pyruvate, which partakes in the TCA cycle at mitochondria, producing acetyl co-enzyme A (ACoA). Through acetyl-CoA carboxylase, ACoA is carboxylated to give malonyl-CoA, from which fatty acids are created – a reaction facilitated by FAS. Triglyceride molecules are synthesised from glycerol-3-phosphate and fatty acids, then transported into the lipid droplet. Dietary lipids in the form of triglycerides and fatty acids are also able to contribute relatively directly to the lipid droplet[43].

Fatty acid uptake

Dietary lipids, including essential fatty acids, also enter adipocytes through cell surface transporters such as CD36[48]. Fatty acids alone are insoluble, therefore are either bound to albumin while in the circulation as an FFA, enabling their transport to peripheral tissues, or complexed with glycerol as a triglyceride[48] (Figure 2). FFAs may be saturated, in the case of palmitate, or unsaturated, such

as oleate. Fatty acids, hydrolysed from the triglycerides in lipoprotein particles, are the predominant molecule through which the body stores energy in adipocytes[49].

Lipolysis

The uptake of fatty acids into tissues can also be regulated by the lipolysis pathway, via enzymatic cell surface protein lipoprotein lipase (LPL), which is expressed by adipocytes and muscle cells[48]. LPL is essential for AT function and is considered a tissue-specific 'gatekeeper', directing calories to the appropriate tissues[50]. The activity of LPL in AT is largely regulated by insulin, as exposure to insulin during adipocyte differentiation positively correlates with LPL mRNA transcription[48]. Glucose increases LPL synthesis and can stimulate LPL activity, as it facilitates its glycosylation, a process necessary for LPL secretion and function[48].

The metabolic process of lipolysis (Figure 4) is the liberation of FFAs and glycerol for utilisation as an energy substrate by organs in response to a caloric deficit. In AT, triglycerides stored in the lipid droplet of adipocytes undergo hydrolysis to mobilise FFAs, which are transported to peripheral tissues[51]. This process requires enzyme lipases, which include adipose triglyceride lipase (ATGL), hormone-sensitive lipase (HSL) and monoglyceride lipase (MGL), and is regulated by catecholamines during periods of fasting[51].

Lipid deposition in AT is regulated by insulin. During periods of feeding, insulin concentrations increase and inhibit lipolysis through cAMP-dependent and

independent mechanisms[51,52]. Independent of cAMP, activated protein phosphatase-1 removes the phosphorylation of HSL, thereby rendering it inactive and unable to cleave a fatty acid chain from diacylglycerol[53]. In the case of cAMP-dependent activation, the insulin receptor is autophosphorylated upon binding, prompting further phosphorylation of insulin receptor subunits (IRS) and signalling via the PI3K-Akt pathway[52]. After a series of phosphorylation events, phosphodiesterase 3B degrades cAMP, preventing any further activation of protein kinase A (PKA) and reducing lipolysis through decreased stimulation of HSL and perilipin[52,54].

Increased basal lipolysis is evident in obesity, and is thought to be intimately associated with reduced insulin sensitivity, as decreased insulin signalling leads to reduced inhibition of lipolysis[55]. Increased expression of leptin, a key hormone regulating energy balance, has been implicated in the rise of basal lipolysis[56]. In obesity, circulating leptin secreted by adipocytes is increased, however leptin signalling is believed to be reduced[57]. The endocrine role of leptin is further discussed in section 1.1.3.

It has been long established that the rate of lipolysis in AT is dependent on the location of its deposition[58]. AT depots in the upper body are more lipolytically active than lower body depots, and visceral fat is more metabolically important for managing fatty acid flux[58]. In particular, abdominal (upper body) adiposity is associated with metabolic complications, where lower body adiposity is associated with increased risk of cardiovascular events[59]. The disruption of fatty acid flux leads to hyperlipidaemia, and toxicity associated with high circulating FFAs[58].

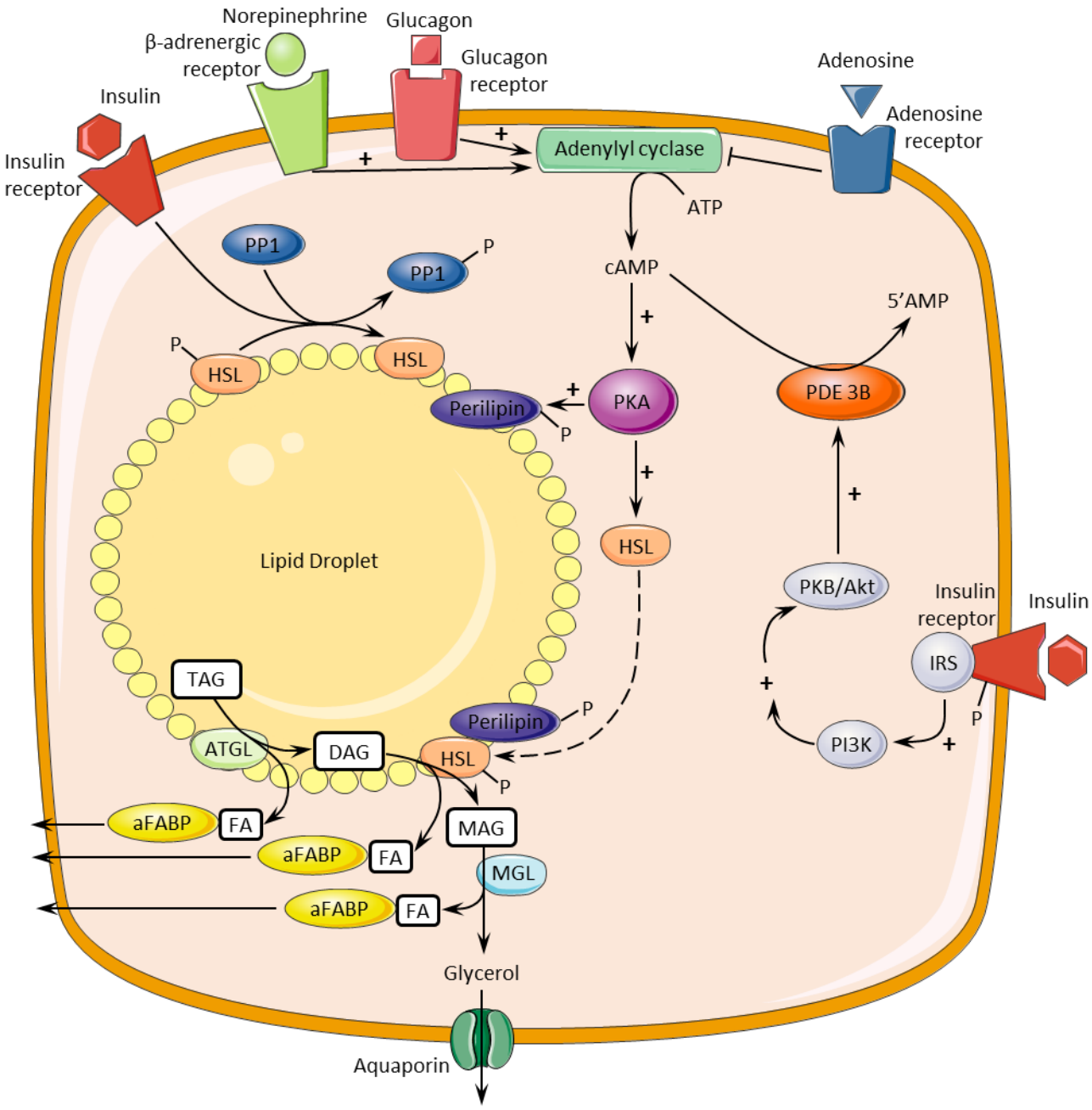

Figure 4: *Lipolysis*. Adapted from Duncan *et al* (2007).

Lipolysis is regulated through a series of extracellular signalling molecules which, through various pathways, either stimulate lipolysis in the event of calorie deficit, or inhibit lipolysis during feeding[52].

1.1.3 *Endocrine function of AT*

Alongside being a fat storage organ, AT has important endocrine functions. Adipokines are signalling molecules secreted by adipocytes, able to act in autocrine/paracrine and endocrine manners[60]. Endocrine signalling enables AT to communicate with other organs of the body, such as the brain and liver, in order to maintain metabolic homeostasis and regulate energy balance, i.e. calorie uptake and energy expenditure[1]. There is some controversy over the use of the term 'adipokine', as some authors define all adipocyte-secreted factors as adipokines, whereas others use the term to refer to cytokines secreted exclusively by AT. In this study, 'adipokine' will be used to refer to all adipocyte-secreted cytokines.

Leptin is a primary adipokine involved in the endocrine action of AT. Also known as the 'satiety hormone' because of its role in regulating calorie intake through suppressing appetite and facilitating weight loss, leptin is encoded by the *OB* gene[61]. Circulating levels of leptin positively correlate with adiposity[62]. Leptin-stimulated activation of leptin receptors (encoded by *OBR*) in the hypothalamus initiates signalling cascades leading to reduced appetite and food intake[63]. Disrupted leptin signalling is thought to contribute to the development of obesity[61].

Adiponectin, encoded by the *ADIPOQ* gene and expressed exclusively by differentiated adipocytes, is an important AT hormone with endocrine function and is highly concentrated in the bloodstream[1]. Decreased levels of circulating adiponectin have been associated with obesity[64], and there is evidence that adiponectin is important in the control of lipid and glucose metabolism in insulin-

sensitive tissues[65]. In addition, reduced adiponectin plasma levels have been associated with insulin resistance, and are purported to directly influence whole-body insulin sensitivity[66,67]. Further to this, fasting hyperinsulinaemia (high circulating levels of insulin) has been shown to be associated with low adiponectin plasma concentrations[68].

Cells of AT secrete various pro-inflammatory cytokines, with the ability to act in an endocrine manner[69]. These include tumour necrosis factor-α (TNF-α)[70], interleukin-6 (IL-6)[71], and monocyte chemoattractant protein (MCP-1)[72]. TNF-α is expressed by adipocytes, as well as cells of the SVF, and increased TNF-α plasma concentrations have been correlated with obesity and insulin resistance[1,73]. TNF-α exerts pro-inflammatory effects on cells of the liver, and negatively regulates expression of genes involved in fatty acid oxidation, as well as glucose uptake and metabolism[74]. Insulin signalling is also directly impaired, as TNF-α-induced signalling results in the degradation of hepatic insulin receptors[75–77]. Indirectly, TNF-α also increases serum fatty acid levels, resulting in insulin resistance[1,78,79].

Similarly, IL-6 and its receptor are expressed by adipocytes[80]. As well as playing a potential role in controlling body fat mass[81], circulating IL-6 levels are positively correlated with obesity and insulin resistance, and may be used as a predictor of cardiovascular disease and T2DM[82].

1.1.4 *Paracrine/autocrine action of AT*

Adipokines control the tissue microenvironment, expansion and inflammatory signalling in AT. Inflammation in dysfunctional AT is discussed in more detail in section 1.2. In addition to its roles in endocrine signalling, leptin is known to have paracrine and autocrine effects on AT. Leptin stimulates basal lipolysis and prevents lipid uptake in adipocytes, thus reducing adiposity in a paracrine manner[83]. It may also influence fat mass and weight loss through this appetite-independent mechanism, involving activation of Janus kinase (JAK)/signal transducer and activator of transcription 1 (STAT) pathways and nuclear translocation of STAT1[84]. Leptin release is correlated with adiposity, therefore obesity may persist as a result of adipocytes becoming resistant to leptin signalling[85]. Leptin also has a pro-inflammatory function in AT, as it upregulates expression of TNF-α in monocytes[86] and induces the production of reactive oxygen species[87].

MCP-1, secreted by adipocytes[88], regulates inflammatory responses by controlling the local infiltration of macrophages, and along with its receptor is significantly upregulated in obese AT[89]. TNF-α, secreted by various cell types in AT, is thought to contribute towards the development of insulin resistance[90] by inducing the release of FFAs from adipocytes[91] Several other classical pro-inflammatory cytokines are also secreted by cells of AT, including IL-1β and interferon-γ (IFN-γ), and influence the function of the tissue[91].

Adiponectin, expressed by adipocytes, acts in an autocrine and paracrine manner to modulate inflammation in AT, by promoting differentiation of AT macrophages

into an anti-inflammatory phenotype[92]. Adiponectin has been found to inhibit the production of IFN-γ in natural killer cells, thereby exerting an anti-inflammatory effect on the tissue microenvironment[93].

Another adipokine with paracrine/autocrine effects is IL-10, secreted by anti-inflammatory macrophages in AT[94]. IL-10 exerts its anti-inflammatory effect via JAK1 and TYK2-mediated recruitment of transcription factor STAT3, which modulates transcription by binding immune response genes[95]. In addition, anti-inflammatory macrophages are capable of secreting transforming growth factor-β (TGF-β), which regulates the differentiation of adipocytes and modulates the deposition of matrix proteins[96]. There are numerous other adipokines and cytokines secreted by cells of adipose tissue, which together with the factors described, contribute to AT homeostasis.

1.1.5 *AT expansion*

AT is required to expand during times of caloric excess and may do so through hypertrophy or hyperplasia[97]. Hypertrophy refers to cell growth, where the diameter of the cell increases as additional lipids are stored in the lipid droplet organelle. Hyperplasia within AT is the differentiation of new adipocytes resulting in increased AT mass[98]. This process is referred to as adipogenesis, where tissue resident fibroblast-like preadipocytes differentiate into mature adipocytes capable of storing lipid[99]. In times of nutritional deficiency, mature adipocytes and preadipocytes within the tissue release anti-adipogenic factors such as IL-6 and TNF which inhibit adipogenesis, likely via the Wnt/β-catenin pathway[98,100]. During periods of overnutrition, where energy intake exceeds energy expenditure,

adipocytes induce preadipocytes to differentiate by secreting pro-adipogenic factors, including transcriptional regulators enhancer binding protein α, β and δ (C/EBP) and peroxisome-proliferator activated receptor-γ (PPAR-γ), alongside inhibitors of anti-adipogenic signals[98].

1.1.6 *ECM remodelling*

To accommodate changes in the lipid storage requirements, and the newly hypertrophic or hyperplastic AT morphology, the ECM surrounding adipocytes is required to remodel[101]. This happens through shifts in the balance between the production and secretion of ECM components, and their degradation. Degradation of ECM components is primarily facilitated by a group of proteolytic enzymes known as the matrix metalloproteinases (MMPs)[101]. The action of these MMPs is inhibited by a family of molecules known as tissue inhibitor of metalloproteinases (TIMPs)[102].

1.2 Adipose tissue dysfunction

The term ‘AT dysfunction’ has been coined in recent years to describe the metabolic state whereby the delicate balance of metabolic processes is disrupted. AT dysfunction is linked with obesity, and is characterised by inflammation, impaired lipid metabolism, and altered adipokine secretion[103]. Long term effects of AT dysfunction include the development of AT fibrosis, insulin resistance and hyperinsulinaemia, and the deposition of lipid at ectopic sites, e.g. muscle and liver[103].

1.2.1 *Obesity*

Recent trend analysis of worldwide adult body mass index (BMI) has predicted that within the next ten years the prevalence of obesity will reach 18% in men and 21% in women[104]. As of 2010, 26% of adult men and women in the UK were obese[105]. This obesity ‘epidemic’ has been largely attributed to a widespread change in lifestyle over the past several decades: physical activity levels, and therefore energy expenditure, have decreased while caloric intake has increased with the abundance of calorie-dense foods[106].

Obesity is implicated in the development of a host of co-morbidities, including colorectal, prostate and breast cancers, sleep apnoea, osteoarthritis, hypertension, coronary heart disease, and atherosclerosis[107–111]. These conditions increase the risk of events like stroke and myocardial infarction[112]. In England alone, the cost of obesity and obesity-related disease was estimated at £27 billion in 2015[113]. Obese individuals also carry increased risk of developing T2DM - in 2012 direct costs of T2DM totalled £8.8 billion, while indirect costs

reached £13 billion[114]. In light of this, it is becoming increasingly pertinent that conditions leading to the development of T2DM are fully understood.

1.2.2 *Obese AT expansion*

In the event of chronic positive energy balance adipokine signalling can become dysregulated, resulting in reduced adipogenesis and decreased capacity for healthy AT expansion, as frequently observed in obesity and insulin resistance[115,116]. This impaired adipogenesis has been attributed to the effects of upregulated Wnt signalling, which inhibits expression of PPARγ and C/EBPα, a key inducer of adipogenesis and lipid storage and a leptin regulator respectively[98].

In the event of reduced adipogenesis, adipocytes become more hypertrophic until eventually their lipid storage capacity is exceeded[98]. Additional 'spill-over' lipid is stored in ectopic sites, in lipid droplets of the functional cells of the liver and pancreas, and skeletal muscle[98]. Some studies suggest that larger hypertrophic adipocytes are fragile and undergo necrotic cell death[117], whereas others give evidence that apoptosis takes place[118]. These dying cells prompt an inflammatory response and infiltration of immune cells, making obesity a disease defined by chronic low-level inflammation[119].

1.2.3 *AT hypoxia*

As adipocytes expand through hypertrophy, they often reach the diffusional limit of oxygen (100-200μm[120]). Healthy expansion of AT requires increased angiogenesis to keep tissue adequately supplied with oxygen, however the rapid

expansion of AT during obesity results in local hypoxia when angiogenesis cannot keep pace[121]. The angiogenic response to hypoxia is controlled by hypoxia inducible factor 1 (HIF1), a heterodimeric protein consisting of α and a β subunits. HIF1α is regulated by oxygen levels: under normoxic conditions it is hydroxylated at two proline residues and tagged for degradation[121]. When the local microenvironment is hypoxic, hydroxylation drops allowing the accumulation of HIF1α. HIF1α is then translocated into the nucleus, where, alongside constitutively-expressed HIF1β, it acts as a transcription factor for angiogenesis-inducing target genes such as vascular endothelial growth factor (*VEGFA*)[121].

Hypoxia is an important inducer of adipocyte death as it induces upregulation of pro-inflammatory TNF-α and impaired insulin signalling, and activates inflammatory signalling pathways which induce necrotic cell death[122,123], triggering an influx of macrophages into the tissue[124]. Adipocytes may also die by apoptosis, the 'programmed cell death'[118]. Apoptotic cell death differs from necrotic cell death in that it involves an intracellular proteolytic cascade which prevents release of cell contents into the environment, which would otherwise trigger an inflammatory, tissue damaging response[125].

1.2.4 *AT inflammation*

Necrotic adipocyte death results in the release of the lipid contents from the cell, eliciting a pro-inflammatory response from the surrounding cells[126–129]. The purpose of inflammation is to protect tissues within an organism from stimuli-mediated harm, initiate healing and restore homeostasis[130]. AT Inflammation is characterised by immune cell influx, increased production of inflammatory

cytokines and activation of inflammatory signalling pathways[119]. Increased adipocyte hypertrophy during AT expansion is correlated with increased adipocyte secretion of pro-inflammatory cytokines, such as interleukin-6 (IL-6), IFN-γ and TNF-α[130].

Various types of immune cells accumulate in obese AT, including lymphocytes, mast cells, neutrophils and macrophages[130,131]. Studies in mice have shown that in the lean state, macrophages make up <10% of the total number of cells in AT, whereas in the extremely obese state they may constitute upwards of 50%[131], suggesting they play an important role in perpetuating inflammation in obese AT.

AT macrophages (ATMs)

It generally accepted that AT resident macrophages derive from blood monocytes, which infiltrate into the tissue via adhesion to capillary endothelial cells and diapedesis, before differentiating into macrophages[131]. Adipokines secreted by mature adipocytes, particularly leptin, facilitate the infiltration and accumulation of macrophages within AT[86,132]. This recruitment of blood monocytes is increased in obesity[133].

Obese adipocytes secrete increased levels of MCP-1, also known as chemokine (C-C motif) ligand 2 (CCL2)[134]. MCP-1 is a chemokine that stimulates the recruitment and migration of monocytes into AT, leading to accumulation of macrophages in the tissue. MCP-1 is secreted in response to pro-inflammatory cytokine signalling, and therefore is upregulated in obese AT[135]. Studies show that MCP-1 knockout in a murine model significantly decreases macrophage

infiltration within AT, and that MCP-1 upregulation is associated with increased macrophage numbers and insulin resistance[89,132].

Monocytic phagocytes (macrophages) are highly plastic cells able to adapt to signals within their microenvironment in response to damaged cells, tissue, cytokines, and can polarise their phenotype to provide the appropriate functionality[136,137]. As a result, they are broadly categorised into M1 and M2 phenotypes[94]. It has been proposed that this functional polarisation may contribute to the maintenance of homeostasis within obese AT[130].

M1 macrophages

M1 macrophages (Figure 6) are pro-inflammatory, and 'classically activated' by IFN-γ[138], bacterial endotoxin lipopolysaccharide (LPS)[139–141] and TNF-α[130]. They contribute to type I inflammation, and remove intracellular pathogens[94]. IFN-γ is the predominant stimulus for M1 activation and is primarily secreted by Th1 cells, although natural killer cells and macrophages are also able to produce IFN-γ[142]. IFN-γ interacts with the IFN-γ receptor, which is composed of IFNGR-1 and IFNGR-2 chains, before STAT1 and other regulatory factors are activated via JAK1/2[143]. These transcription factors modulate the expression of many cell surface markers and adhesion molecules, including essential pro-inflammatory cytokine receptors such as IL-6R and CSF2RB[142].

M1 macrophages recognise pathogen-associated molecular patterns of bacterial products, such as LPS, through pattern recognition receptors on the cell surface, forming part of the innate immune response[142]. In AT, macrophages displaying

M1 characteristics are responsible for 'mopping up' dead adipocytes, by forming crown-like structures surrounding dying adipocytes (Figure 5), allowing the lipid droplet to be 'scavenged' in order to avoid the lipotoxic effects of free lipid[122].

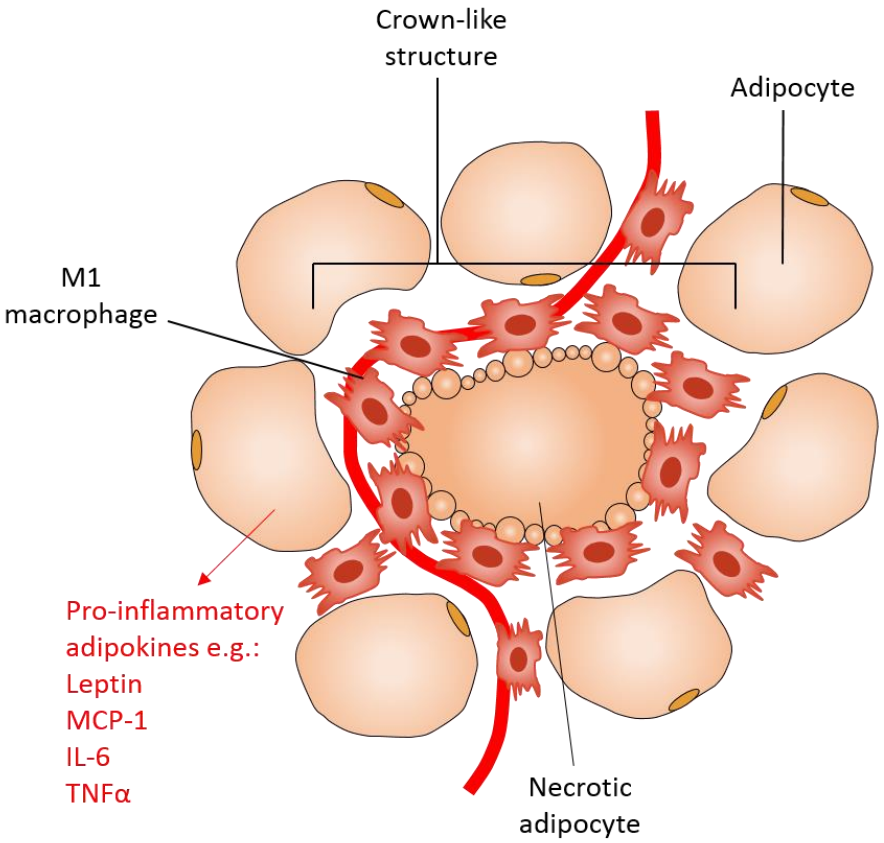

Figure 5: *Crown-like structure in obese adipose tissue.* Adapted from Ouchi *et al* 2011[87].

M2 macrophages

M2 macrophages (Figure 6) are considered to have an 'anti-inflammatory' phenotype and in AT make up the majority of the non-CLS interstitial macrophages[144]. They act to attenuate inflammation and promote tissue

repair[145], or ‘wound-healing’, by promoting the production of ECM components[94,144,146] from cells of the SVF[147,148]. M2 macrophages upregulate production of anti-inflammatory cytokines, such as IL-10, and downregulate production of pro-inflammatory cytokines including IL-1[87]. Although macrophages are not regularly characterised beyond M1 and M2 subtypes, M2 macrophages can be further classified based on the specific physiological stimuli which trigger their polarisation into M2a, M2b and M2c subtypes: IL-4[149] and IL-13[150], toll-like receptor (TLR) ligands[151], and IL-10 respectively (Figure 6)[142,152].

IL-4 is secreted in an autocrine manner by macrophages, as well as by other immune cells such as basophils, eosinophils and Th2 cells[142]. The transcriptomic signature induced by IL-4 in macrophages is believed to lead to decreased phagocytosis and increased macrophage fusion[142]. IL-4 signalling is facilitated by a cell surface receptor complex involving IL4Rα1, which via JAK1/3 activation leads to phosphorylation and nuclear translocation of transcription factor STAT6. IL-13 also signals via a similar mechanism, through binding with the IL13Rα1 (or the controversial IL13R α2) chain[142].

IL-4 and IL-13-stimulated M2a macrophages are known as ‘alternatively activated’ and are thought to be involved in type II inflammatory responses[142,153]. They secrete IL-10 and present mannose and scavenger receptors on the cell surface[142,149]. M2b macrophages, whose differentiation is stimulated by immune complexes and TLR or IL-1 receptor ligands, secrete TNFα, IL-1 and IL-6, as well as high levels of IL-10[94]. They are believed to play a role in the activation of Th2 cells, and are important for immunoregulation[142]. M2c macrophages are stimulated by IL-10, which binds to a dimeric receptor consisting of IL10R1 and

IL10R2 and resulting in receptor autophosphorylation. STAT3 is activated by phosphorylation, dimerises and translocates into the nucleus where acts as a transcription factor to inhibit the expression of pro-inflammatory cytokines[142].

M2c macrophages express signalling lymphocytic activation molecule (SLAM), also known as CD150, and mannose receptor (CD206), as well as secreting IL-10 and TGFβ, and are reported to contribute to matrix deposition and tissue remodelling[142]. M2c macrophages in particular are thought to play an important role in wound healing due to their expression of high levels of TGF-β[94], which contributes to increased ECM production via Smad2/3 signalling pathways[144].

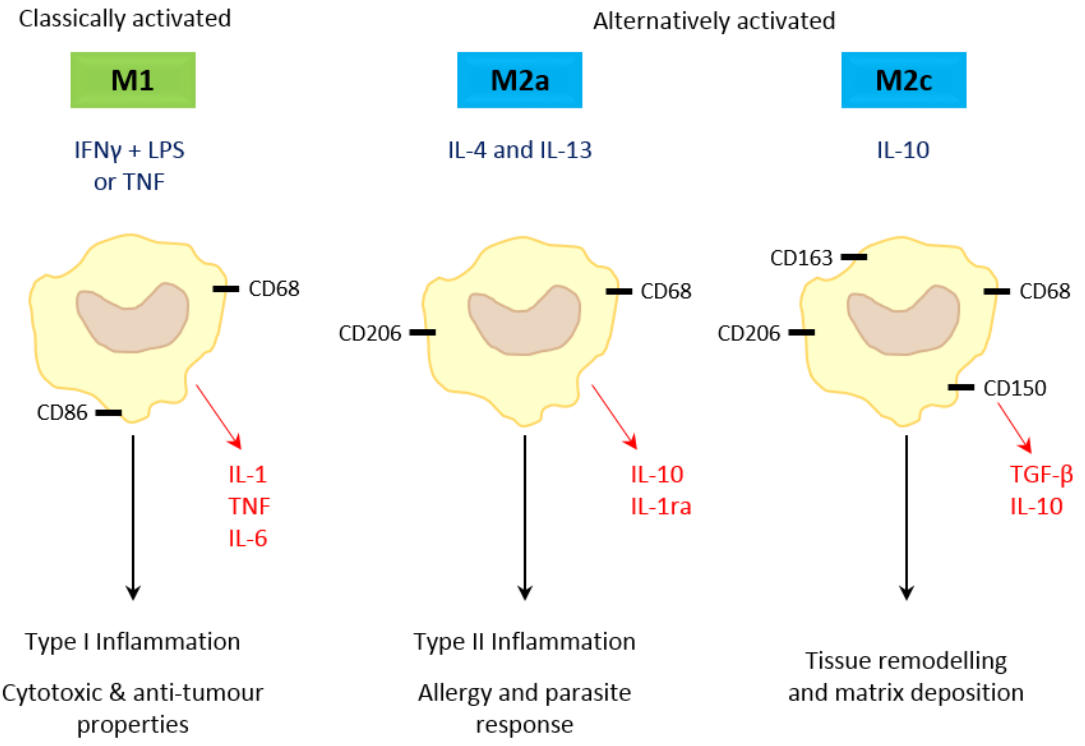

Figure 6: *Functional properties of classically and alternatively activated macrophages.* Adapted from Martinez and Gordon (2014)[142].

The origin of M2 macrophages in AT remains unclear: they may derive from newly infiltrated monocytes or may transdifferentiate from M1 macrophages already in

the tissue. One theory proposes that monocytes are recruited in 'waves' at different stages of the inflammatory response, and are therefore exposed to a different milieu of inflammatory signals, which determines their polarisation into M1 or M2 macrophages[154]. An alternative hypothesis suggests that, given the right environmental signals, M1 macrophages transdifferentiate into anti-inflammatory M2 macrophages[154].

ATMs in obesity

There are contradictory studies regarding the phenotype of macrophages in obese AT. Lumeng *et al* (2007) reported that in mice fed a high fat diet, the accumulating ATMs appear to be of M1 phenotype[155]. ATMs of lean mice expressed markers of M2 macrophages such as arginine (*Arg1*) and mannose receptor 2 (*Mrc2*) more strongly than macrophages in obese mice. They conclude that high expression of IL-10 from M2-polarised macrophages protects adipocytes from TNF-α-mediated downregulation of insulin receptor and GLUT4 expression, and insulin resistance. As such, Lumeng *et al* propose a model of 'phenotypic switching', whereby tissue resident M2 macrophages undergo transformation towards a more pro-inflammatory, M1-like phenotype during positive energy balance[155]. Upregulation of M1 macrophage markers has been shown to positively correlate with markers of insulin resistance[87], therefore it has been suggested that the M1 phenotype is able to promote insulin resistance in obesity, while M2 macrophages may protect against its development[156].

In contrast, it has been reported that human ATMs mainly appear to be of an M2-like phenotype, but are able to secrete high levels of pro-inflammatory cytokines,

such as TNF-α and IL-1β, after stimulation with IFNγ or LPS[157]. In agreement with this mixed inflammatory phenotype, human ATMs are capable of expressing both CD206 and CD11c, M2 and M1 macrophage cell surface markers respectively[158]. Fjeldborg *et al* (2014) also reported elevated numbers of M2 macrophages in obese human subjects, qualified by high expression of M2 macrophage markers CD163 and CD206 and increased secretion of IL-10. In comparison, ATMs from lean subjects expressed significantly lower levels of M2 markers, suggesting that obesity induces macrophages take on an M2-like phenotype[159].

In summary, this evidence suggests an important role for polarised macrophages in the development of dysfunctional obese AT.

1.2.5 ***AT fibrosis***

In obesity, AT expansion via tissue hyperplasia or adipocyte hypertrophy requires the surrounding matrix to adapt through the deposition and degradation of ECM proteins.[97] AT fibrosis is defined as the excessive accumulation of insoluble ECM collagens, which increases tissue rigidity, potentially limiting healthy tissue expansion and therefore lipid storage capacity[144]. It is implicated in the development of AT dysfunction, associated with insulin resistance, T2DM, and non-alcoholic fatty liver disease[160]. ECM collagens have differing functional and structural classifications according to their type, and are be described as fibril-forming, network-forming, or beaded-filament-forming[12].

Fibril-forming collagens in AT fibrosis

Fibril-forming collagens are one of the main fibrous components of the ECM and are essential for providing structural support in tissue[9]. Collagens I, III and V are fibril forming, and undergo much post-translational processing to assemble their triple helical structure[9].

Collagen I precursor α-chains are synthesised in the rough endoplasmic reticulum lumen, where they undergo various processing modifications before disulphide bonds form between the N- and C-terminal sequences, enabling the assembly of the triple helix[12]. *COL1A1* encodes the pro-alpha1 (1) chain of the collagen triple helix, which associates with the pro-alpha (2) chain, encoded by *COL1A2*. Two α1 subunits are bound to a single α2 subunit to establish a heterotrimeric type I collagen monomer[161]. After further processing at the Golgi complex, N- and C- terminal pro-peptides are cleaved and the triple helices are exocytosed to the extracellular space where, through lysyl oxidase (LOX)-mediated covalent bonding, they polymerise to form fibrils[162]. These fibrils then assemble into collagen fibres, as observed in AT[162].

As a fibril-forming collagen, type III collagen undergoes the same process of assembly, differing only in the composition of its triple helix: it is homotrimeric, and is therefore composed of three identical α1 chains, encoded by *COL3A1*[163]. Collagen I and collagen III are co-expressed in fibrous bundles, in areas of fibrosis in human omental AT, and are therefore postulated to contribute to the pathophysiological development of AT fibrosis[148]. It is also believed that fibroblast-like preadipocytes, rather than adipocytes, are the predominant cell

type responsible for the development of obesity-associated AT fibrosis[164]. Macrophage-secreted pro-inflammatory factors have also been implicated in the increased expression of collagen I/III in differentiated preadipocytes[165].

Collagen V also forms fibrils in the ECM, and is reportedly required for the formation of collagen I fibrils in embryonic tissues[166]. Spencer *et al* (2011) report a relationship between collagen V and insulin sensitivity, where increased expression of *COL5A1* mRNA significantly correlated with reduced insulin sensitivity in subcutaneous AT (SCAT)[167], indicating a relationship between AT dysfunction and increased deposition of fibre-forming ECM collagens.

Network-forming collagen IV

Type IV collagen is a network-forming collagen, expressed during adipogenesis and essential for the formation of the basement membrane, which surrounds adipocytes[12,13]. The basement membrane gives structural support to cells, and provides a site for integrin signalling and cell adhesion to take place, as well as being important for the maintenance of tissue function in AT[12,168]. Collagen IV-α1 and collagen IV-α2 are the predominant proteins which constitute the collagen IV trimer in AT, as collagen IV-α3-6 are expressed at relatively low levels[13]. Overexpression of collagen IV has been implicated in the development of pericellular fibrosis, as in obese SCAT, collagen IV surrounding adipocytes has been shown to be increased, along with having a more disorganised pattern of deposition[15]. *COL4A1* expression has also been positively correlated with markers of insulin resistance[15].

Beaded-filament-forming collagen VI

Type VI collagen assembles into 'beaded-filaments', and plays an essential role in providing ECM stability[12]. It is expressed in a wide range of tissue types, as well as in AT. Within the endoplasmic reticulum of the cell, α1, α2 and α3 chain subunits (encoded by *COL6A1, COL6A2, COL6A3* respectively) assemble into triple helical monomers, which align in opposing directions and undergo disulphide bonding to give dimers, before subsequent disulphide bonding creates tetramers which, after modification at the Golgi apparatus, are secreted into the extracellular space[16]. Here, tetramers associate into beaded microfilaments through non-covalent bonds, giving a 'beads on a string' appearance[16].

Collagen VI has been extensively studied as a key ECM component implicated in the development of pericellular fibrosis, and its overexpression is hypothesised to limit adipocyte hypertrophy, exacerbating the pathogenic effects of AT dysfunction[144,169,170]. However, the picture is not clear cut as there is still some debate over the nature of the involvement of collagen VI in AT fibrosis[147].

There is evidence to suggest that collagen VI is significantly enriched in AT depots compared with other tissues[169]. Metabolic stress and impaired glucose tolerance was associated with increased murine *col6a3*, suggesting collagen VI may restrict expansion and contribute to adipocyte dysfunction[169]. Importantly, murine collagen VI knock-out models showed uninhibited adipocyte expansion and reduced inflammation[169]. Subsequently, a distinct correlation between expression of *COL6A3* in abdominal SCAT and BMI was shown, suggesting

increased deposition of collagen VI may be associated with the pathogenesis of obesity in humans, as well as mice[170].

Following these important observations, Spencer *et al* (2010) assessed the influence of insulin sensitivity on induction of human SCAT fibrosis. They noted a significant correlation between increased expression of *COL6A1* and reduced sensitivity to insulin, an indication of insulin resistance[144]. This was supported by a significant inverse correlation between overall fibrosis within human abdominal SCAT sections and insulin sensitivity[144], indicating a role for insulin in the regulation of ECM protein synthesis.

In contrast to studies linking collagen VI increase with obesity, McCulloch *et al* (2015) reported no change in human SCAT *COL6A3* mRNA expression after weight gain, and describe a significant increase in subjects after weight loss[147]. They describe a negative association between *COL6A3* and leptin mRNA expression in SCAT, and demonstrate decreased *COL6A3* expression in SCAT explants after leptin treatment. They propose leptin may regulate *COL6A3* expression by binding leptin receptors on the adipocyte surface and activating undefined paracrine signalling cascades, and suggest that metabolic improvements observed as a result of *Col6* knockout in *ob/ob* mice may be restricted to the murine model only, as the *ob/ob* model induces obesity through disruption of leptin signalling pathways[147]. This suggests conclusions made using murine models may not translate to human obesity. More research is required to accurately determine whether collagen VI does indeed play an important role in human obesity-associated AT fibrosis.

Non-collagenous structural proteins

Elastin, encoded by the *ELN* gene, is essential for tissue recoil, elasticity, and healthy AT expansion. It is secreted as its precursor tropoelastin before assembling into fibres through lysyl oxidase-facilitated cross-linking[9]. Elastin deficiency in mice has been linked to impaired glucose metabolism, suggesting it may be involved in the development of insulin resistance[171]. It was shown to be significantly reduced in obese subjects when compared to lean, and is suggested to be negatively associated with inflammation[167]. Loss of elastin content in obese AT suggests that fibrosis development not only involves excessive deposition of collagens, but also degradation of elastin, limiting the remodelling and lipid storage capacity of the tissue[167]. The factors regulating elastin deposition are relatively poorly understood, but fibres are thought to be degraded by members of the metalloproteinase family, known as metalloelastases, although more work is needed to further elucidate the key molecules involved[172], as well as the role of inflammation in controlling elastin content in obese AT.

Fibronectin is an important fibrous protein, involved in the organisation of the developing ECM, and is encoded by the *FN1* gene[9]. It provides integrin-binding sites, and is essential for directing cell organisation, migration and differentiation, and is therefore important in ECM remodelling[9]. Fibronectin also binds to collagen fibres, contributing to the stabilisation of the ECM[173]. Its increased expression is thought to correlate with measures of metabolic dysregulation in obesity[174].

Molecular regulators of fibrosis

Secreted protein acidic and rich in cysteine (SPARC), also known as osteonectin, is a collagen-binding matricellular protein which helps stabilise the basement membrane[175], and therefore may play an important role in the development of pericellular fibrosis[176]. SPARC has been shown to be overexpressed in obese adipocytes, and this overexpression may be induced by increased TGF-β signalling[15], suggesting that TGF-β secreting macrophages may contribute to fibrosis through SPARC-mediated thickening of the basement membrane. Increased SPARC expression may be upregulated *in vivo* in response to hyperinsulinaemia, and as such, linked with insulin resistance[177].

TGF-β signalling is believed to play a vital role in inducing the development of AT fibrosis[144] by regulating the balance between synthesis of matrix components and their degradation via MMPs, and its expression by adipocytes may be induced by mechanical stress[169]. Members of the TGF-β family are cell signalling molecules responsible for directing the development and behaviour of cells, activating Smad protein pathways and plasminogen activator inhibitor-1 (PAI-1), a protein which inhibits plasmin-mediated ECM degradation[178]. TGF-β isoforms (1 and 3) have been shown to induce upregulation of *PAI-1*, connective tissue growth factor (*CTGF*) and *TGFβ1* genes in adipocytes[15], potentially leading to a positive-feedback loop wherein TGF-β-secreting wound-healing macrophages[94] act as an initiator, and activated adipocytes provide a macrophage-independent source of pro-fibrotic signalling[15].

Lysyl oxidase, encoded by the *LOX* gene, is an enzyme responsible for the covalent cross-linking of collagen and elastin fibres at their lysine residues, establishing the deposition of insoluble matrix components and stabilising the ECM[179]. There is evidence to suggest that *LOX* mRNA is significantly increased in adipocytes from obese AT[180], and that this can be induced by TGF-β1 signalling, therefore contributing to ECM stabilisation in fibrosis[15]. In addition, LOX has been implicated in the development of HIF1α-mediated fibrosis[121].

Hypoxia and fibrosis

There are two main pathways through which hypoxia is thought to cause fibrosis. The first is hypoxia-induced necrotic cell death and infiltration of macrophages which may exert wound-healing, pro-fibrotic characteristics[181]. Alternatively, AT hypoxia induces upregulation of HIF1α[182,183], and reportedly directly mediates the expression of murine *Col1a1, Col3a1, Col6a1* and *Eln*[121]. Its upregulation is thought to play an important role in AT fibrosis through activation of a pro-fibrotic transcriptional programme[121,181].

1.2.6 *Insulin resistance and fibrosis*

Insulin plays an important role in influencing the development of AT, as it regulates the deposition of ECM proteins by enhancing post-transcriptional processing and secretion of ECM collagens[184]. Therefore, increased levels of insulin may be implicated in AT fibrosis.

The term ‘insulin resistance’ refers to the metabolic state in which cells of the body become unresponsive to insulin signalling, and if left untreated, can

progress into T2DM[19]. Reduced insulin sensitivity, or insulin resistance, results in disruption of the normal postprandial response mechanism (described in section 1.1.2), where blood glucose is not effectively utilised by AT, the liver and skeletal muscle - the major insulin response organs. When insulin sensitivity is low, glucose tolerance is usually maintained by a compensatory increase of insulin secretion by pancreatic β-cells[185]. One consequence of this is chronically high concentrations of circulating insulin, known as hyperinsulinaemia[186].

Hyperinsulinaemia is associated with AT dysfunction, and strongly predicts metabolic disease[187]. There are conflicting reports regarding the effect of insulin on AT, as there is evidence to suggest it exerts a pro-inflammatory effect in obese AT via upregulation of MCP-1 in adipocytes[188], however has also been shown to exert a potent anti-inflammatory effect by inhibiting the pro-inflammatory nuclear factor κ B (NFκB)[189]. Boutens *et al* (2015) postulate that insulin resistance in monocytes may influence their functional and inflammatory properties, and suggest the need for studies investigating the effects of insulin signalling patterns on macrophage phenotype[190].

1.2.7 *Insulin resistance and T2DM*

Insulin resistance can lead to the development of T2DM. T2DM is characterised by metabolic disturbances including obesity, dyslipidaemia (abnormal levels of circulating lipid)[181], decreased insulin secretion, reduced insulin sensitivity in peripheral tissues and increased hepatic gluconeogenesis (synthesis of glucose by the liver)[191]. In obesity-related T2DM, the secretory ability of pancreatic β-cells is impaired and glucose remains at a high concentration in the circulation for an

extended period of time (hyperglycaemia)[192]. For T2DM classification, β-cells fail to rapidly release insulin in response to stimulation by circulating glucose, and there is up to 50% apoptosis-related depletion of cells[193]. The remaining cells are not able to maximise their insulin secretion capacity, and once fasting hyperglycaemia has developed, cells have lost up to 75% of their function[193]. This decline is progressive: it is ongoing and associated with declining glycaemic control[193]. Hyperglycaemia is thought to perpetuate insulin insensitivity and have toxic, oxidative stress-related effects on β-cells[194].

Insulin resistance alone is insufficient to cause the development of T2DM. The individual must have a genetic predisposition, and be unable to secrete sufficient quantities of insulin to meet metabolic demand[195]. Additionally, reduced insulin sensitivity prevents insulin-induced inhibition of lipolysis (Figure 4) leading to hyperlipidaemia[192]. It is believed that consistently high plasma FFAs are implicated in perpetuating further insulin resistance and β-cell dysfunction[192].

Chronically poor glycaemic control as a result of β-cell dysfunction leads to glucose toxicity and increased risk of cardiovascular events, diabetic neuropathy, nephropathy and retinopathy[194]. T2DM patients may be treated with insulin replacement therapy in order to improve glycaemic control and thus avoid these pathologies[196]. A side effect of this treatment is chronic hyperinsulinaemia[197], which as previously discussed, may be implicated in the development of AT fibrosis.

1.2.8 *Inflammation and insulin resistance*

A direct link between inflammation and insulin resistance has long since been established[198], as obesity is associated with infiltration and activation of pro-inflammatory macrophages[199]. Pro-inflammatory cytokine TNF-α, secreted by pro-inflammatory ATMs, is capable of inducing insulin resistance in adipocytes in obesity by promoting increased serine/threonine phosphorylation of IRS-1 and inhibiting signal transduction by preventing IRS-1 acting as a substrate for the kinase activity of the insulin receptor[200]. Its upregulation in obese mice resulted in significantly decreased insulin-facilitated uptake of glucose from serum into tissues[90].

Some macrophage-secreted pro-inflammatory factors can block the action of insulin, and may be important modulators of insulin sensitivity[72]. Macrophage secretory products have been shown to downregulate the expression of IRS-1 and GLUT4 in adipocytes, as well inhibit translocation of GLUT4 to the cell surface[201]. This effect was reversed by the neutralisation of TNF-α by anti-TNF-α antibodies, indicating the importance of pro-inflammatory TNF-α in sustained insulin resistance[201].

1.3 Aims and objectives

The development of fibrosis is thought to be caused by a dysregulated response to adipocyte death, where inflammatory signalling triggers an influx of macrophages. These macrophages undergo polarisation and are considered the 'master regulators' of AT fibrosis. This study hypothesised that M2c macrophages, via anabolic TGF-β signalling, are the key cellular drivers of pathogenic AT fibrosis, and that hyperinsulinaemia, a hallmark of insulin resistance, enhances the development of macrophage-mediated AT fibrosis (represented in Figure 7).

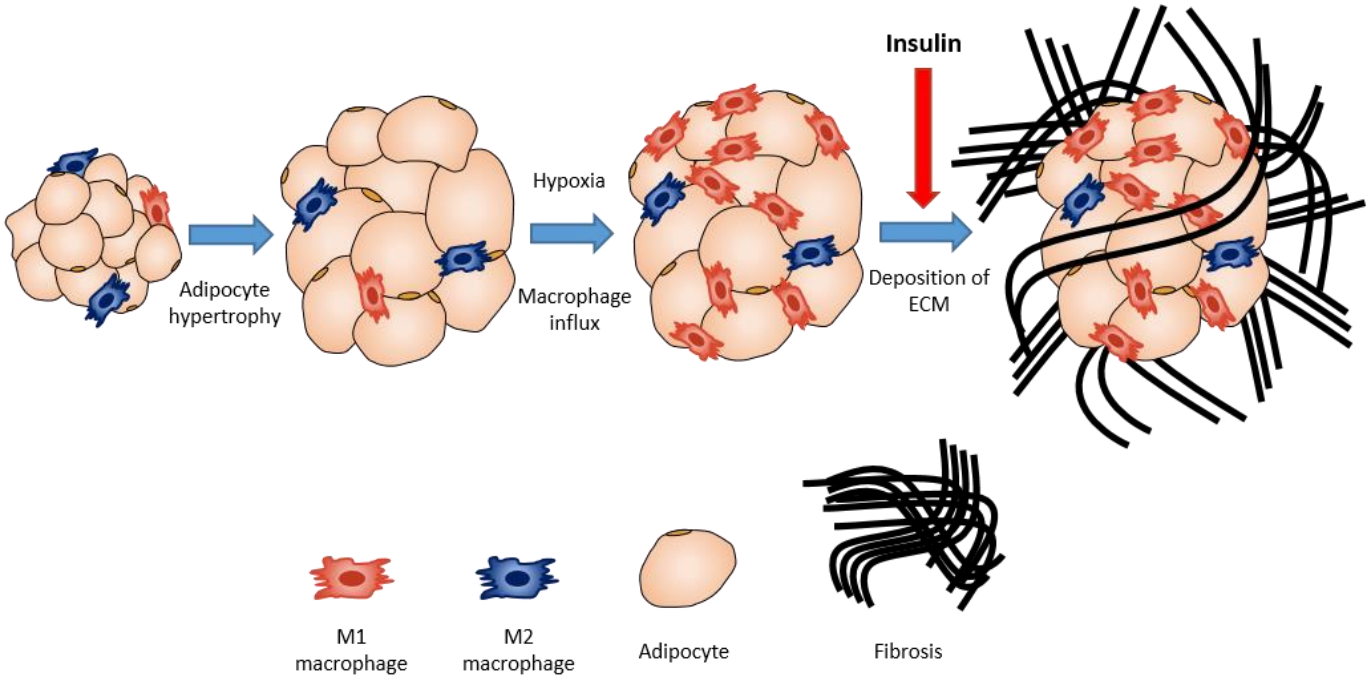

Figure 7: *Schematic representation of hypothesised events leading to adipose tissue fibrosis.* Adipocyte hypertrophy results in local hypoxia, cell death, inflammation and macrophage influx. Macrophage polarisation regulates the deposition of ECM components. When ECM deposition becomes dysregulated, AT develops fibrosis and loses plasticity, leading to ectopic lipid deposition. This effect may be compounded by increased levels of insulin.

This study aimed to build on the current understanding of how obese AT inflammation may lead to fibrosis, by investigating the effects of macrophages and insulin on AT fibrosis – specifically helping to clarify the role of M2a and M2c macrophage subtypes. It also aimed to provide novel insight into a possible pro-fibrotic effect of hyperinsulinaemia on the development of macrophage-mediated AT fibrosis.

Therefore, the objectives of this study were to confirm the pro-fibrotic effects of M2 macrophages (M2a and M2c subtypes) on human AT, to assess how insulin may modulate the effect of M1, M2a and M2c macrophages on the expression of genes associated with fibrosis in AT, and to determine the efficacy of *in vitro* macrophage differentiation protocols, enabling informed conclusions to be drawn about the importance of macrophage phenotype in the development of AT fibrosis.

By further unravelling the factors involved in the development of pathogenic fibrosis in AT, it may be possible in the future to identify cellular or molecular treatment targets with a view to improving AT dysfunction in obesity.

Chapter 2: Methods

The specific procedures and methodology used in order to fulfil the objectives of this study are detailed in this chapter. Briefly, THP-1 monocytes were cultured and differentiated, aiming to represent M1, M2a and M2c macrophages. Omental AT samples were obtained from consenting participants, before being processed and co-cultured with macrophages in the presence of insulin at various concentrations.

2.1 THP-1 cell culture

The THP-1 (Tohoku Hospital Paediatrics-1) cell line is an immortalised proliferating cell line of human leukaemia monocytes, established in 1980 and derived from the blood of a young male patient with acute monocytic leukaemia. THP-1 cells, characterised by their specific human leukocyte antigen type, can proliferate on a scale suitable for use in an *in vitro* study, and have a homogenous genetic background, meaning potential for phenotypic variation is limited. It is also possible to effectively differentiate and polarise THP-1 cells under controlled culture conditions[144], providing a significant advantage over primary monocytes or monocyte-derived macrophages in terms of practicality and reproducibility of results.

RPMI 1640 (Roswell Park Memorial Institute) media, used to culture THP-1 cells, was developed as a suitable medium for the culture of human leukaemic cells, and contains high concentrations of vitamins (e.g. vitamin B_{12}) to support cell growth. RPMI 1640 does not contain growth factors, proteins or lipids so must be

supplemented with foetal bovine serum (FBS). During the manufacture of FBS, erythrocytes, fibrinogen and platelets are removed from calf whole blood to prevent clotting, leaving all other proteins essential for cell culture[202].

The culture medium was supplemented with 1% penicillin and streptomycin (Sigma, St. Louis, MO, USA) antibiotics to prevent bacterial infection. The two were used in combination to protect against gram-positive and gram-negative bacteria, as penicillin disrupts the bacterial cell wall, and streptomycin inhibits protein synthesis in the target bacterial cell by binding and sequestering the 30S ribosomal subunit[202].

For this study, THP-1 cells were removed from storage in liquid nitrogen and swiftly defrosted by hand. The cell suspension was briefly mixed via vortex and pulse-spun in the centrifuge to ensure all cells were collected. Cells were immediately transferred into 10ml of fresh THP-1 culture medium – RPMI 1640 (11mM D-glucose) supplemented with 10% foetal bovine serum (FBS), 1% penicillin streptomycin (P/S) solution (100U/ml penicillin, 100µg/ml streptomycin) and 2mM L-glutamine. The cell suspension was centrifuged at 300 x g for 5 minutes to obtain a cell pellet, then resuspended in 20ml of medium at a concentration of $3x10^5$ cells/ml and added to a $75cm^2$ cell culture flask. Cells were maintained in 5% CO_2, with 100% humidity at 37°C. An additional 20ml of fresh culture medium was added four days later, and cells were split for sub-culture upon reaching a concentration of $1x10^6$ cells/ml. Concentration was determined by dispensing 1µl of diluted cell suspension (1:50) into a cell counting slide and reading using a Bio-Rad TC20™ automated cell counter.

2.2 Subject participation

2.2.1 *Subject recruitment*

Ethical approval for the study was granted by the Ethics Committee and Tissue Bank ECRF Steering Committee. Suitable participants, scheduled to undergo surgical procedures, were identified by clinicians during their routine care. Patients were required to be over the age of 18 and able to provide informed consent. Exclusion criteria prevented the participation of subjects who had undergone bariatric surgery, were actively undergoing steroid treatment or had used steroids in the preceding three months, or had a chronic inflammatory condition requiring use of anti-inflammatory medication. AT samples were held as part of the Royal Devon and Exeter Tissue Bank (TB) for use in this study. Basic patient characteristics are detailed in Table 1.

	Patient	Age	Sex	Weight (kg)	BMI
	1	70	F	68.95	28
	2	48	F	89	28.4
	3	49	F	103	36.1
	4	55	F	90.2	34.4
	5	42	F	71	29.9
	6	42	F	51.4	19.8
	7	64	F	55	20.2
	8	64	F	84.2	35.5
	9	46	F	103.1	35.2
	10	33	F	62.2	21.3
Mean		51.3		77.81	29.72
Median		48.5		77.6	29.9
SD		11.73		18.8	6.32

Table 1: *Patient characteristics.* AT was obtained from ten female patients. Age, weight and BMI information was collected.

2.2.2 *Sample and data collection*

Fresh omental AT (OMAT) samples were collected during routine obstetric/gynaecological surgery from consenting female patients where tissue was removed for pathological analysis and considered surplus to requirements, or where the patient had given consent for a small additional piece of tissue to be taken, and clinicians agreed the process presented no additional medical burden. During the assessment of patient suitability, some basic information was gathered including current and previous weight measurements, blood pressure and medication, and current body mass index (BMI) figures. All tissue samples were assigned a unique TB code to preserve patient anonymity and submerged in room temperature Hank's balanced salt solution (HBSS) immediately after harvest.

2.3 Cell culture

2.3.1 *THP-1 differentiation*

THP-1 cells were observed under the microscope to assess confluency and the accumulation of cell debris – indicative of apoptosis. Cells were then spun at 300 x g for 5 minutes and pellet resuspended in a known quantity of fresh culture medium (10ml per 75cm^2 flask) before being transferred into a single 50ml tube. The cell suspension was diluted accordingly (1:50) then quantified using the Bio-Rad TC20™ Automated Cell Counter. The read-out was used to calculate the volume of suspension needed to give 4x10^6 cells per well in each condition. As 8ml of cell suspension was necessary per condition, four tubes containing this volume were centrifuged and resuspended in media for their corresponding conditions, an overview of which can be found in Table 2. For M1 differentiation,

the THP-1 cell pellet was resuspended in 30ml RPMI 1640 supplemented with 2mM L-glutamine, 20ng/ml LPS and 20ng/ml IFN-γ.

For M2 differentiation, two cell pellets were resuspended in RPMI 1640 supplemented with 2mM L-glutamine and 5nM PMA and incubated at 37°C for 5 minutes. PMA was used in the differentiation process to induce cell cycle arrest and halt proliferation through upregulation of p21, which in turn inhibits cyclin-dependent kinase 2 (CDK2) and prevents cells transitioning from G_1 to S phase of the cell cycle[203].

After incubation, tubes were immediately centrifuged at 300 x g for 5 minutes. One pellet was resuspended in 30ml RPMI 1640 supplemented with 2mM L-glutamine, 1% P/S and 20ng/ml IL-4 in order to induce differentiation into the M2a macrophage subtype, while the second pellet was resuspended in 30ml RPMI 1640 supplemented with 2mM L-glutamine, 1% P/S and 20ng/ml IL-10 to facilitate differentiation into the M2c macrophage subtype. In the case of the undifferentiated THP-1 control, cells were resuspended in 30ml RPMI 1640 supplemented with 2mM L-glutamine 1% P/S. 2ml of each suspension was dispensed into the corresponding wells before plates in were incubated at 37°C for 48 hours.

	THP-1	M (IFNγ +LPS)	M (IL-4)	M (IL-10)
RPMI 1640	✓	✓	✓	✓
2mM L-Glutamine	✓	✓	✓	✓
1% P/S	✓		✓	✓
20ng/ml LPS + 20ng/ml IFNγ		✓		
5nM PMA			✓	✓
20ng/ml IL-4			✓	
20ng/ml IL-10				✓

Table 2: *Composition of media for macrophage differentiation.*

2.3.2 ***THP-1/AT co-culture***

AT samples were stored in HBSS and upon receipt from surgery kept at room temperature for the duration of processing (up to four hours). For each macrophage condition, a small piece of tissue (approximately 3g) was removed from the bulk of the sample before forceps and surgical scissors were used to remove any prominent vasculature and areas of stiffness or scarring. The tissue was then 'minced' using scissors into pieces measuring approximately 500µm^3 to achieve a 'soup-like' consistency. An explant of 250mg (±20mg) was prepared for each duplicate well and spread evenly across the membrane of a Millicell hanging cell culture insert (Fisher Scientific MCHT06H48). If some tissue was surplus, several small pieces (~3-5g) were removed and stored at -80°C. During co-culture set-up, explants were prevented from drying by a small volume (2ml) of RPMI 1640 2mM L-glutamine, 1% P/S. Once prepared, the macrophages in culture were removed from incubation and their differentiation medium gently

aspirated, leaving adherent differentiated macrophages behind. The inserts were dispatched into wells with 2.5ml RPMI 1640 2mM glutamine 1% P/S and either a vehicle control, 1, 10, or 100nM insulin. Figure 8 shows the full experimental set-up. Plates were incubated at 37°C, 5% CO_2 for 48 hours. This procedure was repeated for all macrophage phenotypes, along with a negative control condition without macrophages. Within each experiment, co-culture conditions were performed in duplicate. Ten independent experiments were carried out, each using AT from a single independent donor.

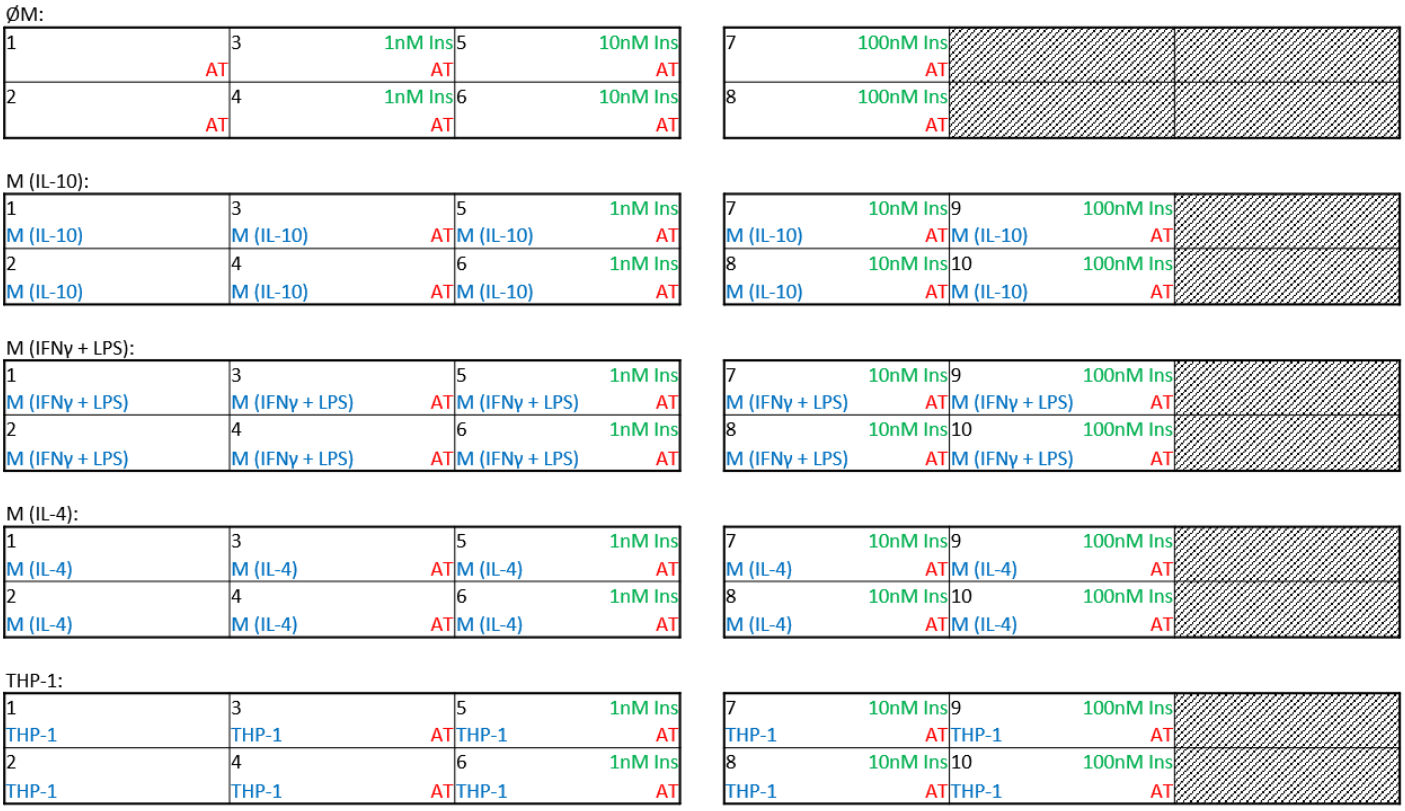

Figure 8: *Representation of co-culture setup, denoting the presence of AT, insulin concentration and macrophage differentiation.* Each cell represents a numbered well in a six-well polystyrene cell culture plate. $4x10^6$ THP-1 cells were plated per well before differentiation was induced. Co-cultures were performed in duplicate. Ten independent experiments were performed, using explants from a single tissue donor in each.

After the co-culture incubation period, AT explants were collected and stored in 1ml TRI Reagent® Solution in preparation for RNA isolation. All media was removed from the culture wells and dispensed into 1.5ml tubes. TRI Reagent® Solution (500µl) was added to the wells and a cell scraper was used to collect differentiated, adherent macrophages from the plastic surface of the wells for storage in a 1.5ml tube. All tubes were preserved at -80°C. This protocol was

repeated for each new tissue sample (ten in total) over the course of several months.

2.4 Expression profiling

2.4.1 *RNA extraction and purity*

AT samples stored at -80°C in TRI Reagent® solution were defrosted by hand and homogenised in the Retsch® MM400 homogeniser at room temperature. A single sterile RNAse-free stainless steel bead was added to each tube before homogenising at 30Hz for approximately 10 minutes, or until the sample appeared fully homogenised. Samples were then centrifuged at 12000 x g for 10 minutes at 4°C and the pink TRI Reagent® phase isolated from the lipid layer and debris pellet. Per 1ml of TRI Reagent®, 200µl of chloroform was added. Samples were shaken vigorously for 15 seconds, then incubated at room temperature for 2-3 minutes. Tubes were spun a second time at 12000 x g at 4°C for 15 minutes to give a clear, aqueous layer containing RNA, an interphase of genomic DNA and denatured proteins, and an organic phenol-chloroform phase containing some DNA and proteins, at the bottom of the tube. The clear aqueous RNA layer was carefully isolated and 500µl of ice-cold isopropanol added. Following thorough agitation and a 10 minute incubation at room temperature, the samples were spun at 12000 x g at 4°C for 10 minutes, allowing the RNA to precipitate into a visible pellet. Pellets were twice washed with 1ml of ice-cold ethanol before being resuspended in RNase-free water and immediately stored on ice. The volume of water used was judged by eye based on the observed size of the pellet, but was typically 12-40µl.

RNA concentrations and purity were subsequently assayed using the Thermo Scientific NanoDrop™ 8000 spectrophotometer. In addition to obtaining a measure of nucleic acid concentration within the sample, sample purity was determined using the 260/280nm and 260/230nm absorbance ratios. All nucleotides (i.e. RNA, ssDNA and dsDNA) absorb light at the 260nm wavelength. Contaminants such as protein and phenol (likely from TRIzol® Reagent) absorb light at 280nm, therefore the 260/280 measurement indicates the relative purity of the sample - a reading in the region of 2.0 is considered 'pure'. A secondary indicator of purity is the 260/230 ratio, which should be 2.0-2.2 when RNA is pure. A lower figure suggests contamination by carbohydrates and phenol, which also absorb UV light at 230nm.

Following the extraction of RNA from all experimental samples, additional genetic material was extracted from three untreated pieces of AT, frozen at the point of receipt during the co-culture set up (section 2.3.2), for use as a calibrator in each qPCR plate, as described in section 2.5. RNA was also extracted from macrophages cultured alone in wells 1 and 2 for each subtype, without AT or insulin treatment, to establish the success of the differentiation protocol. Samples were assayed and diluted as above.

2.4.2 *Sample selection*

Due to resource constraints, AT from six of the initial ten independent experiments was selected for reverse transcription (RT). The selected samples had the highest RNA concentration and $A_{260/280}$ and $A_{260/230}$ wavelength ratios closest to the optimum. See appendix 2 for full details. These participants were

patients 2, 4, 5, 6, 7, and 9 (age: 49.5 ± 7.83, BMI: 27.98 ± 6.12 and weight: 76.62 ± 19.03kg, as detailed in Table 1).

2.4.3 *Reverse transcription*

RT was performed on RNA samples from six participants and calibrator samples (detailed above) to give complimentary DNA (cDNA), using a reaction mix which included random primers, RT enzymes, $MgCl_2$, dNTPs and DNA polymerase. Invitrogen™ SuperScript™ VILO™ cDNA Synthesis Kit (10499763, Fisher Scientific) was used in accordance with the published product information sheet, using the following volumes of VILO™ Reaction Mix (at 5X concentration), SuperScript™ Enzyme Mix (at 10X concentration), RNA and nuclease-free water for a 10µl reaction mix, as shown in Table 3.

Reagent	Volume
5X VILO™ Reaction Mix	2 µl
10X SuperScript™ Enzyme Mix	1 µl
RNA	X µl
Nuclease-free water	up to 10µl

Table 3: *Reverse transcription reaction mix.*

The volumes of RNA and nuclease-free water were dependent on the concentration of the RNA samples (available in appendix 2), and together made up 7µl of the total reaction volume, giving a final RNA concentration of 30ng/µl in each well.

RNA was reverse transcribed in 96-well polypropylene plates, with a total of 300ng of material in each reaction, using the DNA Engine® DYAD™ Peltier Thermal Cycler according to the protocol shown in Figure 9.

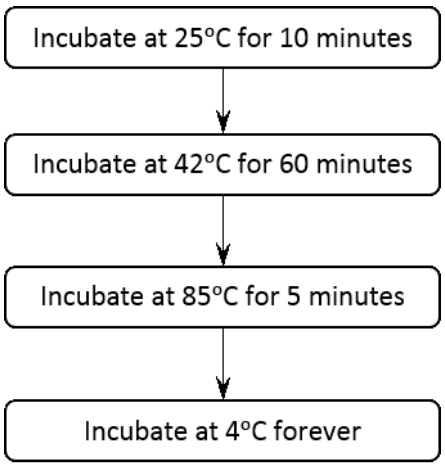

Figure 9: *Reverse transcription thermocycler programme*

The resulting cDNA was diluted using Invitrogen™ Ambion™ nuclease-free water (not DEPC treated) (10185104 Fisher Scientific) to 5ng/µl before storage at -20°C.

2.4.4 ***qRT-PCR***

Quantitative polymerase chain reaction (qPCR), also referred to as real-time polymerase chain reaction, is a method by which the exponential amplification of cDNA is monitored and recorded in real time, allowing the relative expression levels of specific genes of interest (GOIs) to be determined based on the quantity of cDNA in a sample[204]. qPCR was performed on the Applied Biosystems™ QuantStudio™ 12K Flex system, using the QuantStudio™ 12K Flex Software v1.2.2, with the run method set to comparative C_t ($\Delta\Delta C_t$) in a 5µl reaction volume.

cDNA from three participants, and three calibrator samples, were plated along with a no-template control (NTC), onto each 384-well plate.

The reaction mix was prepared in 96-well plates using the volumes described in Table 4, before being mixed well, centrifuged, and carefully dispensed in triplicate into MicroAmp® Optical 384-Well Reaction Plates, then centrifuged again to ensure the liquid fully covered the bottom of each well.

Component	Per well (96w plate)	Per well (384w plate)
2X TaqMan® Universal PCR Master Mix	7.75µl	2.5µl
TaqMan® assay	0.78µl	0.25µl
cDNA	1.55µl	0.5µl
Nuclease-free water	5.43µl	1.75µl

Table 4: *Composition of qPCR reaction mix*

cDNA was denatured as the reaction mix (containing cDNA, master mix, TaqMan® assay and nuclease-free water) was heated to 95°C. The TaqMan® Universal PCR Master Mix (Thermo Fisher Scientific: 404437) includes AmpliTaq Gold® DNA Polymerase, Uracil-DNA Glycosylase (UNG), dNTPs, primers and optimised buffer components. The temperature was reduced to 60°C during the annealing step, where the sequence-specific TaqMan® probes hybridise to the target DNA sequence between two primers, and elongation takes place. TaqMan® probes rely on fluorescence resonance energy transfer (FRET) to emit a signal, with a reporter fluorophore attached to the 5’ end and a ‘quencher’ at

the 3’ end. While in close proximity, energy from the reporter is received by the quencher, thereby preventing the emission of a detectable signal. When Taq polymerase catalyses DNA extension in the elongation phase, the 5’-3’ exonuclease activity of the polymerase cleaves the reporter dye from the probe, releasing it from the suppressive effect of the quencher, allowing the fluorescent signal to be emitted, and the initial quantity of cDNA to be detected and quantified[204]. Denaturation and annealing phases were repeated for 40 cycles, before a threshold cycle (C_t) value, a measure of relative concentration of the target sequence, was ascertained.

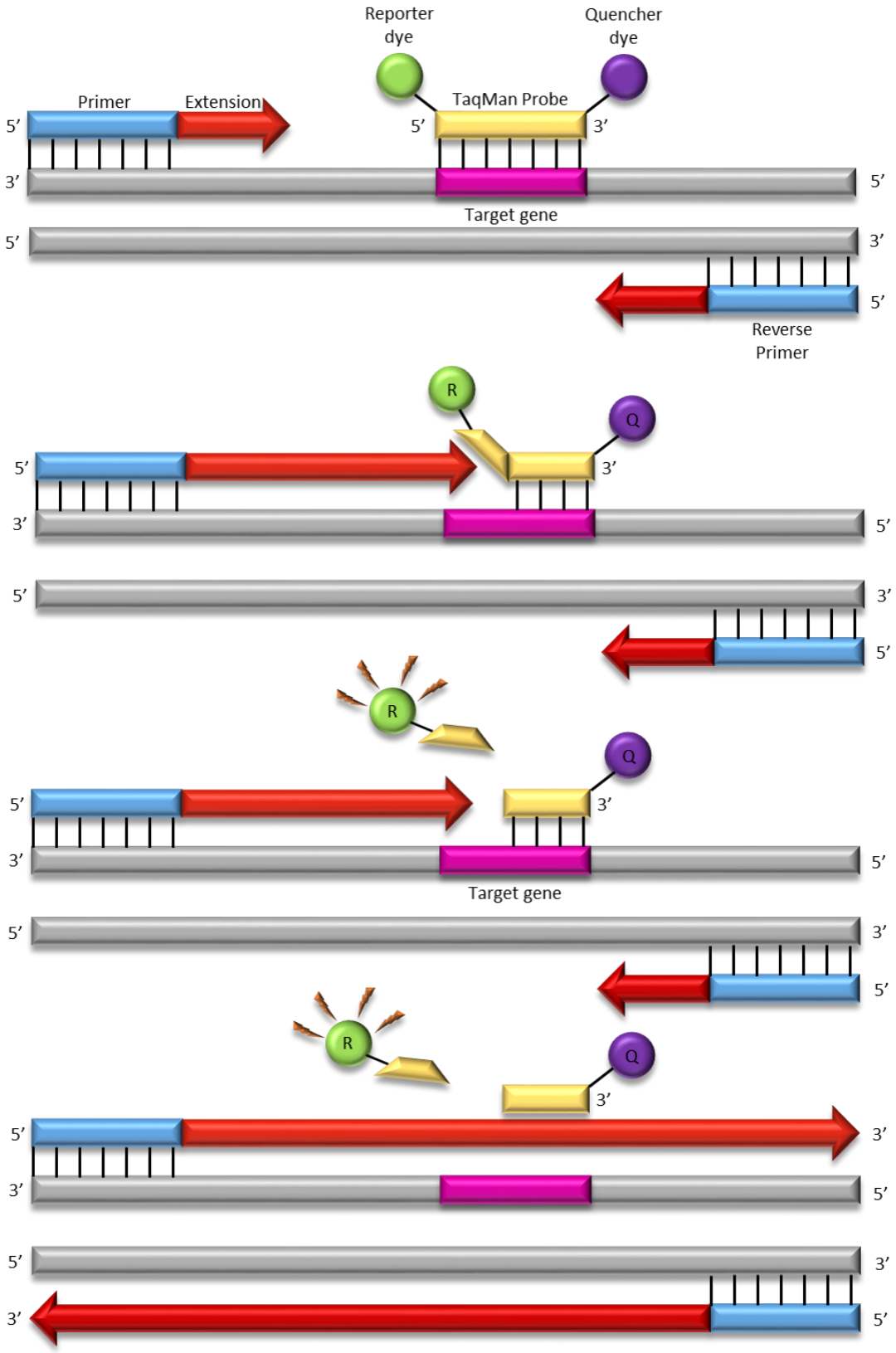

Figure 10: *qPCR amplification of cDNA with FRET signalling.* TaqMan probes bind to the denatured (single-stranded) cDNA template in a sequence-specific manner. Elongation, facilitated by Taq Polymerase, occurs between two primers and its 5'-3' exonuclease activity cleaves the reporter (R) from the quencher (Q), allowing a fluorescent signal to be emitted[205].

In accordance with the Applied Biosystems® TaqMan® Universal PCR Master Mix User Guide[206], the following thermocycler programme (shown in Table 5) was used:

Parameter	UNG incubation	Polymerase activation	PCR (40 cycles)	
	Hold	Hold	Denature	Anneal/extend
Temperature	50°C	95°C	95°C	60°C
Time (mm:ss)	02:00	10:00	00:15	01:00

Table 5: *qPCR run method*

qPCR output data is presented as relative fluorescence against a cycle number, allowing the amplification to be visualised over the course of the cycles. If exponential amplification is observed in an early cycle, the starting material is more abundant than if it was observed in a later cycle. The resulting amplification graph shows a baseline level of fluorescence which is regarded as background signal. Upon completion of all 40 cycles, the QuantStudio 12K Flex software determines a threshold, defining the point at which the signal becomes statistically significant and can be credited to DNA amplification. The point at which the signal curve crosses this threshold is known as the threshold cycle (C_t), and was used to quantify the cDNA of the gene of interest relative to a housekeeping gene[204]. The obtained C_t value is inversely related to the quantity of cDNA in the reaction mix, as a larger quantity of cDNA will reach the 'threshold' at an earlier cycle.

2.4.5 *Enzyme-linked immunosorbent assay (ELISA)*

Multiple sandwich ELISA kits (Table 6) were used to characterise differentiated macrophages based on their secretory products. Individual protocols varied slightly, but broadly assays were performed as follows: high binding capacity flat bottom polystyrene 96-well ELISA microplate wells were coated with capture antibody solution directed toward the protein of interest (human IL-1α, IL-6, IL-10, TNF-α, TGF-β1 or oxidised low-density lipoprotein receptor-1 (OLR-1), kits as detailed in Table 6), sealed and incubated at 4°C overnight (as shown in Figure 11). Wells were washed 3 times with 200 µl phosphate-buffered saline (PBS) 0.05% Tween-20 wash buffer, allowing approximately one minute for soaking between washes. An ELISA plate washer was not available, so all washing and aspiration steps were performed using a P200 8-channel pipette. Wells were blocked with 200 µl sample diluent solution for one hour at room temperature with shaking, then aspirated and washed once with wash buffer. Serial dilution of standards was carried out in duplicate in accordance with each individual kit protocol, and cell culture supernatant samples were added to wells (undiluted in assays measuring IL-6, IL-10, TNF-α, with dilution factor of 2 in IL-1 and OLR-1 assays, and with dilution factor 1.4 for TGF-β) in triplicate. Duplicate blank wells were filled with 100 µl sample diluent. Plates were incubated at room temperature for two hours with shaking, antigen sample aspirated, and washed 3 times with 200 µl wash buffer with soaking. 100 µl of biotin-conjugated detection antibody (diluted according to kit protocol) was added to each well and plates incubated for one hour at room temperature with shaking. Wells were aspirated and washed three times before 100 µl horseradish peroxidase (HRP) enzyme-conjugated streptavidin solution was added, then incubated with shaking at room temperature for 30 minutes. Wells were aspirated and washed five times, and

100 µl tetramethylbenzidine (TMB) substrate solution added. After 15 minutes incubation at room temperature (with shaking), 50 µl of stop solution (1M H_3PO_4) was added to inactivate HRP and halt colour development. Plates were measured at 450nm with corresponding reference wavelength (570nm for IL-6, IL-10, TGF-β1 and TNF-α, 550nm for OLR-1 and 620nm for IL-1α assays) using a PHERAstar FS microplate reader.

Target	Sensitivity	Standard curve range	Dilution factor	Detection wavelength	Source
IL-1α	1.6 pg/ml	1.6-100 pg/ml	2	450 nm	Invitrogen BMS243-2
IL-6	2 pg/ml	2-200 pg/ml	None	450 nm	Invitrogen 88-7066
IL-10	2 pg/ml	2-300 pg/ml	None	450 nm	Invitrogen 88-7106
TNF-α	4 pg/ml	4-500 pg/ml	None	450 nm	Invitrogen 88-7346
TGF-β1	8 pg/ml	8-1000 pg/ml	1.4	450 nm	Invitrogen 88-8350
OLR-1	2 pg/ml	2-500 pg/ml	2	450 nm	ThermoScientific EHOLR1

Table 6: *Parameters of commercial ELISA kits*

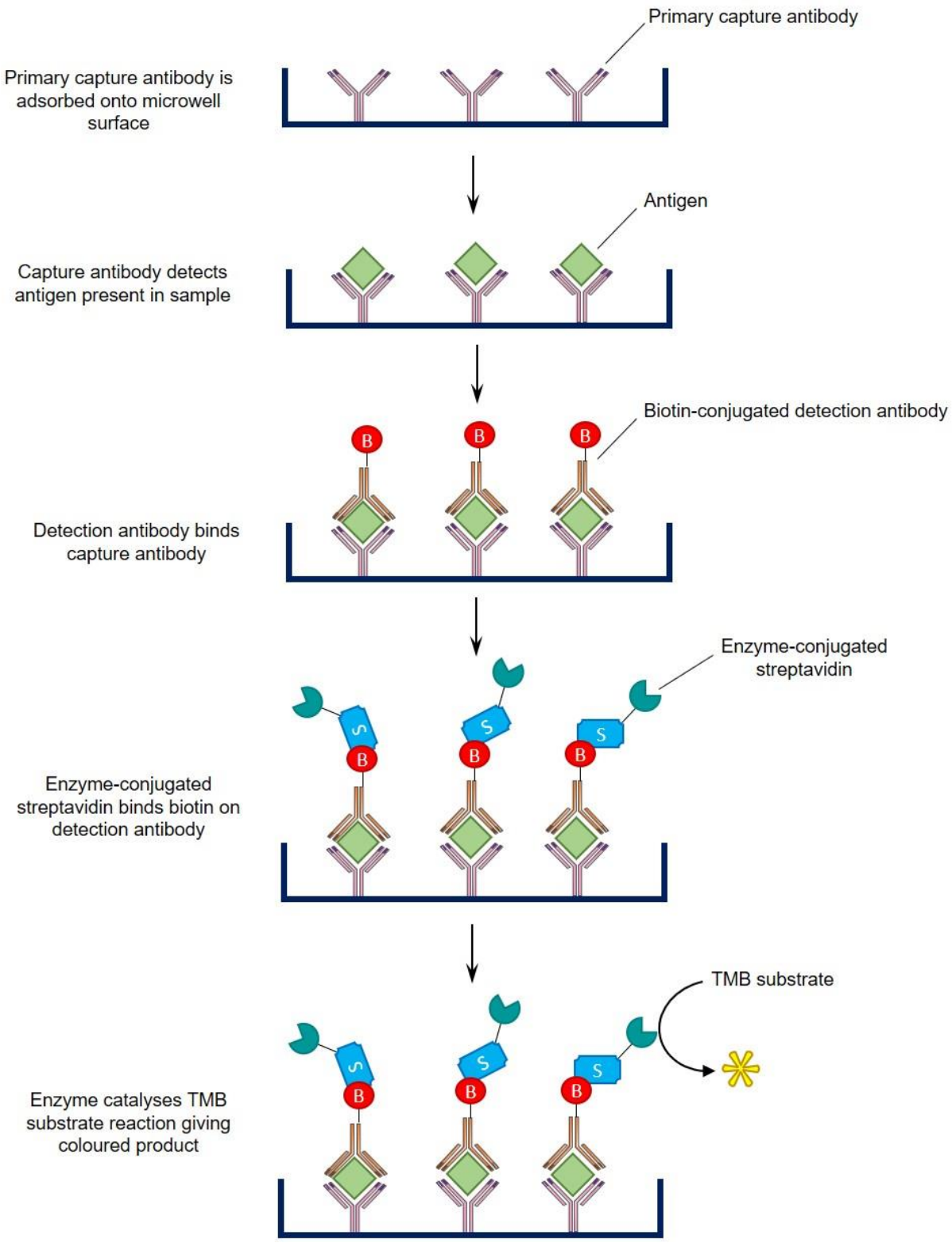

Figure 11: *Biotin-streptavidin sandwich ELISA*. Briefly, the sample antigen binds a capture antibody on surface of microplate wells. A biotin-conjugated detection antibody also binds the antigen, allowing HRP-conjugated streptavidin to bind. When TMB substrate is added, HRP catalyses the formation of a measurable coloured product.

2.5 Expression analysis

2.5.1 *qRT-PCR plate calibrators*

More than one 384-well plate was required per gene for AT-derived cDNA when analysing gene expression. It was therefore necessary to account for any variation between individual plates, i.e. a 'plate effect'. RNA extracted from three untreated AT samples was used to give three plate calibrators, and plated in triplicate as per the experimental samples. The mean and standard deviation (SD) for each set of calibrator triplicates was calculated. Where the SD was ≥0.5 and a single data-point was considered responsible, the outlying value was removed. If the triplicate data-points were spread and a specific outlier could not be identified, no values were removed. These triplicate means were then averaged to give an overall 'calibrator mean' for each plate, allowing for the correction of inter-plate variation using the first plate ('plate A') as reference. Calibrator means for subsequent plates were divided by the calibrator mean of plate A to give a factorial by which all the C_t values for the given plate were divided.

2.5.2 *Quality control*

Microsoft Excel 2013 was used to evaluate the quality and consistency of the raw data. Before any analysis was performed, some data points were removed where AT samples had been eliminated at an earlier stage of processing, e.g. RNA pellet lost during extraction, or RNA concentration was too low to perform RT, and a final concentration of 30ng/µl was not possible within the volume limitations described in Table 3. The standard deviation of corrected C_t values within each triplicate was calculated, and where this exceeded 0.5, triplicates were reviewed.

As before, any single data point deemed responsible for a high standard deviation, was considered an outlier and removed from further calculations. The 'no-template control' (NTC) wells were expected to give an 'undetermined' reading as they contained no genetic material to be amplified. For all experimental genes, no signal was detected in these wells.

2.5.3 ***Housekeeping gene selection***

Housekeeping genes encode proteins required in all cells for basic function and metabolism, therefore they are constitutively active in tissues throughout the body. Such reference genes are used to give meaning to the level of expression of a GOI within a cell as they allow for data to be normalised, and expressed in relative terms, i.e. as a fold increase or decrease[207]. Examples of commonly used housekeeping genes include polyubiquitin C (*UBC*), 18S, glyceraldehyde 3-phosphate dehydrogenase (*GAPDH*), peptidyl-prolyl cis-trans isomerase A (*PPIA*) and TATA-box binding protein (*TBP*).

Polyubiquitin C is an essential source of ubiquitin – a protein which plays an important role in targeting other proteins for degradation[208]. *18S* ribosomal RNA is highly conserved and expressed across many different tissues as it contributes to the small ribosomal subunit, making it essential for protein synthesis and eukaryotic cell function[209]. *GAPDH* is frequently used as a reference gene because it encodes the essential GAPDH enzyme for glycolysis, allowing cells to utilise glucose as an energy source. PPIA is a zinc-dependent DNA binding protein[210] which contributes to the isomerisation of peptide bonds and protein folding in macrophages[211]. TBP is a subunit of a transcription factor active in the

synthesis of RNA polymerase I, II and III. This means that TBP is required before any transcription can take place[212], and so must be active in all active eukaryotic cells.

2.5.1 *Housekeeping gene validation*

Housekeeping genes *18S*, *PPIA*, *TBP* and *UBC* were used as appropriate internal controls for AT-derived cDNA[213–215], and were used to normalise for inconsistencies in quantity of RNA that was reverse transcribed, providing an endogenous reference value in order to determine relative gene expression. C_t value means (corrected for plate variation as detailed in 2.5.1) were initially plotted to give an indication of stability, and appeared relatively consistent across the different experimental conditions. It was essential to also mathematically validate the suitability of the housekeeping genes. This validation of housekeeper stability was performed using the comparative $2^{-\Delta\Delta Ct}$ method[216,217] (detailed below) to identify any significant changes in expression.

2.5.1 *Comparative $2^{-\Delta\Delta Ct}$ method*

The comparative ΔΔCt method[217] was used to quantify changes in gene expression relative to the untreated control condition, with results presented as 'relative expression' (arbitrary units) or as a 'fold change'. The calculations rely on the exponential nature of amplification by PCR and the assumed 100% efficiency of TaqMan® probes. The housekeeper geomean was subtracted from each C_t mean (calculated from triplicate values) to give the ΔC_t. A separate calibrator value for each gene was calculated as the mean of the untreated control samples, i.e. no insulin, no macrophages, across all participants. The

$\Delta\Delta C_t$ was obtained by subtracting the $\Delta Ct_{calibrator}$ from the ΔCt_{sample}. To obtain the fold-change, $2^{(-\Delta\Delta Ct)}$ was calculated. The mean of the $2^{(-\Delta\Delta Ct)}$ values for the two culture wells (see Figure 8 for co-culture layout) was then plotted with the standard deviation.

2.5.2 *ELISA analysis*

The concentration of macrophage-secreted proteins was determined by constructing a standard curve of known concentrations plotted against their respective absorbance (OD). Where instructed, measurements obtained at the reference wavelength (OD_{ref}) were subtracted from values at the detection wavelength ($OD_{detection}$) to give Absorbance (ΔOD_{ref}) for each standard, for which the mean and coefficient of variation (%CV) of technical duplicates was calculated. Where CV exceeded 20%, data points were carefully considered, and removed from the standard curve if necessary. It was acknowledged that removal of data points from the upper and lower bounds of the standard curve impacted the assay detection range. All standard curves contained a minimum of six data points and had an r^2 value between 1 and 0.9956.

The quality of experimental sample data was similarly assessed using Microsoft Excel 2016. Absorbance(ΔOD_{ref}) was obtained, and %CV of technical triplicates calculated. In the majority of assays, some %CV values exceeded 20. This was determined to be largely caused by single outliers, rather than a wide spread of data points. Subsequently, the median was calculated, and interpolated into the equation of the standard curve to calculate the analyte concentration. For assays where samples were diluted, the concentration was multiplied by the dilution

factor. In some samples the calculated concentration fell below the assay detection range, and the analyte was determined to be ‘not detected’. Although it was not possible to determine complete absence of the target protein, these values were corrected to ‘0’ for the purposes of data analysis and graphical presentation.

Protein levels were represented relative to the undifferentiated control cells within each independent experiment, in order to show the effect of differentiation on cytokine secretion. Data points were plotted with mean and standard deviation.

2.5.3 *Statistical analysis*

‘Column statistics’ testing was performed using GraphPad Prism 5 software to determine if data was normally distributed, and therefore the type of statistical test required. All data failed D’Agostino and Pearson omnibus and Shapiro-Wilk normality testing due to small sample size, with only some passing the Kolmogorov-Smirnov test. With at least two out of three normality tests failed, Gaussian distribution was not assumed, and non-parametric tests were selected for all statistical analyses.

2.5.4 *One-way ANOVA (Friedman non-parametric test)*

One-way non-parametric ANOVA (Friedman test) is a statistical technique used to determine whether there is a statistically significant difference between the means of three or more independent groups. The ANOVA alone is not able to determine where the difference occurs, so a post-hoc test is necessary. Dunn’s multiple comparison test was used to specify which means are different from each

other. This test is used when data does not conform to a traditional Gaussian distribution.

2.5.5 *Repeated measures two-way ANOVA*

The non-parametric repeated measures (mixed model) ANOVA (two-way), with Bonferroni multiple comparisons post-hoc test, was used to detect the differences in means within a group. The effect of insulin concentration was assessed by comparing 1nM, 10nM and 100nM concentrations to the 0nM control within each macrophage subtype group. Two-way ANOVA also allows for all the data to be presented at once, giving a broader understanding of the effect of the different experimental conditions in the context of each other.

2.5.6 *Kruskal Wallis test*

A Kruskal Wallis non-parametric test was utilised to analyse data obtained by ELISA as normality tests were not passed. Where a significant difference was found between the four means, Dunn's multiple comparisons post-hoc test was used to pinpoint where means differed significantly from the control (undifferentiated THP-1 condition).

Chapter 3: Quantification of macrophage differentiation

3.1 Introduction

In order to accurately interpret results from the macrophage-AT co-culture experiment, it was necessary to validate the differentiation of THP-1 monocytes into M1, M2a and M2c macrophage subtypes.

THP-1 monocytes were differentiated in culture (detailed in 2.3.1) into M (IFNγ + LPS), M (IL-4) and M (IL-10) macrophages over 48h to reflect M1, M2a and M2c phenotypes respectively. qRT-PCR (detailed in 2.4.4) was used to measure expression of phenotypic cell surface markers: *CD86*, a marker of M1 macrophages[94], *CD206*, a general marker of M2 phenotype macrophages[94,218], as well as *CD150*[94,167] and *CD163*, both reputed markers of M2c macrophages. Supernatant levels of IL-1α, IL-6, IL-10, OLR-1, TGF- β and TNF-α were measured by ELISA to indicate functional differentiation. Data were analysed using one-way ANOVA (Friedman's test or Kruskal Wallis test) with Dunn's multiple comparisons test.

Results were expected to show M (IFNγ + LPS) cells upregulate *CD86* expression, with little to no change in *CD206*, *CD150* and *CD163* expression[218], and secrete increased IL-1α, OLR-1, IL-6 and TNF-α, thereby suggesting an M1-like phenotype. M (IL-4) cells were expected to upregulate *CD206* and secrete IL-10, while M (IL-10) cells were predicted to upregulate *CD206*, *CD150* and *CD163* while secreting IL-10, and TGF-β, suggesting differentiation into M2a- and M2c-like phenotypes respectively.

3.2 Optimisation

The protocol for macrophage differentiation was based on work by Spencer *et al* (2010)[144]. Optimisation of this protocol was completed by Dr E Pastel over the course of three independent experiments, between which small changes were made. Full details and data from the optimisation process can be found in Appendix 1.

After the final differentiation optimisation experiment, cells were analysed by qRT-PCR to quantify expression of *CD68* (pan-macrophage marker), *CD86* (M1 marker), *CD206* (M2 marker) and *CD150* (M2c marker). All differentiated cells expressed higher levels of *CD68* than did undifferentiated THP-1 monocytes, therefore were considered macrophage-like. Cells treated with IFNγ + LPS were seen to upregulate *CD86*, so were believed to be 'M1-like'. Cells treated with PMA + IL-4 or IL-10 expressed higher levels of *CD206* than did cells treated with IFNγ + LPS, therefore were considered M2-like. None of the differentiated cells increased expression of the M2c marker *CD150*.

Statistical analysis could not be performed on these data as each cell culture experiment was carried out only once, with technical duplicates. A full discussion of the limitations of this optimisation can be found in chapter 6. Although seemingly inconclusive, Dr Pastel considered the optimisation of macrophage differentiation protocols to be complete based on these results (further detailed in Appendix 1).

3.3 Results

Briefly, macrophages differentiated using IFNγ + LPS, IL-4 and IL-10 were analysed by qRT-PCR for expression of phenotypic cell surface markers CD86 (M1 marker), CD206 (M2 marker), CD150 (M2c marker) and CD163 (M2c marker). Post-differentiation cell culture medium was collected and analysed by ELISA to quantify secretion of proteins indicative of macrophage functional polarisation, IL-1α, IL-6, IL-10, OLR-1, TNF-α, and TGF-β.

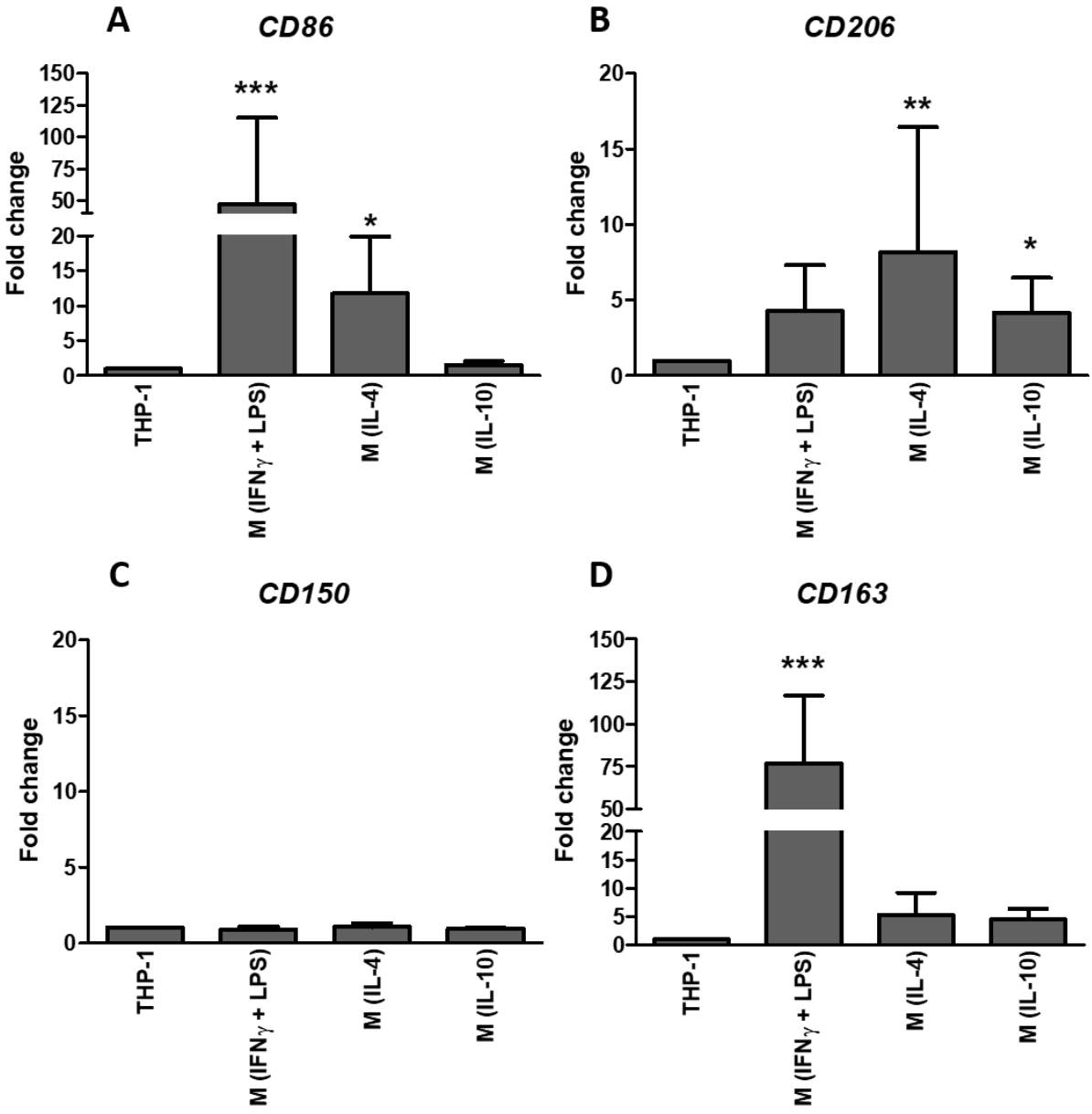

Figure 12: *Relative mRNA expression of macrophage markers in differentiated THP-1 cells.* Markers of macrophage differentiation, A) *CD86*, B) *CD206*, C) *CD150*, and D) *CD163*, in all three differentiated macrophage conditions were compared to undifferentiated THP-1 cells using one-way ANOVA (Friedman's test) with Dunn's multiple comparison post-hoc test (* = $p \leq 0.05$, ** = $p \leq 0.01$, *** = $p \leq 0.001$). Data normalised to undifferentiated THP-1 monocytes. Valued represented as mean fold change ±SD, n=6 independent experiments.

		THP-1			M (IFN + LPS)			M (IL-4)			M (IL-10)		
		Mean fold change	±SD	*p*=	Mean fold change	±SD	*p*=	Mean fold change	±SD	*p*=	Mean fold change	±SD	*p*=
RNA expression	***CD86***	1	0.0	n/a	46.903	68.07	**<0.001**	11.770	8.13	**<0.05**	1.583	0.50	>0.05
	CD206	1	0.0	n/a	4.295	3.04	>0.05	8.167	8.28	**<0.01**	4.157	2.31	**<0.05**
	CD150	1	0.0	n/a	0.869	0.22	>0.05	1.050	0.28	>0.05	0.935	0.11	>0.05
	CD163	1	0.0	n/a	76.944	39.96	**<0.001**	5.253	4.00	>0.05	4.482	1.87	>0.05
Secreted protein	**IL-1α**	1	0.0	n/a	5.243	5.32	**<0.05**	0.902	0.19	>0.05	1.016	1.13	>0.05
	IL-6	1	0.0	n/a	147.449	57.28	**<0.001**	1.000	0.00	>0.05	1.000	0.00	>0.05
	TNF-α	1	0.0	n/a	6.085	7.24	>0.05	1.988	2.75	>0.05	3.115	5.35	>0.05
	OLR-1	1	0.0	n/a	2.111	2.44	>0.05	1.776	2.63	>0.05	2.048	2.50	>0.05
	IL-10	1	0.0	n/a	9.374	13.95	>0.05	11.891	19.22	>0.05	15.698	23.19	>0.05
	TGF-β	1	0.0	n/a	5.466	7.58	>0.05	0.820	0.41	>0.05	2.830	5.44	>0.05

Table 7: *Numerical presentation of quantification of macrophage differentiation*. Relative mRNA expression of macrophage cell surface markers was measured in differentiated macrophages. Protein secretion of cytokines indicative of macrophage functional phenotype was measured by ELISA. Data presented as a mean fold change relative to undifferentiated THP-1 monocytes.

3.3.1 *CD86 expression*

CD86 is expressed on the surface of antigen-presenting cells: it is a co-stimulatory molecule essential for the activation of T-cells in the innate immune response, and a marker of the M1 macrophage phenotype. qRT-PCR was performed on THP-1 differentiated monocytes maintained in culture without AT for a further 48 hours after differentiation. These cells were used as a negative control in the AT-macrophage co-culture experiment. This was followed by statistical analysis by one-way ANOVA with Dunn's multiple comparison post-hoc test, where cells induced to differentiate into M (IFN-γ + LPS), M (IL-4) and M (IL-10) phenotypes were compared with THP-1 cells, the undifferentiated control.

CD86 was shown to be differentially expressed in M (IFN-γ + LPS) cells (Figure 12A) with highly significant mean fold increase of 46.903±68.07 (p≤ 0.001) compared to undifferentiated cells. Although not as highly expressed, there was a significant mean fold increase of 11.77±8.13 of *CD86* in M (IL-4) cells (p≤ 0.05, Figure 12A). M (IL-10) did not significantly upregulate *CD86* (Figure 12A), and fold increase was 1.583±0.49. In comparison to the treated cells, expression of *CD86* in undifferentiated THP-1 cells was extremely low.

3.3.2 *CD206 expression*

The mannose receptor CD206 (MRC1), thought to play an important role in the resolution of inflammation and reduction of pro-inflammatory cytokine release[219], is expressed on the surface of M2 macrophages. Expression of *CD206* in M (IFN-γ + LPS), M (IL-4) and M (IL-10) cells was compared with the untreated THP-1 control (Figure 12B). *CD206* was significantly upregulated in M (IL-4) (p≤0.01) and M (IL-10) (p≤0.05) cells with mean fold changes of 8.167±8.28 and 4.157±2.31 respectively, suggesting effective differentiation towards an M2 phenotype. Although not statistically significant, M (IFN-γ + LPS) cells also exhibited a fold change of 4.29±3.04, suggesting their differentiation may have induced some 'M2-like' characteristics.

3.3.3 *CD150 expression*

CD150 is a cell surface protein expressed by M2c macrophages[220]. It is thought to play an important role in the production of IL-4 from T cells[221], thereby contributing to the resolution of inflammation within AT. Mean fold changes were as follows: M (IFN-γ + LPS) = 0.869±0.22, M (IL-4) = 1.05±0.28, M (IL-10) =

0.935±0.11. None of the differentiation conditions induced significantly increased expression of *CD150* (Figure 12C) compared to undifferentiated THP-1 cells. This result is supported by data from the pilot experiment (see Appendix 1), where no differentiation stimuli upregulated *CD150* expression, and in fact PMA + IL-4 and PMA + IL-10 treatments showed a trend for *CD150* downregulation (Figure 19D). These results suggest that untested changes made to the differentiation protocol during optimisation did not increase *CD150* expression.

3.3.4 ***CD163 expression***

CD163 encodes a scavenger receptor, able to recognise low-density lipoproteins, and is reportedly differentially expressed by M2c macrophages differentiated with IL-10[146]. *CD163* expression in the three differentiation conditions was compared to undifferentiated THP-1 cells. Upregulation of *CD163* by M (IL-4) and M (IL-10) macrophage populations (mean fold changes 5.253±3.99 and 4.482±1.88 respectively) was not significant. Unexpectedly, M (IFNγ + LPS) cells strongly upregulated *CD163* (*p*≤0.001) (Figure 12D*)* with a mean fold change of 76.944±39.96.

The TaqMan assay used to detect *CD163* expression was obtained after the initial differentiation optimisation experiments and the pilot study, therefore it had not previously been possible to determine if expression of *CD163* was high in cells treated with IFNγ + LPS immediately after the 48h differentiation period, or whether expression was induced due to the proceeding 48 hours in culture medium. To answer this question, additional qRT-PCR was performed on cells from the second optimisation experiment (detailed in section 7.1.1) to quantify the

expression of *CD163* both immediately after differentiation and after the additional 48h in culture. In this experiment, several changes had been implemented, including increasing THP-1 cell seeding density from $1x10^6$ to $2x10^6$ cells per well, and increasing the differentiation period from 24h to 48h.

3.3.5 *CD163 expression: second optimisation test*

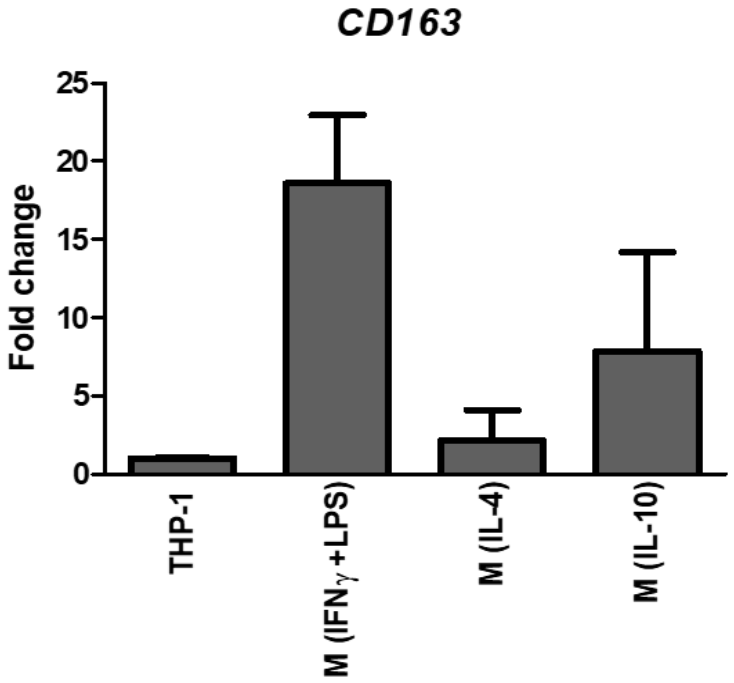

Figure 13: *Relative expression of CD163 in cells from second optimisation test.* Expression of M2c marker *CD163* was measured in undifferentiated THP-1 monocytes, M (IFNγ + LPS), M (IL-4) and M (IL-10) macrophages and analysed using one-way ANOVA followed by Dunn's multiple comparisons post-hoc test. Error bars show mean ±SD, *n*=2 technical replicates.

CD163 (Figure 13) expression was increased in M (IFNγ + LPS) cells from the second differentiation optimisation test (detailed in 7.1.1) when compared to the

undifferentiated control. Mean fold changes were 18.589±4.37, 2.137±1.95 and 7.844±6.35 in M (IFNγ + LPS), M (IL-4) and M (IL-10) populations respectively. Significance could not be calculated as results were based on a single experiment, with technical replicates of two. Although *CD163* expression was more than four times higher after an additional 48h in culture medium (Figure 12D), this result demonstrates that high expression of *CD163* was likely as a direct result of exposure to differentiation stimuli, and cannot be attributed to trans-differentiation[154] of M (IFNγ + LPS) macrophages towards an M2c-like phenotype after the removal of differentiation stimuli. As cell surface marker analysis does not accurately define macrophage function, further techniques were employed to investigate cell differentiation.

3.3.6 ***Secretory profile analysis***

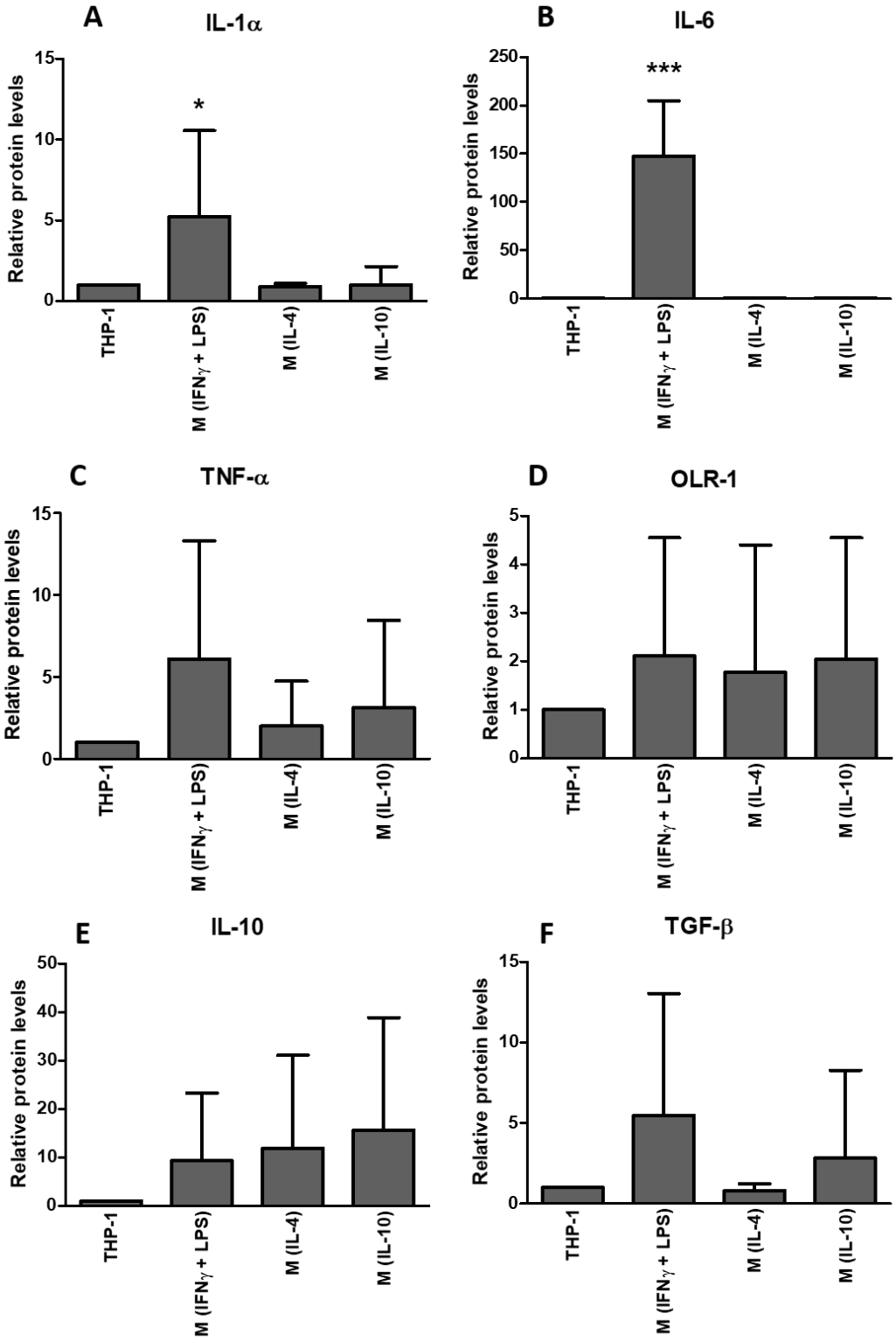

Figure 14: *Relative protein secretion from differentiated macrophages*. Protein secreted by M (IFNγ + LPS), M (IL-4), M (IL-10) and undifferentiated THP-1 cells were analysed by ELISA. Results were normalised and compared to

undifferentiated THP-1 monocytes using Kruskal Wallis with Dunn's multiple comparison test, * = $p<0.05$, ** = $p<0.01$, *** = $p<0.001$. Data represented as mean relative protein levels compared to THP-1 ±SD, *n*=6 independent experiments, except IL-10 where *n*=3.

3.3.7 *IL-1α secretion*

IL-1 is a cytokine with pro-inflammatory activity, and is secreted by M1 macrophages[94]. Cell culture supernatants from differentiated macrophages cultured in the absence of OMAT were analysed by ELISA to assess their secretory profile, giving a more accurate indication of their functional characteristics. IL-1α secretion (Figure 14A) was significantly increased ($p>0.05$) in cells, suggesting macrophages may possess a pro-inflammatory functional phenotype. IL-1α secretion was not increased by differentiation with IL-4 and IL-10, indicating that a pro-inflammatory phenotype was not induced in these cells. Mean fold changes ±SD are detailed in Table 7.

3.3.8 *IL-6 secretion*

M1, but not M2a or M2c macrophages, are characterised by IL-6 secretion[94]. Secreted levels of IL-6 (Figure 14B) were significantly ($p<0.001$) increased by differentiation using IFNγ + LPS, suggesting polarisation of M (IFNγ + LPS) cells to an M1-like phenotype. This upregulation was not observed in M (IL-4) or M (IL-10) macrophages, suggesting these cells do not possess a pro-inflammatory M1-like phenotype.

3.3.9 *TNF-α secretion*

M1 macrophages are a major source of secreted pro-inflammatory TNF-α[94,222]. Secreted TNF-α levels were not significantly increased by any of the differentiation conditions (Figure 14C), however on average cells treated with IFNγ + LPS secreted higher levels of the cytokine than M (IL-4) or M (IL-10) macrophages.

3.3.10 *OLR-1 secretion*

Oxidised low-density lipoprotein receptor 1 (OLR-1), also known as LOX-1, is a type II membrane glycoprotein receptor for oxidised low-density lipoprotein (Ox-LDL). OLR-1 is reportedly upregulated by THP-1 macrophages in response to LPS, TNFα and TGF-β stimuli[223–225]. The receptor is secreted in soluble form[226], and therefore was predicted to be differentially elevated in cell culture supernatant from M (IFNγ + LPS) macrophages. ELISA analysis (Figure 14D) showed OLR-1 secretion was not significantly modulated by differentiation into M (IFNγ + LPS), M (IL-4) or M (IL-10) macrophage phenotypes.

3.3.11 *IL-10 secretion*

Secretion of anti-inflammatory IL-10 (Figure 14E) is indicative of M2a and M2c macrophage phenotypes[94]. IL-10 secretion was not significantly increased by M (IL-10) or M (IL-4) macrophages, however the mean protein level was higher in these conditions than M (IFNγ + LPS).

3.3.12 *TGF-β secretion*

Production and secretion of pro-fibrotic TGF-β is characteristic of M2c macrophages[94], and therefore secretion was expected to be highest in M (IL-10) cells. Secreted TGF-β levels were not significantly upregulated by any means of macrophage differentiation, however did appear to be increased to some degree in M (IFNγ + LPS) and M (IL-10) cell culture.

3.4 Discussion

After differentiation and quantification of marker expression at the RNA level, M (IFNγ + LPS) macrophages were expected to strongly upregulate *CD86*, with little upregulation of M2 markers *CD206*, *CD150* and *CD163* compared to the undifferentiated THP-1 control. M (IL-4) macrophages were expected to show low *CD86*, *CD150* and *CD163* expression, in addition to distinct upregulation of the pan-M2 marker *CD206*. M (IL-10) macrophages were predicted to exhibit low *CD86* expression, with upregulated *CD206*, *CD150* and *CD163*.

This was supported by the findings that M (IFNγ + LPS) cells significantly upregulated *CD86* and secreted high levels of IL-1α and IL-6, and M (IL-4) and M (IL-10) macrophages upregulated *CD206*. However, high expression of *CD163* and elevated secretion of TGF-β from M (IFNγ + LPS) macrophages, and a lack of differential expression of *CD150* in differentiated subpopulations was not the anticipated result, although not altogether surprising based on initial optimisation data (appendix 1). These data establish that further work is needed to fully elucidate the complex cocktail of cytokines and specific cell culture conditions required for effective *in vitro* macrophage polarisation.

3.4.1 ***THP-1 monocytes retain a relatively 'undifferentiated' phenotype***

As anticipated, undifferentiated THP-1 monocytes showed comparatively low mRNA expression of *CD86*, *CD206* and *CD163* markers after 96 hours in culture medium. Low expression of *CD163* in undifferentiated THP-1 monocytes was in line with the findings of Ritter *et al* (1999), who report that unstimulated THP-1

monocytes do not express *CD163* at a significant level[227]. Secretion of IL-1α, TNF-α and IL-6 also remained comparatively low, corroborating previous work by Genin *et al*[228] and suggesting cells maintained an undifferentiated monocyte phenotype.

3.4.2 *IFNγ + LPS induces a mixed macrophage phenotype*

In line with expectations, treatment of THP-1 monocytes with IFNγ and LPS resulted in an approximate mean 8-fold significant ($p<0.001$) upregulation of *CD86* compared to the undifferentiated control, suggesting differentiation into an M1-like phenotype[94]. This is corroborated by the findings of Mia *et al* (2014), who demonstrate stimulation of monocytes with IFNγ + LPS is highly effective for the induction of cell surface CD86 expression[229]. Secretion of IL-1α and IL-6 was also differentially and significantly increased by M (IFNγ + LPS) as expected[230,231], suggesting cells were behaving in a functionally pro-inflammatory manner. Pro-inflammatory TNF-α secretion was expected to be significantly increased by M (IFNγ + LPS) cells. While there was a mean six-fold increase, large variability of data across independent experiments meant this was not statically significant. It must be noted that poor reproducibility and large standard deviations for all the data presented in this chapter limits the definitive characterisation of these cells. Possible reasons for this are explored in depth in Chapter 6.

M (IFNγ + LPS) macrophages did not significantly upregulate *CD206* when compared to the untreated control, likely due to high variability in the data, however there was almost a three-fold mean increase, suggesting some M2-like characteristics. This differs from the findings of Mia *et al* (2014), whose treatment

of human peripheral blood mononuclear cells (PBMCs) with IFNγ and LPS did not increase cell surface CD206 expression, as detected by fluorescence-activated cell sorting (FACS)[229]. In addition to using a different cell type, the differentiation period in their study was only 24h[229], and therefore may not have been sufficient to see increased protein expression on the cell surface. In our study however, 48h of exposure to IFNγ and LPS did result in upregulation of *CD206* mRNA, although it is not possible to determine if the protein level was also increased.

Expression of the M2c marker *CD150* was, as expected, not upregulated in THP-1 monocytes in response to IFNγ + LPS stimulation. Surprisingly, expression of M2c marker *CD163* was increased suggesting a more M2c-like phenotype, which is supported by a non-significant 5.5-fold increase in TGF-β secretion (also demonstrated by Redzic et al (2013)[232]. These data are in sharp contrast to Ritter *et al* (1999), who report that IFNγ-induced stimulation of macrophages, derived from freshly isolated human PBMCs, suppressed *CD163* transcription and cell surface expression, and that LPS-treated monocytes exhibited significantly downregulated expression of *CD163* at the mRNA and protein level[227]. There are some small but important differences in the methodology used by Ritter *et al*, which may, at least partly, explain this difference: when cells were cultured in the absence of serum, an LPS concentration of 1µg/ml was required to stimulate significant downregulation of *CD163*[227]. In contrast, our study used only 10ng/ml LPS in a serum free culture medium. Ritter *et al* also claim that IFNγ suppressed the transcription of *CD163* mRNA when supplied at 10ng/ml, however our data do not support this, as when IFNγ was provided at 20ng/ml, *CD163* was still increased. No information is provided by Ritter *et al* regarding the duration of

exposure to differentiation stimuli. Crucially, monocytes used by Ritter *et al* were freshly isolated from human volunteers, meaning they may respond differently to *in vitro* exposure to differentiation stimuli than the immortalised, leukaemia-derived THP-1 cell line. Further to this, they report that THP-1 monocytes, differentiated into macrophages using only PMA, did not express *CD163* at significant levels.

It was speculated in section 3.3.4, during the additional 48h in culture medium after the differentiation period, in the absence of AT-derived signals or differentiation stimuli, M (IFNγ + LPS) cells may have undergone some transdifferentiation towards a more M2c-like phenotype, thereby resulting in the upregulation of *CD163.* If this were the case, it is possible that at the point of the co-culture setup, M (IFNγ + LPS) cells may have possessed a more traditionally M1-like phenotype, with limited expression of 'M2' markers. To address this, qPCR was performed on macrophages collected immediately after the second differentiation optimisation experiment (see appendix 1), performed by Dr Pastel, in order to measure *CD163* expression. The transdifferentiation theory was consequently disproved, as results revealed a similar pattern of *CD163* expression immediately after 48 hour exposure to differentiation stimuli. This suggests that M (IFNγ+ LPS) cells possessed a mixed M1/M2 phenotype immediately after differentiation and at the beginning of the co-culture period.

Chanput *et al* (2013) treated THP-1 monocytes with 20ng/ml IFNγ and 1μg/ml LPS, and reported increased markers of an M2 phenotype, including *IL10* mRNA and secreted protein, in M1 macrophages[225]. In our study M (IFNγ + LPS) macrophages appeared M1-like with regards to *CD86* expression but secreted

relatively similar levels of IL-10 to M (IL-4) and M (IL-10) macrophages, and slightly enhanced levels of TGF-β. Although neither were significantly increased compared to the control, this may suggest that M (IFNγ + LPS) macrophages possess some M2-like characteristics. Chanput *et al* also propose OLR-1 as a 'new M1 gene', however in our analysis its secretion was not significantly upregulated in response to differentiation stimuli. This may be because they measured OLR-1 mRNA 6h, which may not correspond with an accumulation of secreted protein at the 48h timepoint[225].

Genin *et al* (2015) reported an upregulation of secreted M2 marker chemokine (C-C motif) ligand 18 (CCL18) after differentiation using 10ng/ml LPS and 20ng/ml IFNγ. This effect was not observed when LPS was used at a lower concentration of 10pg/ml, therefore they conclude that high concentrations of LPS induce unspecific expression of M2 markers in pro-inflammatory M1 macrophages. Neither paper specifically reports a change in *CD163* expression in THP-1 cells after treatment with IFNγ and LPS, but taken together their data suggest that using a lower concentration of LPS in the THP-1 differentiation protocol may induce a more definitive M1 macrophage phenotype, without upregulation of M2 markers.

Polarised macrophages resist categorisation into discrete groups, as M1 and M2 represent extremes of macrophage activation, where most cells fall somewhere between the two phenotypes. Spencer *et al* (2010) report a mixed M1/M2 phenotype in around 60% of *in vivo* non-CLS ATMs in lean human subjects, which stained positive for CD86 and CD206 via immunofluorescence[144]. Zeyda *et al* (2007) also show that despite characterising AT macrophages as M2-like

according to their expression of cell surface markers, cells were still capable of producing pro-inflammatory cytokines[157]. Considering this, the apparent mixed M1/M2 phenotype of M (IFNγ + LPS) cells may represent the observed mixed phenotypes of AT macrophages *in vivo*.

3.4.3 *M (IL-4) macrophages significantly upregulate CD206*

M (IL-4) macrophages significantly upregulated expression of *CD86* compared with the undifferentiated control, although the expression of *CD86* was 3.5-fold higher for cells treated with IFNγ + LPS. M (IL-4) macrophages upregulated M2 marker *CD206* significantly and the most strongly of all the treated cells (consistent with previous studies[146,231]), with expression 2.7-fold higher than M (IFNγ + LPS) cells and 8-fold higher than THP-1 monocytes, therefore suggesting the expected differentiation to an M2 phenotype. *CD150* (M2c marker) expression was, as anticipated, not upregulated in M (IL-4) macrophages.

CD163 expression, however, was non-significantly upregulated in M (IL-4) macrophages, contrary to the findings of Porcheray *et al* (2005) who determine that IL-4 strongly reduces CD163 on the surface of macrophages[218]. This discrepancy may be attributed to methodological differences: their study utilises primary human monocytes derived from PBMCs, cultured with macrophage-colony stimulating factor (M-CSF) and granulocyte macrophage-colony stimulating factor (GM-CSF) to maintain a 'neutral' environment with respect to *CD206* and *CD163* expression. Mature macrophages were stimulated with a selection of pro- and anti-inflammatory molecules over four days, at 10ng/ml[218]. Although more convenient for use in *in vitro* studies, THP-1 monocytes may not

respond precisely the same way to pro- and anti-inflammatory stimuli as endogenous monocytes. Obtaining and isolating PBMCs from human subjects is a laborious, time-intensive process, but cells are likely to more accurately represent the behaviour of ATMs *in vivo*. No *in vitro* biological model is perfect, but in the absence of monetary or practical limitations, the 'gold standard' experiment would involve the use of patient-matched PBMCs and OMAT, preferably from a cohort of healthy-BMI individuals.

The differentiation protocol used by Porcheray *et al* (2005) may also recreate the *in vivo* differentiation process more accurately as cells were first slowly matured into macrophages, before being exposed to polarising pro- and anti-inflammatory molecules over a longer period of time[218]. Flow cytometric analysis, as opposed to qRT-PCR, quantified cell surface CD206 and CD163. Due to the transient nature of mRNA transcripts and the opportunity for post-transcriptional modifications, quantification methods detecting cell surface protein levels may provide a more definitive picture of macrophage phenotype.

ELISA analysis from differentiated macrophages showed secretion of pro-inflammatory cytokines IL-1α, IL-6 and TNF-α from M (IL-4) macrophages was not significantly increased, consistent with the findings of Lolmede *et al* (2009)[231], suggesting cells were not of a functionally pro-inflammatory phenotype. M (IL-4) macrophages as expected did not significantly increase TGF-β secretion[94], but also did not increase IL-10 secretion[94]. This outcome is not traditionally expected, but has been shown in previous studies[228,231]. A limited consensus on how to identify M2a macrophages means that their characterisation is often defined relative to M1 or M2c polarised macrophages[231]. Analysis of M (IL-4)

macrophages showed they appeared to somewhat conform with the expected functional phenotype for M2a-like cells, but their phenotype cannot be precisely defined. As such, these cells will be considered 'broadly M2-like'. Quantification of secreted VEGF or membrane bound CD36 may have aided the accurate classification of an M2a phenotype[231].

3.4.4 *M (IL-10) macrophages do not possess a distinct M2c phenotype*

As predicted, THP-1 monocytes, treated with PMA + IL-10 to induce differentiation to an M2c-like phenotype, did not significantly upregulate M1 marker *CD86.* Equally, secretion of IL-1α and IL-6 was not increased, suggesting cells did not possess a pro-inflammatory phenotype. Although slightly elevated, TNF-α and OLR-1 secretion was not significantly different from THP-1 monocytes. mRNA of the reputed M2c specific marker *CD150*[144] was also not upregulated, and expression of M2c-specific *CD163* was modestly upregulated, but still lower than expression induced in the M (IFNγ + LPS) and M (IL-4) populations, in direct contrast to previous reports[146,218,231].

Porcheray *et al* (2005) demonstrated that in human macrophages (PBMC-derived) IL-10 strongly upregulated cell surface presentation of CD163, but CD206 was unchanged. They report CD163 and CD206 are induced in a mutually exclusive fashion after stimulation with anti-inflammatory molecules[218], implying they represent distinct macrophage populations. This suggests CD206 may be more specific to M2a macrophages, and not the pan-M2 marker as described[94,144,233,234]. Our results support this in part, as although there was

significant upregulation of *CD206* by M (IL-10) cells, there was approximately 1.8–fold higher expression of *CD206* from M (IL-4) macrophages. This implies that studies exploring the link between AT fibrosis and AT macrophages may inadvertently fail to identify the primary fibrosis-inducing M2c macrophages when using only CD206 as a pan-M2 marker. Spencer *et al* (2010) oppose this claimed mutually exclusive expression, and state that *in vivo* CD150-positive ATMs were all also CD206-positive[144].

A strong and significantly increased secretion of TGF-β and IL-10 was expected[94,144,231], but was not shown by M (IL-10) macrophages. Overall, phenotypic analysis suggests limited differentiation into a functional M2c phenotype.

3.5 Summary

In conclusion, the differentiation protocol used in this study produced some of the expected outcomes: M (IFNγ + LPS) cells strongly upregulated M1 marker *CD86* and secreted inflammatory cytokines, M (IL-4) and M (IL-10) cells significantly upregulated *CD206* and *CD163* markers and did not increase inflammatory cytokine secretion. Unexpected strong upregulation of *CD163* and some TGF-β secretion from M (IFNγ + LPS) macrophages suggests these cells possess a distinctly mixed phenotype. No significant, strongly increased secretion of TGF-β or IL-10 from M (IL-10) macrophages suggests an overtly M2c-like phenotype was not induced. Proposed changes to the differentiation protocol are explored in chapter 6.

The THP-1 differentiation protocol, adapted from published methodology[144], was thought to be adequately optimised by Dr Pastel (see appendix 1) before starting these experiments, however phenotypic analysis clearly demonstrates this was not the case, and highlights the critical importance of robust protocol optimisation and validation before beginning key experiments.

Chapter 4: The influence of macrophages on adipose tissue fibrosis

4.1 Introduction

Fibrosis is increasingly recognised as an important factor in the development of AT dysfunction, as it has been hypothesised to limit adipocyte expansion, resulting in the pathogenic deposition of dietary lipids at ectopic sites. AT macrophage numbers are greatly increased in obesity, likely in response to higher rates of adipocyte death[133]. The development of fibrosis in AT is strongly associated with the macrophage infiltration, and is thought to be influenced by their pro-inflammatory (M1) or anti-inflammatory/'wound-healing' (M2) phenotype. M2 macrophages can be further classified to encompass M2a and M2c phenotypes, with M2a macrophages important in the removal of parasites, and M2c macrophages thought to play a major role in ECM deposition and remodelling[94].

Using an *in vitro* model of AT inflammation, this study aimed to confirm that M2 macrophages, and M2c in particular, are the primary cellular mediators of fibrosis, and potently induce upregulation of genes associated with fibrosis (encoding structural ECM components collagens I, III, IV, V, VI, fibronectin and elastin, and regulators of matrix deposition TGF-β, lysyl oxidase and SPARC) in AT.

After initial optimisation of methods (see appendix 1), THP-1 monocytes were treated with LPS + IFN-γ, PMA + IL-4, or PMA + IL-10 for 48 hours to induce differentiation. Polarised macrophages are referred to as M (IFNγ+LPS), M (IL-4)

and M (IL-10), to acknowledge that phenotypic analysis suggested these cells could not be discretely classified as M1, M2a or M2c-like respectively.

These macrophages, along with an undifferentiated control and an AT-only condition, were co-cultured with patient-derived OMAT explants for 48 hours, before qRT-PCR was performed on OMAT samples. TaqMan probes were used for a selection of genes encoding structural ECM proteins (*COL1A1*, *COL3A1, COL4A1, COL5A3, COL6A3, TGFβ1, FN1* and *ELN),* and molecular mediators (*SPARC* and *LOX*) shown to be implicated in the development of AT fibrosis. Friedman's one-way ANOVA with Dunn's multiple comparisons test was used for statistical analysis.

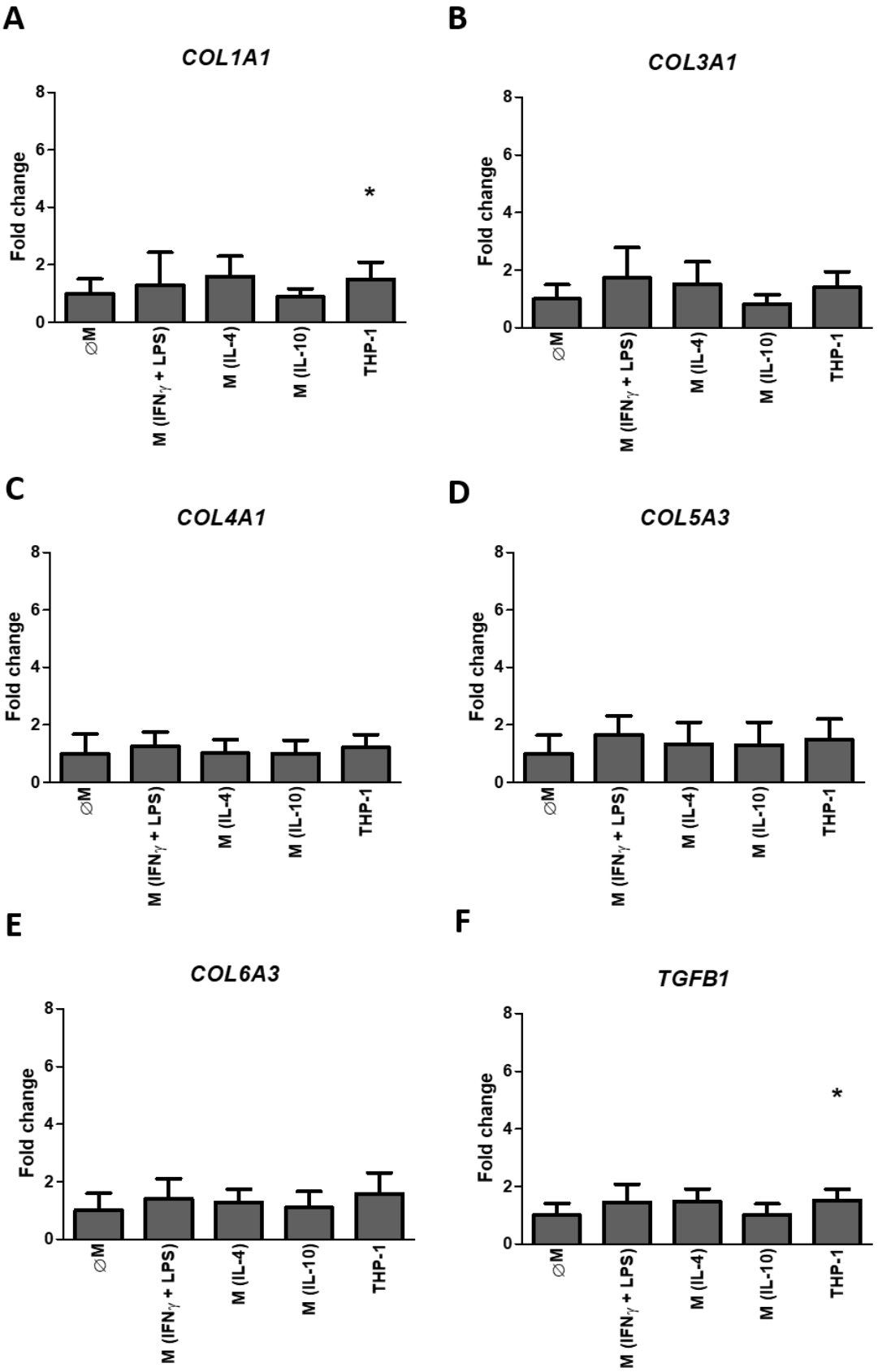
A
COL1A1
Fold change
8
6
4
2
0
*
∅M
M (IFNγ + LPS)
M (IL-4)
M (IL-10)
THP-1
B
COL3A1
Fold change
8
6
4
2
0
∅M
M (IFNγ + LPS)
M (IL-4)
M (IL-10)
THP-1
C
COL4A1
Fold change
8
6
4
2
0
∅M
M (IFNγ + LPS)
M (IL-4)
M (IL-10)
THP-1
D
COL5A3
Fold change
8
6
4
2
0
∅M
M (IFNγ + LPS)
M (IL-4)
M (IL-10)
THP-1
E
COL6A3
Fold change
8
6
4
2
0
∅M
M (IFNγ + LPS)
M (IL-4)
M (IL-10)
THP-1
F
TGFB1
Fold change
8
6
4
2
0
*
∅M
M (IFNγ + LPS)
M (IL-4)
M (IL-10)
THP-1

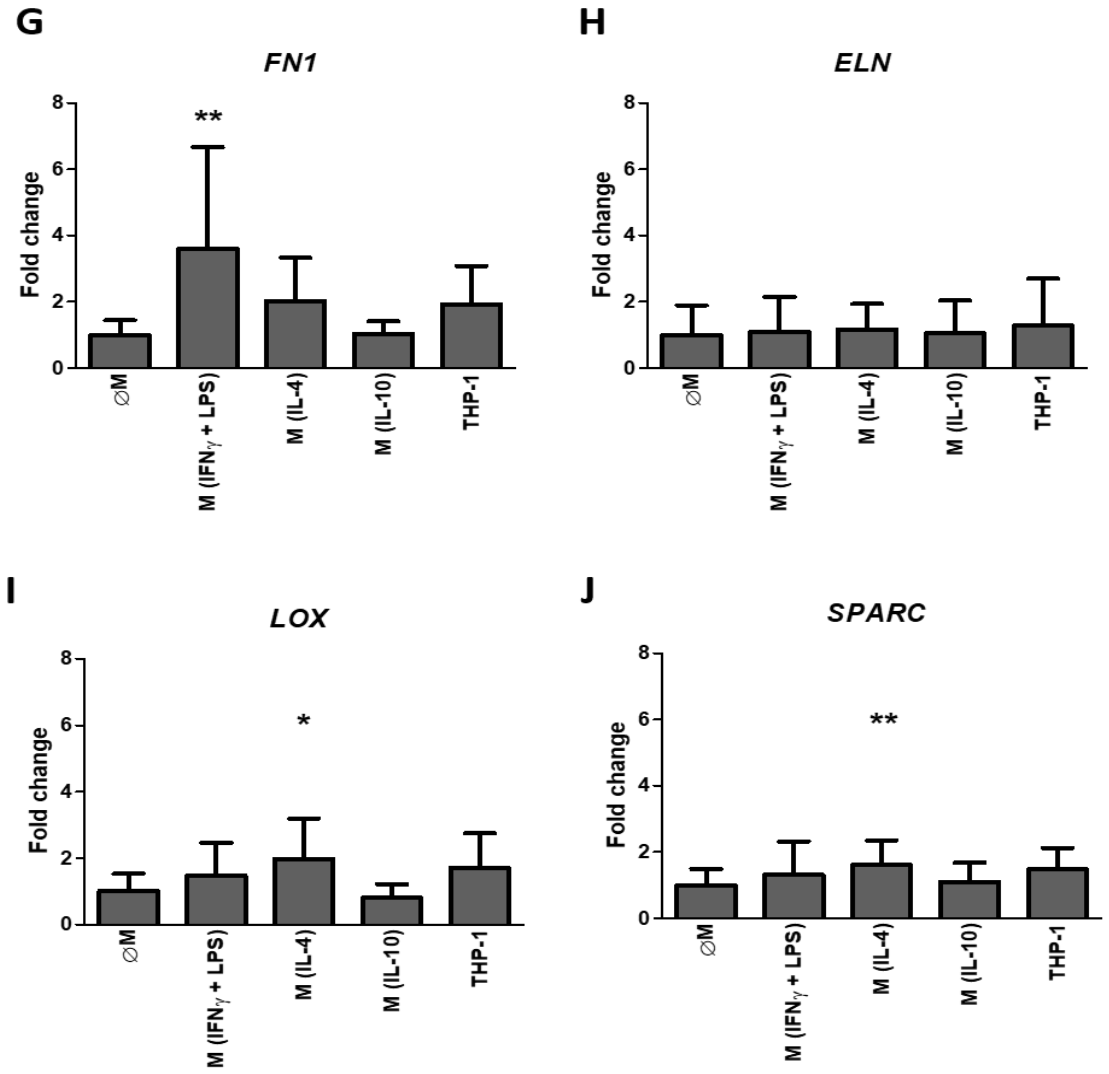

Figure 15: *Relative expression of genes associated with fibrosis in AT after culture alone (ØM), or with M (IFNγ+LPS), M (IL-4), M (IL-10) or THP-1 cells.* THP-1 monocytes were treated with LPS + IFNγ, PMA + IL-4 and PMA + IL-10 to induce differentiation into M (IFNγ+LPS), M (IL-4) and M (IL-10) macrophages respectively over the course of 48 hours, before co-culture with OMAT explants for a further 48 hours. Expression of genes associated with fibrosis was measured in OMAT explants using qRT-PCR relative to the geomean of housekeeping genes *PPIA*, *UBC* and *TBP*. Results were normalised and compared to the ØM (no macrophage) AT control condition (left column) using Friedman's ANOVA followed by Dunn's multiple comparisons test. Data presented as mean fold change ±SD, n=6 independent experiments. (* = p<0.05, ** = p<0.01)

	Ø M			M (IFN + LPS)			M (IL-4)			M (IL-10)			THP-1		
	Mean fold change	±SD	*p=*	Mean fold change	±SD	*p=*	Mean fold change	±SD	*p=*	Mean fold change	±SD	*p=*	Mean fold change	±SD	*p=*
COL1A1	1	0.512	n/a	1.298	1.135	>0.05	*1.592*	0.702	>0.05	0.887	0.281	>0.05	1.489	0.600	**<0.05**
COL3A1	1	0.496	n/a	1.726	1.060	>0.05	1.504	0.786	>0.05	0.832	0.311	>0.05	1.763	0.557	>0.05
COL4A1	1	0.675	n/a	1.257	0.500	>0.05	1.007	0.479	>0.05	1.004	0.457	>0.05	1.218	0.448	>0.05
COL5A3	1	0.643	n/a	1.655	0.663	>0.05	1.338	0.755	>0.05	1.294	0.803	>0.05	*1.485*	0.726	>0.05
COL6A3	1	0.596	n/a	1.402	0.706	>0.05	1.275	0.462	>0.05	1.101	0.559	>0.05	1.576	0.727	>0.05
TGFB1	1	0.416	n/a	1.458	0.616	>0.05	1.48	0.430	>0.05	1.017	0.376	>0.05	*1.51*	0.394	**<0.05**
FN1	1	0.443	n/a	3.601	3.065	**<0.01**	2.027	1.305	>0.05	1.03	0.383	>0.05	1.927	1.159	>0.05
ELN	1	0.896	n/a	1.089	1.052	>0.05	1.161	0.774	>0.05	1.041	1.005	>0.05	1.279	1.422	>0.05
LOX	1	0.529	n/a	1.473	0.998	>0.05	1.976	1.220	**<0.05**	0.81	0.407	>0.05	1.704	1.036	>0.05
SPARC	1	0.495	n/a	1.307	1.014	>0.05	1.613	0.741	**<0.01**	1.1	0.584	>0.05	1.477	0.643	>0.05

Table 8: *Relative expression of genes associated with fibrosis in AT after culture alone (ØM), or with M (IFNγ+LPS), M (IL-4), M (IL-10) and THP-1 cells.* Numerical representation of data presented in Figure 15, with mean fold change ±SD and significance.

4.2.1 *M (IFNγ + LPS) macrophages*

The effect of co-culture with differentiated macrophages on the transcription of genes associated with fibrosis is presented in Figure 15 and detailed in Table 8. Co-culture with IFNγ + LPS-treated THP-1 monocytes for 48 hours significantly ($p \leq 0.01$) upregulated expression of *FN1* 3.6-fold (Figure 15G) in OMAT, when compared with the control condition without macrophages (ØM). Expression of *COL1A1, COL3A1, COL4A1 COL5A3, COL6A3, TGFβ1, ELN, LOX* and *SPARC* was not significantly influenced by co-culture with M (IFN-γ + LPS) macrophages.

4.2.2 *M (IL-4) macrophages*

PMA + IL-4 treated THP-1 cells induced significant ($p<0.05$) upregulation of *LOX* 1.98-fold, (Figure 15I) and *SPARC* ($p<0.01$) 1.61-fold (Figure 15J) in OMAT when compared with the negative control condition (ØM). Expression of *COL1A1, COL3A1, COL4A1, COL5A3, COL6A3, TGFβ1, FN1*, and *ELN* did not appear to be upregulated after co-culture with M (IL-4) macrophages.

4.2.3 *M (IL-10) macrophages*

THP-1 monocytes treated with PMA + IL-10 did not significantly alter expression of any of the genes analysed when compared to the negative control (Figure 15). In some assays, e.g. *COL4A1*, *COL6A3, TGFβ1, FN1, LOX* and *SPARC*, gene expression closely matches the observed 'baseline' expression level of OMAT alone in the no-macrophage (ØM) condition, suggesting co-culture with M (IL-10) macrophages may have little influence on the expression of fibrosis-associated genes in OMAT.

4.2.4 ***THP-1 monocytes***

Undifferentiated THP-1 monocytes significantly upregulated the expression of *COL1A1 (*$p<0.05$) 1.49-fold, and *TGFβ1* ($p<0.05$) 1.51-fold (Figure 15A and F) in OMAT after co-culture for 48 hours when compared with the negative control. Expression of *COL3A1*, *COL4A1*, *COL5A3 COL6A3, FN1*, *ELN, LOX and SPARC* was not significantly modulated by co-culture with undifferentiated THP-1 cells.

4.3 Discussion

M (IL-10) macrophages, initially expected to possess an M2c-like phenotype, were hypothesised to be the key cellular inducers of fibrosis development in AT, and as such were expected to upregulate genes associated with fibrosis more potently than M (IFNγ + LPS), M (IL4) or THP-1 cells. The key finding of this experiment was that M (IL-10) cells did not induce significant upregulation of any genes encoding molecular regulators or structural components of ECM in human OMAT, however given that quantification of macrophage differentiation (Chapter 3) revealed that these cells did not appear M2c-like, this result was not unexpected.

M (IFNγ + LPS) macrophages upregulated pro-fibrotic gene expression in OMAT more strongly than expected for a pro-inflammatory cell type, however macrophage differentiation quantification revealed these cells potentially possessed a mixed M1/M2 phenotype. Consequently, a slight pro-fibrotic effect of these cells on AT was not entirely unexpected.

M (IL-4) macrophages demonstrated upregulation of only *SPARC* and *LOX*, important molecular mediators of fibrosis, results supported by the broadly M2-like phenotype that was demonstrated in Chapter 3. Unexpectedly, given they do not appear to possess an M1 or M2-like phenotype, co-culture with undifferentiated THP-1 monocytes also upregulated the expression of genes with structural and regulatory functions.

4.3.1 *Co-culture with M (IL-10) macrophages did not upregulate expression of pro-fibrotic genes in OMAT*

M2c macrophages secrete TGF-β[94,235], which, upon activation by molecules such as matrix metalloproteins and thrombopondin-1 (TSP-1)[236], induces a signal transduction pathway involving the phosphorylation of Smad proteins (including Smad2 and Smad3) resulting in their translocation and accumulation in the nucleus to act as regulatory transcription factors for genes – some of which are involved in promoting fibrosis in AT[94,237]. In light of this, M (IL-10) macrophages were hypothesised to induce a fibrotic transcriptional programme in OMAT and upregulate genes associated with the development of fibrosis, particularly fibronectin and collagen I, as evidenced by Ignotz and Massagué (1986)[238]. Neither were upregulated as a result of co-culture with M (IL-10) macrophages, likely because these cells did not demonstrate an M2c-like phenotype as the initial THP-1 differentiation step was not effective.

When considering the expression profiles of OMAT cultured with differentially treated macrophages, it becomes clear that the M (IL-10) macrophage condition consistently results in lower expression of genes associated with fibrosis than the M (IFNγ + LPS), M (IL-4) or THP-1 conditions, opposing evidence presented in the literature. If M (IL-10) cells had remained largely undifferentiated, similar levels of gene expression in OMAT co-cultured with M (IL-10) and THP-1 cells would be expected. For many genes (e.g. *COL1A1*, *TGFβ1*, *FN1*, *LOX* and *SPARC*) however, expression was slightly higher with THP-1 co-culture. Indeed, expression levels more closely matched that of the control condition without macrophages, suggesting that the M (IL-10) cells were potentially apoptotic. In

order to determine if this was the case, various indicators of cell death could have been measured, had the experimental design allowed.

Within the limitations of the experimental methods used in this study, ELISA analysis could be employed to quantify release of cytochrome *c* into the culture supernatant, although it would not be possible to determine whether cytochrome *c* was secreted by the OMAT explant or the differentiated macrophages. Levels of apoptosis could have been gauged by performing further qRT-PCR to detect changes in the mRNA level of members of the Bcl-2 family, which regulate apoptosis. Upregulation of pro-apoptotic genes, such as *BAX*, *BAK* and various caspases, and downregulation of anti-apoptotic members such as *BCL-2* and *BCL-XL*[239], would suggest increased cellular apoptosis.

Apoptosis relies on many post-translational modifications and protein-protein interactions, therefore a gene expression assay is unlikely to reliably quantify apoptosis in a cell population. In future studies measuring the respective protein levels of these genes by western blot could prove a more informative technique. Alternatively, experimental methods of future studies should be adapted to allow accurate quantification of apoptosis at the single cell level, for example via Annexin V-enabled cell surface phosphatidylserine quantification by flow cytometry[239].

4.3.2 *Co-culture with THP-1 monocytes influences AT expression of fibril-forming collagen I and TGFB1*

Undifferentiated THP-1 monocytes appeared to upregulate some genes associated with fibrosis in OMAT. After co-culture, these cells induced significantly increased expression of *COL1A1* and *TGFβ1* in OMAT compared to the control, and a non-significant increase in *FN1* and *LOX*. This suggests that these THP-1 monocytes possess a pro-fibrotic phenotype. ATM phenotype is strongly influenced by the surrounding microenvironment, which is altered in obesity. Therefore, where production and accumulation of pro-fibrotic cytokines such as IL-10 is already high in co-cultured AT explants, this may influence THP-1 cells, pushing them towards an M2-like or M2c-like functional phenotype[94,240], potentially able to secrete TGF-β. In future, it would be informative to observe the influence of AT on macrophage phenotype, comparing differentiation markers and secretory factors before and after co-culture.

TGF-β reportedly induces human AT progenitor cells to take on a myofibrobast-like phenotype with capacity for pro-collagen secretion[241], thereby contributing to the development of fibrosis in AT. In this study, *TGFβ1* expression in OMAT was not changed by co-culture with M (IFN-γ + LPS), M (IL-4) or M (IL-10) cells. There was however a significant ($p<0.05$) *TGFβ1* upregulation in OMAT co-cultured with THP-1 monocytes. This does not measure subsequent secretion and activation of the TGF-β1 protein, therefore no conclusions can be drawn beyond the gene expression level. As the hypothesised mechanism of induced AT fibrosis is dependent on macrophage-secreted TGF-β signalling, quantification of AT *TGFB1* does not give appropriate information to make inferences about potential

levels of macrophage-induced TGF-β signalling in cells. For this, downstream targets of TGF-β (such as *PAI-1*) should have been quantified.

Spencer *et al* (2010) detected upregulation of *PAI-1* mRNA as a measure of TGF-β signalling in adipocytes. PAI-1 is a downstream marker and is transcribed as a result of TGF-β signal propagation via the TGF-β receptor tyrosine kinase, and so quantifies the functional activity of TGF-β, as opposed to merely its transcriptional expression[144]. Their results show that conditioned medium from IL-4 treated THP-1 monocytes induced the highest expression of *PAI-1* mRNA in adipocytes. This study is not consistent with our findings, as only THP-1 monocytes upregulated *TGF-β1* when compared with the negative control. There is no indication that Spencer *et al* carried out validation of the functional phenotype of their differentiated macrophages, therefore it is difficult to draw conclusions about the mechanisms through which these macrophages may be acting on adipocytes.

THP-1 monocyte populations induced OMAT explants to significantly upregulate *COL1A1* mRNA ($p < 0.05$), supported by a previous study by Gagnon *et al* (2012), in which human abdominal subcutaneous preadipocytes treated with THP-1 macrophage conditioned media upregulated expression of collagen I/III, identified using immunocytochemistry[165]. This study relied on detecting fluorescence from a collagen I/III antibody, and therefore did not allow either collagen to be accurately quantified.

Collagen type I is fibril-forming and provides structural integrity to AT. Type III collagen is known to co-localise with type I collagen in humans[12], leading to speculation that the two may be co-expressed. With this in mind, it is logical to expect their expression profiles after macrophage co-culture to appear similar. To a certain extent, this is true: fold change in OMAT after treatment with M (IL-4), M (IL-10) and THP-1 populations was very similar, with M (IFNγ + LPS) co-culture the only condition to induce higher expression of *COL3A1* than *COL1A1*.

Finlin *et al* (2012) showed a similar profile of expression in adipocytes differentiated from adult-derived human adipose stem cells, after macrophage co-culture. They also demonstrated type I collagen mRNA levels in adipocytes were not significantly changed by co-culture with M1, M2a or M2c macrophages when compared with adipocytes cultured alone, and suggest collagen I regulation by macrophage-derived signals may be more complex than initially thought[146]. Divoux *et al* (2010) establish that the SVF is the major source of *COL1A1* in AT[148], demonstrating why a study using only adipocytes may be of limited use. For this reason, whole OMAT explants were used in this study.

4.3.3 ***M (IFNγ + LPS) macrophages upregulate FN1 in AT***

Fibronectin is a glycoprotein abundant in the ECM, important for binding collagens and regulating cell growth, differentiation and migration. It is a target gene of TGF-β[236], and therefore thought to contribute to tissue stiffness when overexpressed in obesity.

It was originally hypothesised that *FN1* expression would be upregulated in AT after co-culture with M (IL-4) and M (IL-10) macrophages, however *FN1* mRNA expression was only significantly ($p<0.01$) increased after co-culture with M (IFNγ + LPS) macrophages. Given these cells were demonstrated to have a mixed M1/M2 phenotype, this may be the result of some degree of pro-fibrotic signalling.

Gagnon *et al* (2012) demonstrated that factors secreted by monocyte-derived macrophages increased the secretion of fibronectin protein from human subcutaneous preadipocytes[165], however their study did not differentiate macrophages into different subtypes. The results of our study support this increased production of fibronectin, suggesting that transcription and translation may be rapidly induced in response to inflammatory macrophage-secreted stimuli within a 48h period.

Despite concluding that M (IFNγ + LPS) macrophages likely possessed a mixed M1/M2 phenotype and therefore may be to some extent functionally pro-fibrotic, these cells did not induce significant upregulation of any other genes analysed. These results are challenging to place in the context of the current literature, as most relevant *in vitro* studies focus on the fibrotic effects of discretely defined macrophages subtypes. However, evidence of a ~60% prevalence of mixed M1/M2 phenotype of macrophages in lean human AT, with a shift towards an M2 phenotype and association with fibrosis in obese AT[144], suggests that these mixed phenotype macrophages may not play a major role in the development of AT fibrosis.

Despite evidence that *LOX* expression in AT is upregulated in response to an inflammatory stimulus[242], M (IFNγ + LPS) macrophages, which secreted pro-inflammatory IL-1 and IL-6, did not effect its expression in AT. The macrophage phenotyping data is based on differentiated macrophages cultured alone, therefore it may be that factors secreted by AT during the co-culture influenced the functional phenotype of M (IFNγ + LPS) macrophages.

As M (IFNγ + LPS) macrophages had demonstrated a mixed M1/M2 phenotype with some degree of increased TGF-β secretion, and preadipocytes are thought to be the predominant collagen-secreting cells in AT, it was hypothesised that their co-culture with whole OMAT explants may induce upregulation of *COL4A1,* thereby contributing to AT dysfunction in obesity. Type IV collagen is network-forming, and supports the formation of basement membranes (BM) within AT[12], providing a site for integrin signalling[15]. Basement membrane 'thickening' is the result of collagen IV overexpression and deposition into the space between AT cells in obesity, and although not abundant in areas of fibrosis, is associated with AT dysfunction[15] potentially through the constriction of adipocyte expansion, limiting lipid storage (as detailed in Chapter 1). The results showed that co-culture of AT with macrophages of all phenotypes did not induce upregulation of *COL4A1*.

This mirrors the findings of Reggio and colleagues (2016) in studies using SCAT, where the effect of pro-fibrotic TGF-β isoforms on the expression of type IV collagen in AT was explored. They determined that pro-fibrotic *TGF-β* isoforms were only capable of inducing *COL4A1* expression in endothelial cells, and did not upregulate *COL4A1* in adipocytes[15]. In contrast, Spencer *et al* (2011)

reported that collagen IV was expressed by both AT and adipocytes in culture, although the origin of these adipocytes is not described[167].

It is important to note that although *COL4A1*, along with *COL4A2*, is the most common collagen IV α-chain, collagen IV can possess chains α1-α6 and can exist in three heterotrimeric forms: α1α1α2, α3α4α5, and α5α5α6[243]. As such, it may be that co-culture with TGF-β secreting macrophages upregulates a collagen IV gene other than *COL4A1*, and contributes to BM 'thickening' and AT dysfunction through production of the α3α4α5 or α5α5α6 collagen IV heterotrimers[243], an effect not represented by these data. This may be unlikely, as during adipogenesis at least, α3-6 chains are thought to be expressed at only low levels[13].

COL5A3 was hypothesised to be upregulated in response to exposure to macrophages displaying characteristics of M2c macrophages, which to some extent applies to M (IFNγ + LPS) macrophages. Type V collagen is fibril-forming, and is known to co-distribute with collagen I[12]. Its upregulation is thought to contribute to AT dysfunction by inhibiting angiogenesis, the importance of which is discussed in Chapter 1[167]. Spencer *et al* (2011) established collagen V as a key contributor to AT fibrosis, with significantly higher expression in obese subjects, as opposed to lean[167]. *COL5A3* expression was unchanged by co-culture with differentiated or undifferentiated macrophages. This contrasts with the findings of Spencer *et al* (2011). After co-culture of M1, M2a and M2c macrophages (obtained using very similar differentiation methods) with adipocytes, their quantification of collagen V mRNA showed significant upregulation in adipocytes exposed to M2a ($p < 0.001$) and M2c ($p < 0.05$)

macrophages, but no significant change after co-culture with M1 macrophages[167]. As with many other co-culture studies, their experimental model is not representative of AT *in vivo*, and does not account for the effect of macrophages on gene expression in cells of the SVF (including the fibroblast-like preadipocytes). The adipocytes used were also differentiated *in vitro* from human stem cells, as opposed to being isolated as mature primary cells, which may influence the cell characteristics. By using whole AT explants, our study may better represent levels of *COL5A3* mRNA *in vivo*. However, it is important to note that Spencer *et al*'s co-culture duration was 72h, as opposed to the 48h in this study, therefore it is feasible to speculate that if given an additional 24h in culture, M (IL-4) and M (IL-10) macrophages may have upregulated *COL5A3* in AT.

Based on the findings of Spencer and colleagues (2010)[144], it was postulated that collagen VI mRNA may be upregulated in response to co-culture with M2-like cells, therefore based on the data validating macrophage differentiation, may be influenced by M (IL-4) and possibly M (IFNγ + LPS) macrophages. Type VI collagen has been implicated in mice as a key ECM component responsible for adipocyte dysfunction, as it is thought to physically prevent the hypertrophic expansion of individual adipocytes in obesity, and therefore limit lipid storage[169,170]. Our study showed limited upregulation of collagen VI mRNA. This discrepancy may be explained by differences in transcript quantification: Spencer *et al* used a primer sequence specific for *COL6A1*, whereas in this study the TaqMan assay was specific to *COL6A3*. Type VI collagen α-chains are known to be expressed in different proportions during different phases of wound healing, which may account for this difference[244], and shows just one limitation of relying on RNA analysis. Another important methodological difference is the duration of

the co-culture. Spencer *et al* co-cultured adipocytes with macrophages over the course of 72 hours, in contrast to the 48 hours in this study. It is possible that this period was not long enough to induce a transcriptional programme resulting in significant *COL6A3* upregulation, as perhaps macrophages induce this effect indirectly.

Again, it is important to note that Spencer *et al* used only adipocytes for their co-culture, obtained through *in vitro* differentiation of human adipocyte stem cells, and therefore unlikely to display precisely the same characteristics and expression profile as adipocytes differentiated *in vivo*. The OMAT explant model used in this study should represent a more sophisticated method of mimicking the *in vivo* microenvironment, as importantly it includes the SVF of the tissue, including resident fibroblast-like preadipocytes which are responsible for the majority of ECM component expression, including *COL6A3,* in AT[147,164]. As a result, the experimental model used in this study is more likely to present a realistic picture of how collagen VI expression is influenced by macrophage phenotype.

Pasarica *et al* (2009) suggest a link between *COL6A3* and inflammation in obesity, as they observed a concomitant increase in *COL6A3* and macrophage content in human abdominal SCAT[170]. They postulate that high *COL6A3* expression contributes towards increased inflammation in obese AT[170]. The results of our study suggest that the inverse of this relationship is not correct, as increased inflammation (i.e. high numbers of macrophages) does not induce increased *COL6A3* expression in AT, suggesting a more complex regulatory relationship. As an M2c-like macrophage with high expression of pro-fibrotic TGF-

β and IL-10 was not achieved, it is not possible to conclude whether these data support the theory proposed by McCulloch *et al* (2015)[147], that *COL6A3* may not play an essential role in the development of fibrosis in human obesity as previously suggested.

As a critical component of the AT ECM, elastin helps maintain tissue elasticity and is essential for effective remodelling. Encoded by the *ELN* gene, elastin protein levels have been shown to be reduced in obesity, and morphological changes in elastin fibrils have also been reported[167]. The resulting tissue stiffening may contribute towards AT dysfunction by limiting adipocyte expandability. Based on evidence from Spencer *et al* (2011) that elastin expression was predictably downregulated in adipocytes after co-culture with M2 macrophages[167], it was hypothesised that M (IL-4) macrophages, considered broadly M2-like, would induce downregulation of *ELN1* expression in AT. Results of the co-culture experiment did not reflect this, as macrophages of any phenotype did not induce any change in *ELN* expression from OMAT explants. This may be because no differentiated cells appeared to possess a strongly pro-fibrotic phenotype. Spencer *et al*'s use of adipocytes differentiated *in vitro* from human adipose stem cells, rather than an explant model, may cause them to overstate the effect of macrophage phenotype on AT fibrosis. Our study shows that in the context of whole AT, the downregulation of *ELN* within an adipocyte-only population may not be relevant to this *ex vivo* model. Spencer *et al* observed this downregulation after 72h of co-culture, therefore 48h may not have been enough time to induce detectable *ELN* downregulation.

4.3.4 *M (IL-4) macrophages upregulated expression of LOX and SPARC in AT*

Expression of *LOX* and *SPARC* in OMAT was confirmed and shown to be significantly upregulated ($p<0.05$ and <0.01 respectively) in explants after co-culture with M (IL-4) macrophages, suggesting the broadly M2-like characteristics and secretory profile of these cells may enhance the capacity of AT to deposit collagen[245], inhibit adipogenesis promoting adipocyte hypertrophy[246], and form cross-links within and between collagen and elastin fibres[247].

Lysyl oxidase is required for remodelling of AT in obesity, is predominantly expressed by cells of AT SVF, and is associated with AT inflammation and development of fibrosis[242]. As such, its expression was expected to be increased by co-culture with M2-like macrophages. It is an enzyme which acts to catalyse covalent cross-linking within fibril-forming collagen and elastin fibrils, providing essential stability to insoluble fibres in the ECM, and tensile strength[9,248]. In addition to its expression in VAT[242], *LOX* mRNA is significantly upregulated in the SCAT of obese subjects[180] and as a result of hypoxia[121], suggesting it may also play a role in AT dysfunction. It has not yet been fully established how inflammation, and more specifically macrophage phenotype, may influence the expression of *LOX* in AT.

As the purpose of LOX is to facilitate the cross-linking of collagen and elastin fibres in AT, it was expected that *LOX* could present a similar profile of expression as *COL1A1*, *COL3A1* and *COL5A3*, which encode the fibril-forming collagens. This is not the case, and it may be that *LOX* upregulation occurs at a different

stage during the development of fibrosis, for example in direct response to, or in anticipation of, collagen upregulation. Adipocyte-macrophage co-culture experiments performed by Spencer *et al* (2010) demonstrated upregulation of pro-fibrotic genes in RNA analysed at a 48 hour timepoint[144], and as such provided the basis of the methodology used in this study. The potential limitations of choosing this 48 timepoint for RNA analysis are discussed further in Chapter 6.

SPARC is a matricellular protein predominantly secreted by adipocytes in AT[249]. It is believed to be involved in the regulation of AT expansion, specifically in cell-matrix interactions during AT hyperplasia and adipogenesis[250] and the formation of collagen fibrils, as it is tightly associated with collagen I expression and the tensile strength of the tissue[245]. Kos *et al* (2009) demonstrated that *SPARC* expression is increased with obesity in humans[177], while its role as a mediator of the development of tissue fibrosis has also been established[251].

Despite the importance of SPARC in the development of fibrosis and the clear link between fibrosis and inflammation, there has been little investigation into how pro-inflammatory and anti-inflammatory macrophages may modulate the expression of *SPARC* in AT. This study showed significant ($p<0.01$) upregulation of *SPARC* mRNA in OMAT explants co-cultured with M (IL-4) macrophages. *SPARC* expression is reportedly intricately linked with TGF-β activity[252]. It is well established that SPARC is regulated by TGF-β[252,253]. Secretory profile analysis of M (IL-4) macrophages revealed TGF-β secretion was as expected not induced by differentiation stimuli, however it is possible that co-culture with OMAT may have induced a phenotypic change whereby TGF-β is expressed and thus exerts

a pro-fibrotic effect on AT. To determine this, it would be necessary to measure the upregulation of downstream markers of activate TGF- β signalling such as Smad2/3 and *PAI-1* in AT.

Wrana *et al* (1991) showed that human fibroblast cells stimulated with TGF-β demonstrate increased SPARC accumulation, but in contrast to our findings, observed no change in *SPARC* transcript levels, therefore determining that TGF-β controls SPARC production through post-transcriptional modifications in the nucleus[252]. This suggests that analysis of *SPARC* expression at the RNA level may not be appropriate in order to make conclusions about TGF-β-mediated effects of macrophages on SPARC in AT fibrosis. Alternatively, it is possible that SPARC may be upregulated by M (IL-4) macrophage by an as yet undefined novel TGF-β-independent signalling pathway.

The experimental model utilised by Wrana *et al* does however differ considerably[252], and their observations were made in human fibroblast cells. As Kos *et al* (2009) reported that the majority of SPARC expression derives from adipocytes, rather than the fibroblast-like preadipocyte cells[177], these findings may have limited relevance to the question of macrophage-induced fibrosis in obese AT.

4.3.5 ***Limitations***

It is important to recognise the experimental limitations when interpreting these data. The analysed macrophages were differentiated and cultured in the absence of OMAT, and therefore cannot provide insight into the potential influence of

OMAT explants on the macrophage phenotype during co-culture. *In vivo,* macrophage phenotype depends on microenvironmental cues, which likely vary greatly between subjects depending on levels of AT inflammation. AT possesses inherent morphological heterogeneity, with some areas more heavily fibrotic than others, and pockets of pro-inflammatory macrophages arranged into 'crown-like structures'[144]. As a result, there are likely to be local microenvironmental differences between explants originating from the same piece of tissue, making consistency between experimental duplicates challenging, although this may be overcome by the 'homogenising' effect when AT explants were processed during co-culture setup. Although macrophages are known to be capable of transdifferentiation in response to environmental signals[154], this phenomenon is unlikely to have influenced the outcome of this experiment as macrophages were seeded at a supraphysiological concentration of $4x10^6$ cells/well, and in theory relatively insensitive to small microenvironmental changes - though this potential effect cannot be discounted. Experimental limitations are comprehensively discussed in Chapter 6.

To better understand how OMAT explants directly influence macrophage phenotype, it would be informative to measure the expression of phenotypic and functional markers in macrophages collected after co-culture, and compare to cells cultured without AT. Unfortunately, secreted products from co-cultured macrophages cannot be measured in isolation as it is not possible to determine the origin of protein in the common medium.

4.4 Summary

The results discussed in this chapter provide some evidence to support a potentially important role for mixed M1/M2 macrophages in the development of AT fibrosis, but are inconclusive with relation to the proposed hypothesis that M2c macrophages are the most potent inducers of pro-fibrotic gene upregulation in AT. Upregulation of molecular mediators of fibrosis by M (IL-4) macrophages supports a role for macrophages displaying M2-like characteristics in the development of AT fibrosis.

Chapter 5: The influence of insulin on macrophage-mediated AT fibrosis

5.1 Introduction

Insulin resistance, associated with T2DM, results in chronic hyperinsulinaemia as cells become unresponsive to insulin. Insulin is an important regulator of ECM development, and reportedly controls the post-transcriptional processing and secretion of collagen[184]. It was hypothesised that hyperinsulinaemia with AT macrophages may contribute to the development of fibrosis, thus furthering the pathogenesis of AT dysfunction.

To explore this, an *in vitro* model of hyperinsulinaemia in AT was used. Given that M (IL-4) macrophages were shown to be broadly M2-like, and that M (IFNγ + LPS) macrophages possessed a mixed functional M1/M2 phenotype, their co-culture with OMAT and insulin was expected to upregulate expression of pro-fibrotic genes in OMAT in a concentration-dependent manner, more strongly than co-culture without insulin.

Briefly, OMAT explants were co-cultured with differentiated THP-1 macrophages, of M (IFNγ + LPS), M (IL-4) and M (IL-10) phenotypes, in the presence of insulin (1nM, 10nM, 100nM) for 48 hours. An undifferentiated THP-1 population, a no-macrophage condition (ØM) and a no-insulin vehicle condition were used as controls. Gene expression (*COL1A1*, *COL3A1, COL4A1, COL5A3, COL6A3, TGFβ1, FN1, ELN, SPARC* and *LOX)* was measured using qRT-PCR. Statistical analysis was performed using two-way ANOVA followed by Bonferroni post hoc test.

5.2 Results

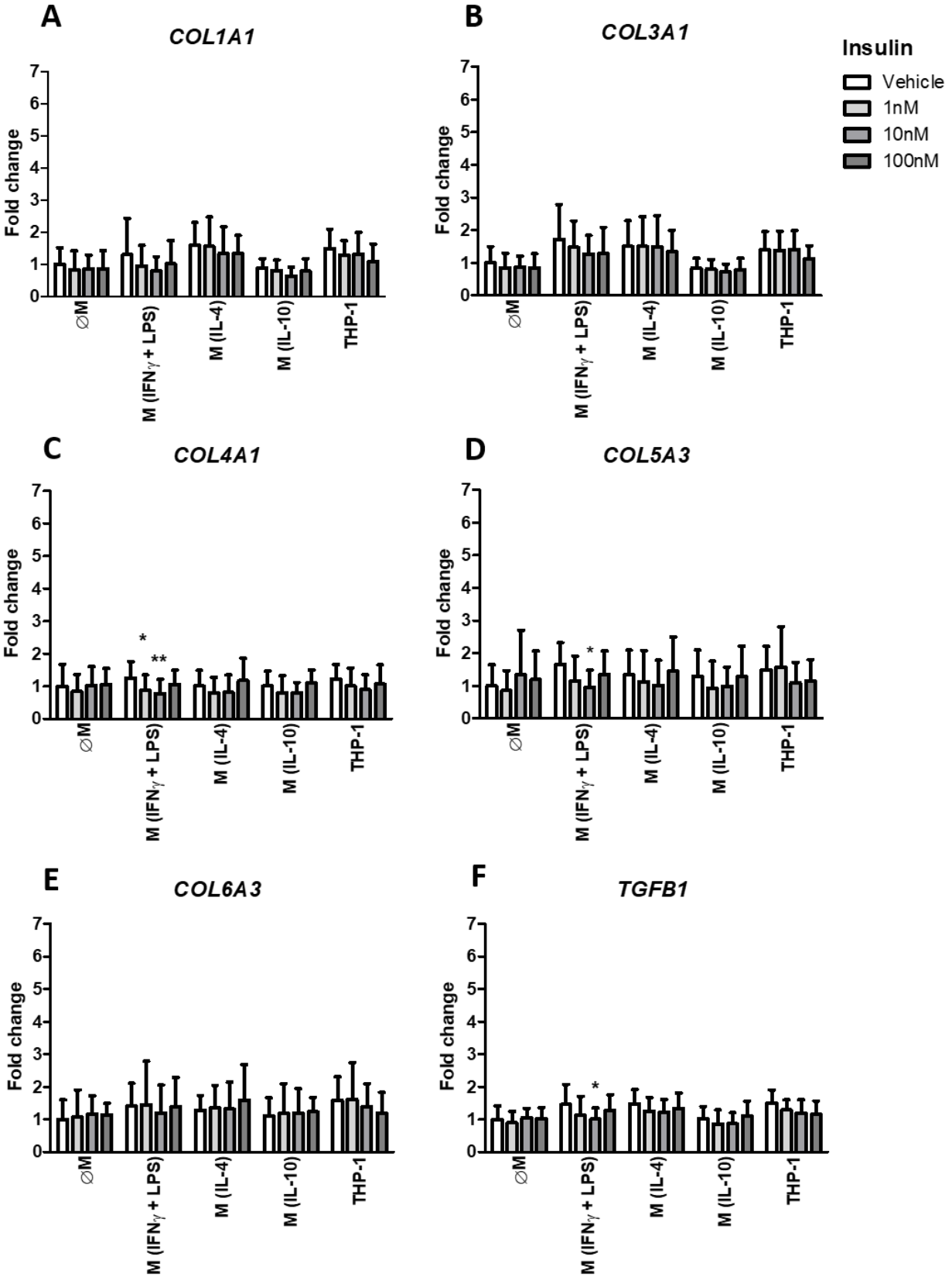
A
COL1A1
B
COL3A1
Insulin
Vehicle
1nM
10nM
100nM
C
COL4A1
D
COL5A3
E
COL6A3
F
TGFB1
Fold change
0
1
2
3
4
5
6
7
*
**
∅M
M (IFNγ + LPS)
M (IL-4)
M (IL-10)
THP-1

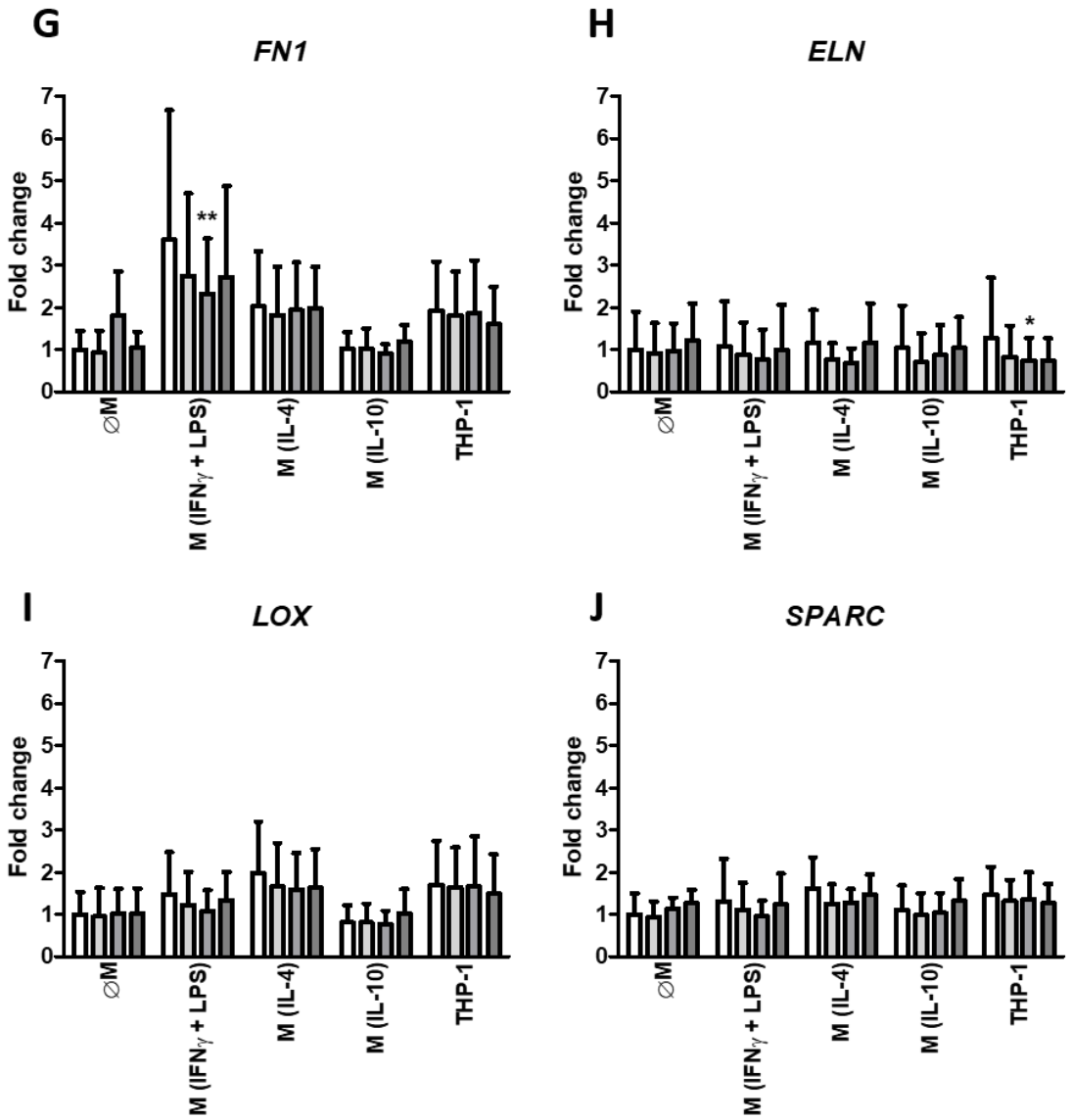

Figure 16: *Effect of insulin on AT gene expression after co-culture with macrophages.* OMAT explants were cultured alone (ØM), with M (IFNγ + LPS), M (IL-4), M (IL-10) or THP-1 cells. Repeated measures two-way ANOVA followed by Bonferroni multiple comparisons post-hoc test was used to show how insulin concentration changed pro-fibrotic gene expression in AT (* = p<0.05, ** = p<0.01), in each macrophage co-culture compared with the vehicle only condition. Values were normalised to the vehicle insulin negative control (ØM, first column). Error bars denote mean fold change ±SD. n=6 independent experiments.

Ø M:

	Vehicle			1nM Ins			10nM Ins			100nM Ins		
	Mean fold change	±SD	*p=*	Mean fold change	±SD	*p=*	Mean fold change	±SD	*p=*	Mean fold change	±SD	*p=*
COL1A1	1	0.512	>0.05	0.826329	0.589	>0.05	*0.859335*	0.427	>0.05	0.868718	0.554	>0.05
COL3A1	1	0.496	>0.05	0.843931	0.452	>0.05	0.868739	0.336	>0.05	0.843003	0.430	>0.05
COL4A1	1	0.675	>0.05	0.845692	0.514	>0.05	1.025859	0.584	>0.05	1.053246	0.491	>0.05
COL5A3	1	0.643	>0.05	0.853848	0.614	>0.05	1.338843	1.357	>0.05	1.190687	0.883	>0.05
COL6A3	1	0.596	>0.05	1.072967	0.830	>0.05	1.1577	0.567	>0.05	1.142458	0.351	>0.05
TGFB1	1	0.416	>0.05	0.895572	0.349	>0.05	1.04386	0.292	>0.05	1.020915	0.338	>0.05
FN1	1	0.443	>0.05	0.921809	0.527	>0.05	1.070483	0.380	>0.05	1.047114	0.372	>0.05
ELN	1	0.896	>0.05	0.907886	0.714	>0.05	0.967167	0.652	>0.05	1.216308	0.876	>0.05
LOX	1	0.529	>0.05	0.949	0.678	>0.05	1.016339	0.584	>0.05	1.015027	0.598	>0.05
SPARC	1	0.495	>0.05	0.930671	0.377	>0.05	1.131934	0.266	>0.05	1.261654	0.321	>0.05

M (IFN + LPS):

	Vehicle			1nM Ins			10nM Ins			100nM Ins		
	Mean fold change	±SD	*p=*	Mean fold change	±SD	*p=*	Mean fold change	±SD	*p=*	Mean fold change	±SD	*p=*
COL1A1	1.297606	1.135	>0.05	0.942447	0.649	>0.05	*0.794422*	0.439	>0.05	1.010595	0.728	>0.05
COL3A1	1.726029	1.060	>0.05	1.470462	0.814	>0.05	1.269358	0.572	>0.05	1.278878	0.804	>0.05
COL4A1	1.256997	0.500	>0.05	0.873317	0.471	**<0.05**	0.779964	0.429	**<0.01**	1.0502	0.440	>0.05
COL5A3	1.654953	0.663	>0.05	1.145431	0.769	>0.05	0.956363	0.526	**<0.05**	1.34903	0.719	>0.05
COL6A3	1.402245	0.706	>0.05	1.4449	1.341	>0.05	1.193935	0.856	>0.05	1.383824	0.906	>0.05
TGFB1	1.457994	0.616	>0.05	1.123606	0.584	>0.05	1.00424	0.344	**<0.05**	1.280862	0.474	>0.05
FN1	3.60057	3.065	>0.05	2.744286	1.951	>0.05	2.320956	1.304	**<0.01**	2.722372	2.144	>0.05
ELN	1.088938	1.052	>0.05	0.889387	0.751	>0.05	0.764274	0.712	>0.05	0.994117	1.068	>0.05
LOX	1.473125	0.998	>0.05	1.229164	0.782	>0.05	1.075711	0.499	>0.05	1.330207	0.672	>0.05
SPARC	1.307239	1.014	>0.05	1.112546	0.634	>0.05	0.953334	0.370	>0.05	1.237896	0.724	>0.05

M (IL-4):

	Vehicle			1nM Ins			10nM Ins			100nM Ins		
	Mean fold change	±SD	*p=*	Mean fold change	±SD	*p=*	Mean fold change	±SD	*p=*	Mean fold change	±SD	*p=*
COL1A1	1.591926	0.702	>0.05	1.552641	0.919	>0.05	*1.332016*	0.836	>0.05	1.325094	0.577	>0.05
COL3A1	1.503721	0.786	>0.05	1.504899	0.908	>0.05	1.496833	0.950	>0.05	1.336912	0.660	>0.05
COL4A1	1.007384	0.479	>0.05	0.801651	0.471	>0.05	0.815543	0.531	>0.05	1.177703	0.688	>0.05
COL5A3	1.337758	0.755	>0.05	1.124891	0.959	>0.05	1.010052	0.771	>0.05	1.453957	1.045	>0.05
COL6A3	1.274632	0.462	>0.05	1.351698	0.695	>0.05	1.317804	0.824	>0.05	1.582285	1.097	>0.05
TGFB1	1.479646	0.430	>0.05	1.259812	0.409	>0.05	1.213751	0.395	>0.05	1.34021	0.470	>0.05
FN1	2.02683	1.305	>0.05	1.809445	1.151	>0.05	1.935379	1.124	>0.05	1.974972	0.987	>0.05
ELN	1.161201	0.774	>0.05	0.76431	0.391	>0.05	0.693873	0.330	>0.05	1.159616	0.932	>0.05
LOX	1.975803	1.220	>0.05	1.653083	1.042	>0.05	1.591617	0.863	>0.05	1.630749	0.918	>0.05
SPARC	1.613228	0.643	>0.05	1.249228	0.501	>0.05	1.272251	0.621	>0.05	1.464601	0.461	>0.05

M (IL-10):

	Vehicle			1nM Ins			10nM Ins			100nM Ins		
	Mean fold change	±SD	*p*=	Mean fold change	±SD	*p*=	Mean fold change	±SD	*p*=	Mean fold change	±SD	*p*=
COL1A1	0.887032	0.281	>0.05	0.807559	0.321	>0.05	*0.641491*	0.274	>0.05	0.784141	0.390	>0.05
COL3A1	0.832308	0.311	>0.05	0.803837	0.300	>0.05	0.720826	0.237	>0.05	0.791794	0.346	>0.05
COL4A1	1.004136	0.457	>0.05	0.798935	0.522	>0.05	0.325768	0.780	>0.05	1.0502	0.440	>0.05
COL5A3	1.293697	0.803	>0.05	0.928291	0.822	>0.05	0.988183	0.589	>0.05	1.279604	0.938	>0.05
COL6A3	1.101412	0.559	>0.05	1.180079	0.919	>0.05	1.19297	0.744	>0.05	1.231874	0.445	>0.05
TGFB1	1.017386	0.376	>0.05	0.854064	0.439	>0.05	0.864115	0.340	>0.05	1.099933	0.460	>0.05
FN1	1.029773	0.383	>0.05	1.023898	0.479	>0.05	0.906357	0.217	>0.05	1.188985	0.393	>0.05
ELN	1.040601	1.005	>0.05	0.702212	0.684	>0.05	0.871788	0.707	>0.05	1.037867	0.731	>0.05
LOX	0.809876	0.407	>0.05	0.808078	0.446	>0.05	0.766791	0.320	>0.05	1.018522	0.580	>0.05
SPARC	1.100055	0.584	>0.05	0.985525	0.519	>0.05	1.033926	0.474	>0.05	1.32023	0.515	>0.05

THP-1:

	Vehicle			1nM Ins			10nM Ins			100nM Ins		
	Mean fold change	±SD	*p*=	Mean fold change	±SD	*p*=	Mean fold change	±SD	*p*=	Mean fold change	±SD	*p*=
COL1A1	1.489362	0.600	>0.05	1.28828	0.441	>0.05	*1.308531*	0.686	>0.05	1.086505	0.551	>0.05
COL3A1	1.39599	0.557	>0.05	1.382983	0.586	>0.05	1.407703	0.581	>0.05	1.116305	0.403	>0.05
COL4A1	1.217838	0.448	>0.05	1.009044	0.553	>0.05	0.894603	0.458	>0.05	1.0666	0.584	>0.05
COL5A3	1.485299	0.726	>0.05	1.563386	1.245	>0.05	1.089152	0.633	>0.05	1.149917	0.654	>0.05
COL6A3	1.575927	0.727	>0.05	1.606958	1.131	>0.05	1.390597	0.703	>0.05	1.190461	0.633	>0.05
TGFB1	1.509778	0.394	>0.05	1.284906	0.308	>0.05	1.190737	0.408	>0.05	1.154454	0.415	>0.05
FN1	1.922608	1.159	>0.05	1.813231	1.039	>0.05	1.86662	1.248	>0.05	1.602222	0.893	>0.05
ELN	1.278922	1.422	>0.05	0.834166	0.732	>0.05	0.736641	0.539	**<0.05**	0.738785	0.524	>0.05
LOX	1.703976	1.036	>0.05	1.632361	0.949	>0.05	1.657393	1.194	>0.05	1.49298	0.922	>0.05
SPARC	1.477039	0.643	>0.05	1.317511	0.501	>0.05	1.370212	0.621	>0.05	1.263729	0.461	>0.05

Table 9: *Effect of insulin on expression of genes associated with fibrosis in OMAT after co-culture with differentiated macrophages.* Data displayed in Figure 16 is given here in numerical form categorised by macrophage subtype. Values were normalised to the no macrophage vehicle insulin negative control (ØM). Mean fold change given ±SD, with significance. *n*=6 independent experiments.

5.2.1 *ØM (no macrophages)*

Culture of OMAT explants with insulin in the absence of macrophages did not reveal any significant concentration-dependent changes in expression of genes associated with fibrosis. In *ELN* (Figure 16H) and *SPARC* (Figure 16J) however, there was a small, non-significant trend increase from 1nM to 100nM insulin,

when compared with the vehicle only condition. Comprehensive details of mean fold changes ±SD can be found in Table 9.

5.2.2 *M (IFNγ + LPS) macrophages*

When cultured with 10nM insulin, M (IFNγ + LPS) macrophage co-culture significantly downregulated *COL4A1* ($p \leq 0.01$, Figure 16C), *COL5A3* ($p \leq 0.05$, Figure 16D), *TGFβ1* ($p \leq 0.05$, Figure 16F) and *FN1* ($p \leq 0.01$, Figure 16G) in OMAT, when compared with the vehicle only condition. In the case of *COL4A1*, the 1nM insulin condition also showed significant downregulation ($p < 0.05$, Figure 16C). This general trend was reflected in expression of *COL1A1* (Figure 16A), *COL3A1* (Figure 16B), *ELN* (Figure 16H), *LOX* (Figure 16I) and *SPARC* (Figure 16J), despite not achieving significance.

5.2.3 *M (IL-4) macrophages*

When treated with 1nM, 10nM or 100nM insulin, there was no insulin-mediated M (IL-4) effect on the expression of any of the pro-fibrotic genes analysed, when compared to the vehicle control.

5.2.4 *M (IL-10)*

Upon co-culture with insulin and M (IL-10) macrophages, there was no significantly modulation of pro-fibrotic gene expression in OMAT. Although M (IL-10) macrophages and insulin may appear to influence expression of some pro-fibrotic genes, the pattern of expression is very similar to that of the ØM (no macrophage) condition, suggesting any observed effect is likely a result of insulin acting directly on AT explants, rather than a combined macrophage-insulin effect.

5.2.5 ***THP-1 monocytes***

Co-culture of OMAT explants with undifferentiated THP-1 monocytes, treated with 10nM insulin, resulted in significantly ($p<0.05$) decreased *ELN* expression in OMAT (Figure 16H), when compared with the vehicle control. Despite changes at 1nM and 100nM concentrations not proving significant, these results suggest there may be a concentration-dependent downregulation of *ELN*. A similar tendency is found in the expression of *TGFβ1* (Figure 16F). To some extent, a similar pattern of a downward trend in expression, relative to insulin concentration, can also be seen in *COL1A1* (Figure 16A), *COL3A1* (Figure 16B) and *COL6A3* (Figure 16E). There appeared to be no distinguishable effect of insulin concentration with THP-1 cells on *COL4A1* (Figure 16C), *COL5A3* (Figure 16D), *FN1* (Figure 16G), *LOX* (Figure 16I) and *SPARC* (Figure 16J) expression.

5.3 Discussion

In contrast to expectations, there was no observable upregulation of pro-fibrotic genes with insulin treatment, which suggests that insulin does not contribute towards pathogenic macrophage-mediated fibrosis in obesity. Instead, insulin appears to moderate the slight pro-fibrotic effects of M (IFNγ + LPS) macrophages and THP-1 monocytes. As previously discussed, M (IL-10) cells, treated with PMA + IL-10 did not appear to be functionally M2c-like, and may be apoptotic. Consequently, their combined effect with insulin, which largely appears similar to the no macrophage condition, will not be discussed further in the following sections.

5.3.1 *Insulin alone does not modulate expression of genes associated with fibrosis in OMAT explants*

Based on the reported anti-inflammatory effects of insulin[189], and its propensity to increase pro-fibrotic SPARC in AT[177], insulin was hypothesised to upregulate genes associated with fibrosis in OMAT. There was no significant concentration-dependent change in expression of pro-fibrotic genes in OMAT explants treated with insulin (at 1nM, 10nM and 100nM) and cultured for 48 hours in the absence of macrophages (ØM condition), when compared to the vehicle control.

These unexpected results may be explained by the methods chosen to analyse changes in the development of fibrosis in this study. It may be that insulin-mediated effects on fibrosis development occur at the level of protein expression, secretion or processing, and therefore changes will not be detected in the transcription levels of structural components (such as collagens) or molecular

mediators (i.e. *LOX* and *SPARC*). This is supported by the findings of Wang *et al* (2006), who used an *in vitro* model of mouse-derived 3T3-L1 adipocytes treated with insulin, and determined that insulin does not alter expression of ECM components (e.g. *Col5a3* and *Col6a3*) at the mRNA level. Insulin does however modulate the transcription of enzymes associated with the processing of ECM component proteins, such as procollagen C-endopeptidase enhancer protein (*Pcolce*), which through post-transcriptional processing, help stabilise structural proteins within the ECM[184]. As RNA was extracted from AT explants, it would be possible in future to perform further qRT-PCR to quantify how insulin concentration modulates expression of human ECM protein-processing enzymes and tissue inhibitor of metalloproteinases (e.g. *TIMP1* and *TIMP4*), to more effectively elucidate how insulin contributes to ECM remodelling in obesity[184]. In future studies, it would also be pertinent to measure changes in insoluble collagen fibre deposition or biomechanical properties[254], as a means of robustly quantifying fibrosis.

Contrary to expectations[177], there was no significant insulin-dependent modulation of *SPARC* expression in OMAT explants. This could be a feature of the timepoint at which expression was analysed after co-culture, as Kos *et al* (2009) report a significant increase in SPARC protein, measured by western[255] blot, when human OMAT was treated with 1nM ($p<0.05$) and 100nM ($p<0.01$) insulin for 24h *in vitro,* in comparison to the untreated control[177]. Their study reveals that SPARC protein levels are measurably elevated at the 24h timepoint, suggesting RNA levels of *SPARC* are likely to be detectably increased around or before this timepoint. At the 48 hr timepoint, it is possible that sustained exposure to high levels of newly secreted SPARC protein may have activated protective

autocrine positive feedback cell signalling mechanisms via the SPARC receptor, whereby transcription of *SPARC* RNA is downregulated in response[256]. This highlights the critical need for careful consideration of previously obtained data, thorough literature review and complete optimisation of *in vitro* protocols when refining methodology, particularly in studies using precious human samples. Further limitations stemming from inadequate optimisation of this study are discussed in Chapter 6.

5.3.2 *Insulin may modulate the pro-fibrotic effect of M (IFNγ + LPS) macrophages*

The role of insulin in the development of fibrosis is currently unclear. A report of its anti-inflammatory effects on mononuclear cells[189] led to the hypothesis that insulin treatment may upregulate genes associated with fibrosis in AT by modulating the function or phenotype of the macrophages.

As discussed previously, co-culture of OMAT explants with M (IFNγ + LPS) macrophages resulted in increased expression of *FN1*, supporting the evidence that these cells to some extent functionally pro-fibrotic. The addition of 1nM or 10nM insulin to the co-culture results in significantly decreased expression of *COL4A1*, *COL5A3*, *TGFβ1* and *FN1* in OMAT, when compared with the vehicle control. Although not significant, this observable tendency also persists in the expression of *COL1A1*, *COL3A1*, *ELN*, *LOX* and *SPARC*. This may be because insulin does exert a pro-inflammatory effect on macrophages, causing them to downregulate any anti-inflammatory, pro-fibrotic transcriptional programme. This is in keeping with the findings of Tada Iida *et al* (2001), who conclude that insulin

is capable of upregulating TNF-α expression in macrophages[257]. Consequently, downregulation of pro-fibrotic genes in OMAT by insulin and M (IFNγ + LPS) macrophages may be explained by the pro-inflammatory effect of insulin, pushing macrophages closer towards a full M1 phenotype, thereby reducing any wound-healing pro-fibrotic influence on OMAT. To confirm this, it would be necessary to examine the effect of insulin alone on macrophage phenotype. Unfortunately, a macrophage-insulin condition was not included in this study. The significant limitations of this are further discussed in Chapter 6.

Pedersen *et al* (2015) clearly demonstrate a positive correlation between hyperinsulinaemia and AT inflammation in mice, where pro-inflammatory cytokines were upregulated with increased insulin and downregulated with decreased insulin, concluding that hyperinsulinaemia directly drives AT inflammation in obese mice[188]. This suggests that *in vivo* the pro-inflammatory effect of hyperinsulinaemia may result in increased numbers of infiltrating blood monocyte-derived M1 macrophages, secreting pro-inflammatory cytokines such as TNFα and IL-1[94] which may induce existing macrophages to take on a pro-inflammatory phenotype[157]. This may lead to decreased pro-fibrotic signalling and therefore decreased pro-fibrotic gene expression.

5.3.3 *The anti-fibrotic effect of insulin and M (IFNγ + LPS) macrophages is not concentration-dependent*

In contrast to expectations of a linear correlation between insulin concentration and degree of pro-fibrotic gene expression, insulin-mediated downregulation of pro-fibrotic genes did not follow a linear concentration-dependent trend. In many

of the genes analysed (e.g. *COL4A1*, *COL5A3*, *TGFB1* and *FN1*), the expression after co-culture with M (IFNγ + LPS) macrophages across all four insulin conditions resembles a 'U-shaped' curve, with higher pro-fibrotic gene expression at 100nM insulin, as shown in Figure 16. This effect may be attributed to mechanisms regulating insulin signalling.

A typical physiological fasting plasma insulin level in a healthy adult under normoglycaemic conditions is 20-140 pmol/l[258], whereas fasting insulin levels in hyperinsulinaemic individuals tend to be upwards of 100pmol/l[259]. Extreme hyperinsulinaemia (represented by 1nM or 10nM conditions[260,261]) is symptomatic of severe insulin resistance in very poorly controlled type 2 diabetes, which is in turn associated with AT fibrosis and dysfunction[160].

Adipocytes negatively regulate insulin signalling by internalising insulin receptors in a 'monoexponential' concentration-dependent and time-dependent manner in response to insulin, meaning that the percentage of insulin receptors internalised increases with both the concentration and time of exposure[262]. Maximal insulin receptor loss is achieved at 100ng/ml insulin[262] (~17nM), therefore it is reasonable to assume cells would have very high levels of insulin receptor internalisation after 48 hours of culture with 10nM or 100nM insulin. As such, treatment with insulin at lower concentrations and for a shorter length of time should have been explored. Negative regulation of insulin signalling could provide an explanation for the observed 'U-shaped' response to insulin concentration, as insulin may exert an anti-fibrotic effect at 1nM and 10nM concentrations while signalling is active, but receptor internalisation or inhibition of downstream signal transduction, as discussed in 1.1.2, prevents this at 100nM.

During the optimisation and design stage of this *ex vivo* cell culture experiment, no consideration was given to the concept that treatment with high concentrations of insulin does not guarantee high levels of insulin signalling in AT. A molecular readout for insulin signalling (such as insulin receptor tyrosine phosphorylation by western blot[32], GLUT4 surface expression by flow cytometry[263] or RNA analysis of *PTPN1* expression[33]) should have been included to understand how insulin signalling is regulated at various concentrations, and to aid optimisation. This would provide greater understanding of how insulin modulates the development of fibrosis, whether that be as a direct or indirect result of traditional insulin signalling pathways.

An alternative explanation may be the activation of insulin-like growth factor (IGF) receptors. Matsui-Hirai *et al* (2011) reported a similar U-shaped effect of supraphysiological levels of insulin (such as 100nM) when measuring its effects on endothelial senescence *in vitro*, although they concluded that this effect only occurred in the presence of high glucose concentrations[264]. They speculate that at supraphysiologically high concentrations, insulin activates IGF receptors[265], which are also expressed on the surface of adipocytes as their signalling is important for differentiation and lipid accumulation[266]. Increased IGF receptor mediated PI3K and MAPK signalling[267] may have influenced pro-fibrotic gene expression. This is reflected by the increased expression of some pro-fibrotic genes in AT when co-cultured with M (IFNγ + LPS) macrophages and 100nM insulin, compared with the downregulation observed at the 1nM and 10nM concentrations. In future it would be informative to expand on the insulin concentrations used, e.g. 0.5nM 1nM, 3nM, 7nM and 10nM, to determine if the

resulting expression level follows this U-shaped curve. It is important to recognise that the vehicle condition is not entirely physiologically accurate, as insulin is required to facilitate the uptake of glucose in adipocytes, and therefore its absence may potentially disrupt normal cell function.

Macrophages express insulin receptors[268], but also express GLUT1 and GLUT3 transporters enabling glucose uptake through insulin-independent facilitated diffusion[269]. This suggests that insulin signalling may be in part required for regulatory functions other than glucose utilisation. It is known that insulin stimulates the IR/IRS2/PI3K/AKT signalling cascade in macrophages, but the effect on the MAPK pathway, which is known to regulate gene expression, is not yet clarified[270]. In an *in vitro* study using bovine monocyte derived macrophages, Eger *et al* (2016) found that macrophages, after differentiation into M1 and M2 subsets, did not appear to express GLUT4 receptors, and therefore the addition of insulin to their culture medium did not increase their glucose uptake[271]. Interestingly, they also discovered that M2 (CD163+) macrophages consumed glucose more readily from their culture medium than M1 (CD11b+) and M0 cells. Although Eger *et al* do not further characterise their M2 macrophages into M2a and M2c subpopulations, this raises the possibility that the M (IL-10) cells in this study were not provided with sufficient glucose in their culture medium, hence their postulated apoptosis (see section 4.3.1).

Insensitivity of macrophages to insulin could potentially alter their functional phenotype, and therefore modulate their effect on ATs. Macrophages *in vivo* can become insensitive to insulin during obesity-induced insulin resistance[272], and high insulin concentration *in vitro* (e.g. 100nM) for 48 hours is sufficient to induce

insulin resistance in macrophages[273]. Insulin resistance in macrophages, which demonstrate metabolic changes and reduced Akt2 phosphorylation, has been suggested to promote an M2-like phenotype[272]. Induction of an insulin resistant, pro-fibrotic M2-like macrophage phenotype at 100nM may at least partly explain the observed 'U-shaped' pattern of expression of pro-fibrotic genes in AT.

PTP1B, an inhibitor of insulin signalling which can be induced by TNF-α[274], also plays a role in the polarisation of macrophages by downregulating cytokine receptor signalling via JAK2 and tyrosine kinase 2 (TYK2) dephosphorylation, and so acting as a negative regulator of JAK/STAT-mediated inflammation[275]. PTP1B-mediated insulin resistance may have pushed mixed phenotype M (IFN-γ + LPS) macrophages closer to a pro-fibrotic M2-like phenotype, which could explain the increased expression of pro-fibrotic genes at 100nM insulin. This is at odds with Tada Iida *et al* (2001), who report that insulin acts on THP-1 macrophages in a concentration-dependent manner to upregulate mRNA expression of TNF-α through an extracellular kinase-dependent pathway[257], implying that insulin influences macrophages to adopt a pro-inflammatory functional phenotype, rather than an anti-inflammatory, pro-fibrotic phenotype.

The potential influence of insulin resistance in macrophages was not considered in this experimental design. Macrophages were not stimulated with insulin in the absence of OMAT, therefore it is not possible to deduce a direct effect on their insulin sensitivity or phenotype. A controlled experiment should be designed wherein differentiated macrophages are treated with insulin at a broad range of concentrations (e.g. 0.1nM, 0.5nM, 1nM, 5nM, 10nM, 50nM, 100nM), before

phenotypic markers and secreted proteins (e.g. TGF-β) are measured by ELISA or western blot. Flow cytometry should also be performed to better understand the phenotypic profile of individual cells after their exposure to insulin, as macrophages are capable of possessing a mixed phenotype[144].

5.3.4 *Insulin and M (IL-4) macrophages do not significantly modulate pro-fibrotic gene expression*

Expression of *LOX* and *SPARC* in OMAT was increased by co-culture with M (IL-4) macrophages, therefore it was hypothesised that this effect may be enhanced by insulin. The addition of insulin at 1nM, 10nM and 100nM concentrations did not significantly modulate the expression of the pro-fibrotic genes analysed. In some genes, e.g. *COL4A1, COL5A3, TGF-β, ELN* and *SPARC*, the effect of insulin concentration on OMAT gene expression again resulted in a 'U-shaped' response curve, likely due to internalisation of insulin receptors as discussed above (section 5.3.3). The pro- or anti-inflammatory effects of insulin are not yet fully elucidated, with conflicting reports of its action[276,277]. These results suggest that insulin action in AT and macrophages warrants further investigation to clarify the mechanistic effects of hyperinsulinaemia and its role in AT dysfunction.

Studies in human monocyte-like (U937) and rat adipocyte cell lines have shown that PMA, used during the differentiation of M (IL-4) and M (IL-10) cells, inhibits insulin binding and induces receptor internalisation[278]. Although THP-1 cells were only treated with PMA for a short time, this may in part explain why co-culture with insulin did not significantly modulate their effect on pro-fibrotic genes in AT.

5.3.5 *Insulin downregulates ELN expression in AT with undifferentiated THP-1 monocyte co-culture*

Co-culture of undifferentiated THP-1 monocytes with insulin and AT resulted in significant downregulation of *ELN* expression in the 10nM insulin condition relative to the vehicle control, potentially demonstrating the first stages of loss of elasticity, as has been observed in obese SCAT[167]. Following this, there was also some decreased expression in the 1nM and 100nM insulin conditions, although this did not reach statistical significance. In the case of the other pro-fibrotic genes analysed, insulin concentration did not induce significant changes in expression, however there was a slight tendency decrease in *COL1A1, COL3A1, COL6A3* and *TGFβ1*.

Insulin is a potent growth factor, regulating growth and differentiation of cells[279], therefore it is possible that culture with insulin at different concentrations may provide a stimulus to influence the function and phenotype of these undifferentiated macrophages. In an *in vitro* study using human hepatic cells, Iwasaki *et al* (2009) report that insulin initially exerts an anti-inflammatory effect on cells, but after 36 hours of chronic insulin exposure, mimicking the microenvironment of insulin resistance, pro-inflammatory effects were observed through the stimulated transcriptional activity of NFκB, a key transcription factor facilitating the expression of many genes associated with inflammation[277]. To clarify whether this is the case in our experimental model, it would be necessary to measure the accumulation of molecular mediators of inflammation and fibrosis (e.g. MCP-1 and TGF-β), secreted by both AT and macrophages into the media, at various time-points during the co-culture period using ELISA, or analyse cells by western blot. It may be of interest to explore whether there is a similar shift

from an anti-inflammatory/pro-fibrotic to pro-inflammatory microenvironment when macrophages are treated with insulin, measuring protein levels of secreted cytokines at different timepoints between 6h and 72h.

5.4 **Summary**

There are conflicting reports regarding the role of insulin in AT inflammation and fibrosis, therefore it was unsurprising that insulin did not exert a pro-fibrotic effect as hypothesised, and instead may have a slight anti-fibrotic influence. After phenotypic analysis of differentiation showed discrete M1, M2a and M2c macrophage populations had not been achieved, the effect of macrophage phenotype along with insulin on the development of AT fibrosis became more difficult to define. The observed ‘U-shaped’ concentration-dependent effect was not initially anticipated, but appears to be explained upon reviewing the negative regulatory mechanisms involved in insulin signalling. It is clear that the role insulin may play in the development of fibrosis is more complex than initially thought, and requires further investigation.

Chapter 6: Discussion

This study aimed to investigate how macrophages and hyperinsulinaemia, a hallmark of insulin resistance, contribute towards the development of AT fibrosis. The objective was to better define the influence of macrophages and their phenotype, along with insulin, on the expression of genes associated with fibrosis in OMAT. The response of THP-1 monocytes to *in vitro* differentiation was assessed, and the effect of polarised macrophages alone, and with insulin, on OMAT gene expression was analysed.

6.1 Main conclusions

Analysis of macrophage markers showed differentiation of M (IL-4) macrophages induced a broadly M2-like phenotype as opposed to the expected M2a-like phenotype, however differentiation of M (IL-10) macrophages clearly did not induce an M2c-like macrophage. As previously discussed, cells may have become apoptotic during the differentiation period, however as apoptosis was not measured in this study, this cannot be assumed to be the cause of lower than expected gene expression. As such, conclusions about the role of M2c macrophages in AT fibrosis cannot be made based on the results of this study. If these data were replicated with viable macrophages shown to be of an M2c-like phenotype, this may call into question the consensus on the role of M2c macrophages in AT fibrosis.

Much of the literature regarding the 'wound-healing' function of M2 macrophages implicates M2c macrophages as key inducers of AT fibrosis[94,233] due to their reportedly strong secretion of TGF-β isoforms[94]. TGFβ-1 upregulates expression

of fibrous ECM proteins in AT[15] by inducing a pro-fibrotic transcriptional programme via Smad signalling[178,238], hence the hypothesis that genes associated with fibrosis would be more strongly upregulated by co-culture with M2c-like macrophages than with M1 or M2a-like macrophages.

Of the differentiated macrophages, TGF-β was most strongly secreted by M (IFNγ +LPS) cells. Phenotypic analysis of M (IFNγ + LPS) macrophages suggests cells possessed a mixed M1/M2 phenotype. Considering mixed-phenotype macrophages are reported *in vivo*[144,145], these cells may be more closely representative of human ATMs. M (IFNγ + LPS) macrophages were able to induce significant upregulation of *FN1* in OMAT. This was attenuated by insulin, suggesting a protective anti-fibrotic role, which could be explained by the proposed pro-inflammatory effect of insulin[188,257] pushing AT macrophages towards a more M1-like functional phenotype, and therefore reducing their secretion of TGF-β. Further experimentation and macrophage characterisation would be required to provide evidence for this. TGF-β signalling in AT could be more thoroughly investigated by quantifying phosphorylation of Smad2/3 proteins, and expression of downstream targets such as *PAI-1*, which is transcriptionally regulated by TGF-β[144,280].

The findings of our study to some extent support a pro-fibrotic role for broadly M2-like macrophages, as molecular mediators of fibrosis *LOX* and *SPARC* were significantly upregulated in AT after co-culture with M (IL-4) macrophages. This pro-fibrotic view is supported by Spencer *et al* (2010), where stem-cell derived adipocytes cultured in M2 macrophage-conditioned medium expressed two fold higher levels of *PAI-1* than adipocytes cultured in M1 macrophage-conditioned

medium[144], indicating increased TGF-β signalling. It is important to note that Spencer *et al* do not publish supporting data validating the phenotype of their differentiated macrophages. The findings of our study highlight the importance of assessing the efficacy of macrophage differentiation, a step which is often overlooked in similar co-culture studies[144,146].

Insulin at physiologically relevant concentrations was shown to have slight anti-fibrotic effects on macrophage-mediated gene upregulation in OMAT. The concentration-dependent effect of insulin was 'U-shaped', and this pattern was observed across various genes with all three macrophage types, and may be caused by feedback mechanisms inhibiting insulin signal propagation, including insulin receptor internalisation, in response to high concentrations of insulin.

In future, conclusions about the role of macrophage subtypes and insulin in the development of AT fibrosis may only be made after considerable optimisation and revisions to experimental design.

6.2 Study strengths

6.2.1 *AT explants*

A defining feature of this study was the use of human OMAT explants in culture, providing advantages over co-culture studies which use only mouse or human-derived adipocytes[144,146,184]. Human explants allow for the physiological AT environment to be recreated more closely, and provide all of the cells of AT (including preadipocytes and endothelial cells of the SVF) in the correct proportions, enabling a greater and more physiologically accurate range of cell

interactions. The SVF, containing the preadipocyte cells, is responsible for the majority of expression of genes associated with fibrosis[147,164], therefore using AT explants in macrophage co-culture is a more informative technique, rather than just adipocytes cultured with a conditioned medium, and is likely to provide a better picture of how macrophages and insulin influence the development of fibrosis in AT *in vivo*.

Specific inclusion and exclusion criteria (detailed in section 2.2.1) were implemented when recruiting subjects to the study to limit confounding factors in the experiment. Metformin, a commonly prescribed anti-diabetic drug, has been found to attenuate fibrosis by inhibiting TGF-β1/Smad3 activation[281,282] therefore patients undergoing treatment for T2DM were excluded.

6.3 Study limitations

6.3.1 *Participants*

OMAT samples were obtained through routine gynaecological procedures (see section 2.2.1), therefore all participants were female. Although it is well established that AT deposition is strikingly different between males and females, differences in metabolism have not been well described[283]. As a result, it cannot be assumed that these results would be reproduced in male-derived explants. One important factor to note in an all-female cohort is the potential impact of the peri-menopausal or post-menopausal state on AT metabolism. The age of the subjects in this study varied from 42 to 64 and were likely to include individuals at various stages of menopause. There are reported differences in

subcutaneous[284] and omental[285] AT metabolism as a result of menopausal changes, raising the likelihood of variability in fibrosis development.

The BMI of subjects covered a wide range, from 19.8 to 36.1, which may have impacted the *in vitro* transcriptomic indictors of fibrosis development and contributed to high variability of data. In AT from obese individuals, the percentage of macrophages with an M2 phenotype is shown to be almost five times higher than in lean individuals[144], suggesting that AT from obese donors could already be inflamed and have high baseline levels of fibrosis or expression of pro-fibrotic genes. The addition of pro-fibrotic macrophages *in vitro* may have a limited influence if TGF-β signalling is already highly active. Of the six explants analysed, only two donors were of a healthy BMI – neither obese nor overweight. In future studies, an overweight or obese BMI could be considered exclusion criteria, however this would dramatically reduce the availability of donated OMAT. An alternative may be to assign donors into cohorts according to BMI and analyse data with reference to each cohort. This may reduce the variability of results and increase the significance of any findings.

6.3.2 ***Use of THP-1 monocyte line***

The practicalities of using THP-1 monocytes over primary cells were an important consideration during the design of this experiment. THP-1 cells did not require blood sample collection or cell isolation, as necessary to obtain primary PBMCs. THP-1 monocytes are derived from a single source so are genetically homogenous, and therefore their use simplifies the analysis and interpretation of

results, and should increase reproducibility and consistency between experiments.

There are some limitations to using THP-1 monocytes, which are acute myeloid leukaemia-derived. Cancer cells undergo a metabolic switch, favouring anaerobic glycolysis (resulting in the production and secretion of lactate) over oxidative phosphorylation, even in the presence of adequate oxygen[286]. There is a clear link between glycolysis and inflammation, as monocytes with increased glucose consumption can demonstrate highly upregulated pyruvate kinase M2 (PKM2), which upregulates IL-6 and IL-1β via pSTAT3[287]. M2 macrophages utilise oxidative phosphorylation, whereas M1 macrophages favour glycolysis for ATP production. Glycolysis-derived metabolites fuel the pentose phosphate pathway, which increases amino acid synthesis and allows for additional protein synthesis[288]. This suggests a potentially increased capacity for protein secretion and extracellular signalling from leukaemia-derived THP-1 monocytes, compared to primary PBMCs, as well as a metabolic profile primed for pro-inflammatory macrophage differentiation, which may account for the challenges encountered during polarisation.

When compared to PBMCs, key immuno-metabolic *genes KYNU, IL6, IL10, CCL4* and *IL1R2* are reduced or not expressed in THP-1 cells, suggesting responses to microenvironmental stimuli may differ[289]. *In vitro* cultured THP-1 cells respond differently to the same stimulus when compared to PBMC-derived macrophages[290], and behave differently under differentiation-inducing conditions, reportedly expressing M2c marker *CD163* mRNA at a much lower level than PBMCs[227]. Although a study using donor-matched OMAT and differentiated

PBMCs may more closely represent biological conditions *in vivo*, the logistical limitations and time constraints of blood and tissue collection prevented this, along with the added ethical complexity of performing a blood collection procedure.

6.3.3 ***Optimisation experiments***

Insufficient optimisation of cell culture protocols and experimental design is one of the biggest limitations associated with this study (see section 7 for optimisation data). Thorough optimisation and validation of THP-1 differentiation was critical for the generation of good quality, meaningful data. Differentiation was optimised over three separate experiments where n=2, therefore no statistical test could be applied. An accurate consensus on the outcome of macrophage differentiation cannot confidently be drawn based on such a small dataset. These experiments should have been continued up to at least n=3 independent identical experiments before progressing to a larger scale study, especially as successful macrophage differentiation underpinned the whole study. As discussed in this chapter, RNA analysis of cell surface markers was inappropriately employed to validate differentiation.

A pilot co-culture experiment was performed, however the collected OMAT explant was not analysed, as the experiment was used to review the seeding density and sustained differentiation of THP-1 monocytes. In the final analysis (Figure 19), the phenotype of M (IL-4) and M (IL-10) cells had not been clearly defined, yet protocols were considered sufficiently optimised to progress to a larger study using precious human tissue. Despite choosing to quantify RNA

expression, the timepoint for this analysis was not optimised with regards to the chosen genes, and was simply chosen based on work by Spencer *et al* (2010)[144]. A comprehensive discussion of how optimisation should be performed is included in 6.4.

6.3.4 ***Determination of macrophage phenotypes***

The methods used to determine the phenotype of differentiated macrophages present significant limitations. qRT-PCR was used to assess how strongly differentiated macrophages upregulated expression of their respective cell surface markers. Performing this analysis at the RNA level was wholly inappropriate due to regulation of post-transcriptional, post-translational and membrane trafficking processes. RNA levels of surface markers may not correspond with presented proteins on the cell surface, and the timepoint at which RNA was obtained is likely to be critically important for the presence of gene transcripts. Flow cytometry should have been used, and would have allowed for assessment of phenotypic heterogeneity within the differentiated cell population. RNA analysis could have provided valuable phenotyping information, had genes indicating functional macrophage characteristics (e.g. pro- and anti-inflammatory cytokines) been analysed.

Macrophage-secreted proteins suggesting functional phenotype were analysed by ELISA. The accuracy of any ELISA interpretation is reliant on construction of a standard curve, therefore a high r^2 value (>0.95) is critical for good quality data. One ELISA plate for detection of IL-10 could not be included in the dataset because the standard curve r^2 value was too low, therefore only three

experiments were analysed for this protein. Unfortunately, standard deviations were very high, likely because insufficient optimisation of macrophage differentiation led to poor reproducibility and consistency across independent experiments. For example, considerable variability may have arisen from differences in attachment rate or viability of differentiating macrophages, which was not controlled for.

Detection of OLR-1 relies on membrane shedding, therefore production of the protein may not directly correlate with secretion. Analysing secreted proteins in cell culture medium was only used for determining macrophage phenotype after differentiation treatment, as the co-culture experimental design did not include a macrophage-insulin condition. This control should have been included, and the lack of data regarding how insulin influences macrophage phenotype severely limited the interpretation of data collected in this study.

6.3.5 *OMAT and macrophage co-culture*

Despite providing the benefits of an *ex vivo* tissue system for co-culture, AT explants present unique challenges, as the cellular composition will vary between subjects. Although weighed to 250±20mg before co-culture, explants will contain adipocytes, preadipocytes and resident macrophages in different numbers. Gene expression was calculated relative to the expression of housekeeping genes, so should normalise any effect caused by differing cell numbers. Macrophages were seeded consistently at a density of $4x10^6$ per well, meaning that the same number of macrophages may have exhibited a larger effect on AT gene expression if there were fewer adipocytes (or preadipocytes) present. As a result, explants with

fewer cells may give an exaggerated impression of the effect of macrophages on fibrotic gene expression.

The supraphysiological quantity of macrophages should reduce the effects of any tissue-resident macrophages, but these endogenous cells may still contribute towards high variability of gene expression between subjects. Due to AT heterogeneity, there may also be small differences between explants obtained from the same donor, leading to inconsistency within experimental duplicates as well as control explants. This heterogeneity was observed during tissue processing, as some areas of OMAT were more heavily vascularised or fibrotic than others. The most prominent areas of fibrosis and vasculature were removed, but some inherent variation of tissue morphology will inevitably remain.

The quantity of macrophages in the co-culture medium depended on their differentiation. $4x10^6$ THP-1 cells per well were initially seeded in suspension and their differentiation medium was removed after 48h, on the assumption that macrophages would adhere during differentiation. A significant number of suspended cells would have been removed had culture conditions failed to effectively induce differentiation. As a result, macrophage number will have inevitably varied between culture conditions and individual experiments, potentially precluding the detection of a macrophage-induced effect on OMAT, and introducing yet more variability. This issue should have been identified and rectified during optimisation, as differentiated macrophages could have been re-seeded at the correct cell density and allowed to attach for 24 hours before co-culture set up. Their viability in response to differentiation stimuli, particularly

inflammatory IFNγ and LPS[228], should have been considered and could have been investigated using a simple alamarBlue assay.

Another point of variation in AT explants is the production and secretion of adipokines, such as adiponectin, which may differ between explants. Adiponectin is reported to promote polarisation towards an M2 macrophage phenotype in human PBMCs, and be capable of inducing M1-to-M2 transdifferentiation[291,292], so could influence the phenotype of differentiated macrophages in co-culture. As a result, AT gene expression in the studied participants may be influenced. Had experimental design been more carefully considered, an aliquot of macrophages could have been collected, stained, fixed and analysed by flow cytometry to answer this question.

LPS induces an M1 phenotype in macrophages via TLR4 receptor activation and stimulation of pro-inflammatory signalling pathways, however there is evidence that some FFAs behave as ligands for these receptors, and play a role in the development of insulin resistance in obesity[140]. Processing AT explants into 500µm^3 pieces caused significant lysis of adipocytes and allowed lipid to escape. During set-up of the co-culture experiments, the amount of lipid appeared to vary between samples of different subjects, as some explants were distinctly more 'oily' than others. This may have resulted in uncontrolled activation of macrophage TLR4 receptors, promoting an M1, pro-inflammatory phenotype. Such exposure to high levels of FFAs does not accurately represent conditions *in vivo*, and again it is not possible to retrospectively measure the potential effect of this on macrophage phenotype by appropriate means, such as flow cytometry.

Although the co-culture assay was carried out at *n*=10, due to limited time and resources only 6 explants were analysed. In future, analysis of these samples could increase the significance of findings, however with such a flawed experimental design, this is unlikely to be a good use of resources.

Insulin treatment was not optimised by any means. Chosen concentrations were loosely based on Kos *et al* (2009)[177], but the complexity of insulin signalling was not appreciated, and negative regulation of insulin signalling in response to high insulin concentration was not considered. The potential for inducing insulin resistance in macrophages *in vitro* by treating with such high concentrations of insulin was also not recognised, and may have introduced a confounding variable preventing meaningful interpretation of results. Another fundamental flaw was that a simple readout for validating insulin signalling in AT or macrophages, e.g. western blot of IRS-1 tyrosine phosphorylation or flow cytometric detection of externalised insulin receptor, was not included, hampering results interpretation.

6.3.6 ***RNA analysis of pro-fibrotic genes***

Analysis of gene expression by RNA was the sole readout for this experiment examining fibrosis. Fundamentally, fibrosis occurs at the extra-cellular protein level, with much opportunity for post-transcriptional and post-translational regulation. mRNA and protein abundance only partially correlate[293], therefore RNA analysis alone does not provide sufficient information to make conclusions about the development of fibrosis. For example, TGF-β is synthesised in inactive precursor form and must undergo proteolytic processing into its bioactive form[294]. This additional level of processing further reduces the likelihood that RNA levels

of TGF-β correlate with the abundance of the active protein. In combination with techniques analysing protein production and secretion however, RNA analysis can be a useful tool to help build a clearer picture of biological processes and their regulation.

A 48 hour timepoint was chosen based on a previous co-culture study[144] where gene expression of cytokines in macrophages was analysed. This was not optimised, and it was not considered that different genes may be expressed at different timepoints in the development of fibrosis. A comprehensive literature review suggests that 24 hours is a more appropriate timepoint to analyse molecular mediators of fibrosis (e.g. *CTGF* and *TSP-1*)[146]. Previous work by Kos *et al* (2009) even demonstrates an insulin-induced SPARC protein increase after 24 hours, suggesting 48 hours may be too late to detect RNA upregulation. In designing analysis timepoints for such an experiment, it is critical to understand and consider the sequence of events involved in gene expression, from transcription, RNA processing and export, to translation, protein maturation and finally secretion.

Insulin may act in a post-transcriptional manner to influence fibrosis[184], therefore it is inappropriate to analyse its effect on matrix components at only the RNA level. Were comprehensive literature searches performed, and insulin treatment optimised, the experimental design could have included analysis of the matrix processing enzymes targeted by insulin, such as *PCOLCE*[184].

6.3.7 ***Summary***

Numerous fundamental flaws in experimental design severely hampered the interpretation of results obtained in this study. Appropriate optimisation would have highlighted these and informed refinements to the study design, preventing wasted time and resources. Human tissue samples were generously donated by patients undergoing surgery, therefore researchers had a moral obligation to conduct well-planned studies generating meaningful data, with potential for a wider impact in the field.

6.4 Further work

The following work should be carried out to generate good quality publishable data, addressing the original goals of this study and enabling conclusions to be drawn.

6.4.1 *Optimisation of macrophage differentiation and phenotypic classification*

The methodology used in published studies requiring macrophage differentiation varies greatly. This study used all cytokines at a concentration of 20ng/ml to induce differentiation, as per methods used by Spencer *et al* (2010) and Finlin *et al* (2013)[144,146], however Mia *et al* (2014) purport to achieve strong M1 differentiation in PBMC-derived macrophages using IFNγ at 20ng/ml and LPS at 50ng/ml, over just 24h. By contrast, Porcheray *et al* (2005) used all cytokines at 10ng/ml to stimulate cell differentiation over four days[218].

To optimise macrophage differentiation, a range of cell treatment times should be tested and could include 24, 48, 72 and 96 hours. The concentration of cytokines used to induce differentiation could be altered and increased. Increasing LPS concentration to 50ng/ml may, in addition to IFNγ, provide a strong enough stimulus to push monocytes closer towards an M1-like phenotype, limiting expression of M2c marker *CD163* and secretion of TGF-β. Alternatively, or in addition, pro-inflammatory TNF-α could be used to enhance differentiation into an pro-inflammatory phenotype[94]. Macrophage viability must be assessed during optimisation of differentiation protocols.

Genin *et al* (2015) and Chanput *et al* (2013) used IFNγ and LPS to differentiate THP-1 monocytes into M1 macrophages, but also used PMA to induce initial 'monocyte-to-macrophage' differentiation before polarisation. Genin *et al* used PMA at 150nM for 24h before an additional 24h of control medium[228], whereas Chanput *et al* (2013) obtained a 'macrophage-like state' by treating cells with 100ng/ml for 48h[225]. Our study exposed cells to 5nM PMA for only five minutes during M (IL-4) and M (IL-10) differentiation, as per methods published by Spencer[144]. Inclusion of a 'monocyte-to-macrophage' step may enhance differentiation into a defined pro-inflammatory M1-like phenotype.

A combination of IL-4, IL-10 and TGF-β could be used to upregulate IL-10 secretion[229]. TGF-β in isolation has been reported to be a potent inducer of CD206 expression[218,295] and downregulator of CD163[218], suggesting it could be utilised to promote differentiation into M2 (or more specifically, M2a)-like macrophages in culture. As IL-13 is an established inducer of M2a expression[94] and thought to act on macrophages via the same signalling pathway as IL-4[296], incorporating it into the M2a differentiation condition may induce a more M2a-like phenotype[94].

Macrophage differentiation should be validated using flow cytometry for cell surface markers, and would ideally include CD80 (monocyte marker), CD68 (pan-macrophage marker), CD86 (M1 marker), CD206 (pan-M2 marker), and CD163 (M2c marker). M1 macrophages are expected to be $CD68^{+}CD80^{+}CD86^{high}CD206^{low}CD163^{low}$, whereas M2a and M2c macrophages are expected to be $CD68^{+}CD80^{-}CD86^{low}CD206^{high}CD163^{low}$ and $CD68^{+}CD80^{-}CD86^{low}CD206^{high}CD163^{low}$ respectively[94,297]. In practical terms, the number of

markers analysed simultaneously may need to be reduced due to fluorophore spectral overlap, therefore CD68 and CD80 could be removed. Critically, a marker of cell viability should be used to identify dead cells, allowing differentiation protocols to be modified to address cell mortality if required.

Additional differentiation markers could be used to help give a more complete picture of macrophage polarisation. Co-stimulatory molecules CD40 and CD80, as well as CD274 which encodes the programmed death-ligand 1, are present on the surface of antigen presenting cells, and may better detect if macrophages are M1-like[157,229,234]. As subtypes of M2 macrophages are still relatively poorly defined, it is difficult to identify undisputed markers which allow for confident characterisation of M2a or M2c macrophage subtypes *in vitro*. The use of CD163 as an M2c marker is contested, as Barros *et al* (2013) believe it to be expressed by macrophages not of the M2 phenotype[298]. In addition, Lech *et al* (2012) controversially claim M2a cells are the primary pro-fibrotic macrophage phenotype, able to secrete TGF, CTGF and ECM molecules[299]. For these reasons, it is imperative to also classify AT macrophages in accordance with their functional characteristics and activation, as suggested by Murray *et al* (2014)[300].

ELISA should be used to quantify IL-1β, IL-6, TNF-α, IL-10 and TGF-β secretion from macrophages, with M1 macrophage supernatant expected to be IL-1β^{high}IL-6^{high}TNF^{high}IL-10^{low}TGF-β^{low}, M2a supernatant IL-1β^{low}IL-6^{low}TNFα^{low}IL-10^{intermediate}TGF-β^{low} and M2c supernatant IL-1β^{low}IL-6^{low}TNFα^{low}IL-10^{high}TGF-β^{high} [94,229]. RNA analysis should also be performed to assess genetic upregulation of these secreted products.

6.4.2 *Optimisation of co-culture conditions*

Following optimisation and validation of macrophage differentiation, conditions for AT/macrophage co-culture must be optimised. Should fresh human AT samples be scarce, preliminary optimisation experiments may be performed on culture-expanded human preadipocyte cells, or murine cell line 3T3-L1.

Differentiated macrophages should be trypsinised and seeded at the optimised density and co-cultured with AT on hanging cell culture inserts. Ideally, AT donors would have a healthy range BMI. The co-culture should be initially performed as a time course, with preliminary timepoints of 24, 36, and 48 hours. Cells/AT explants should be collected and aliquoted for RNA and protein analysis.

Initial AT protein analysis by western blot could focus on detection of type I, III, IV, V and VI collagens, fibronectin and elastin, and may also include targets of TGF-β and insulin signalling e.g. pSmad2/3 and pIRS-1, allowing insulin concentration to be optimised. RNA analysis could centre around detection of molecular mediators of fibrosis, such as *LOX*, *SPARC*, *CTGF*[144,301], and *TSP-1*[302–304]. Critically, AT should be collected and processed for a hydroxyproline assay, a molecule essential for collagen helix stabilisation and indicative of mature collagen deposition. Timepoint optimisation for this particular assay is imperative and may require a significantly longer co-culture period, allowing for expression, processing, secretion and assembly of fibril-forming collagen. The number of genes and proteins of interest and timepoints analysed should be refined based on the results obtained. Should co-culture data suggest increased AT fibrosis after co-culture with M2c-like macrophages, a TGF-β receptor inhibitor

(SB505124[146]) condition could be added to determine specificity to TGF-β signalling.

6.4.3 *Effect of insulin on macrophage phenotype*

The effect of insulin on macrophages is controversial, as there are claims of pro- and anti-inflammatory effects. Ghanim *et al* (2001, 2008) report that insulin exerts a potently anti-inflammatory effect on human blood mononuclear cells *in vitro*[189,305]. Brundage *et al* (2008) determine that THP-1-derived macrophages stimulated with LPS increased TNF-α and IL-6 secretion after treatment with 100nM insulin, therefore exerting a pro-inflammatory effect on macrophages[306].

Essentially, AT-free insulin and differentiated macrophage control conditions must be included for analysis of any pro-fibrotic or pro-inflammatory effect on macrophage phenotype. As macrophage-secreted products could not be analysed from co-culture medium, pro- and anti-inflammatory cytokines (e.g. IL-6, IL-1β, TNF-α, IL-10, TGF-β) may be detected at the RNA or protein level. After co-culture, an additional aliquot of macrophages could be collected from each condition for cell surface marker analysis by flow cytometry, to determine if transdifferentiation from an M1-like to M2-like cell or vice versa[139,218] has taken place in response to insulin or AT-derived signals. These data may later inform understanding of AT fibrosis phenotypes.

6.5 Future perspectives

6.5.1 *Macrophage classification*

Murray and colleagues (2014) discuss the issues and controversy surrounding activation and nomenclature of macrophages *in vitro.* They specifically highlight a lack of common consensus regarding macrophage classification, with different groups choosing to adopt various terms to describe phenotypes[300]. The restrictive and outdated nature of the existing terms, based on a limited set of ligands, no longer accurately reflect the complexity of macrophage phenotype and activation[142].

To allow direct comparisons to be drawn between studies, it would be pertinent to publish a standardised protocol for macrophage differentiation into polarised populations, named according to the activation stimuli, e.g. M(IL-10), or M(IL-4), as directed by Murray *et al* (2014). They also suggest a consensus is needed to standardise macrophage characterisation[300], enabling better interpretation of studies such as this, where macrophage phenotype cannot be discretely described. In the context of this study, accurate differentiation and phenotyping of macrophages is essential to determine how macrophages of pro- and anti-inflammatory phenotypes modulate AT fibrosis on their own and as a result of interactions with insulin.

6.6 Final conclusions

This study used AT-macrophage co-culture with insulin with the aim to demonstrate the importance of polarised macrophages in the development of fibrosis in AT, and how this may be differentially modulated by hyperinsulinaemic conditions. The results suggest that M (IL-4) macrophages may play a role in upregulating molecular mediators of fibrosis *LOX* and *SPARC* in OMAT, and M (IFNγ+LPS) macrophages, which differentiation analysis suggests possess a mixed M1/M2 phenotype, may increase OMAT *FN1* expression. Insulin appeared to reduce expression of some pro-fibrotic genes in OMAT and M (IFNγ+LPS) macrophage co-culture at 1nM and 10nM concentrations, but not at the supraphysiological 100nM condition. A lack of strongly increased TGF-β or IL-10 secretion from M (IL-10) macrophages indicated these cells were not functionally M2c-like, therefore the effect of M2c macrophages remains unclear.

Numerous fundamental flaws in experimental design and a lack of optimisation introduced inherent variability and various other confounding factors to this study, precluding scientifically robust conclusions from being drawn. Experiments would need to be thoroughly optimised and repeated with the changes recommended in section 6.4 to truly assess the roles of polarised macrophages and hyperinsulinaemia on the development of fibrosis in AT, as well as the direct effect of insulin levels on macrophage phenotypes.

Appendix 1

7.1 Optimisation experiments

7.1.1 *THP-1 differentiation*

Methods for THP-1 differentiation were adapted and optimised by Dr E Pastel based on methodology published by Spencer *et al* (2010)[144]. Initial experimentation used THP-1 monocytes at a density of $1x10^6$ cells in 2ml of serum-free 2mM L-glutamine enriched RPMI media per well of a 6 well plate (105,000 cells/cm^2), with M1 differentiation molecules LPS and IFN-γ at 20ng/ml and 20ng/ml respectively. For M2a and M2c differentiation, cells were initially treated with 5nM PMA in the same composition of RPMI for 5 minutes at room temperature, before seeding in 1% penicillin-streptomycin, serum-free RPMI with 20ng/ml IL-4 or 20ng/ml IL-10 for M2a and M2c differentiation respectively. Duplicate cultures were incubated overnight at 37°C, before RNA was extracted and qRT-PCR performed in triplicate to indicate differentiation relative to an untreated THP-1 control.

RNA pellets were observed to be very small after extraction, therefore an increased number of cells per well was considered necessary to obtain more nucleic acid in future experiments. Reverse transcription was carried out using SuperScript™ VILO™ cDNA Synthesis Kit (Invitrogen). qPCR was carried out using TaqMan probes for *CD68* (pan macrophage marker), *CD86* (M1 marker), *CD206* (pan M2 marker) and *CD150* (M2c marker) transcripts.

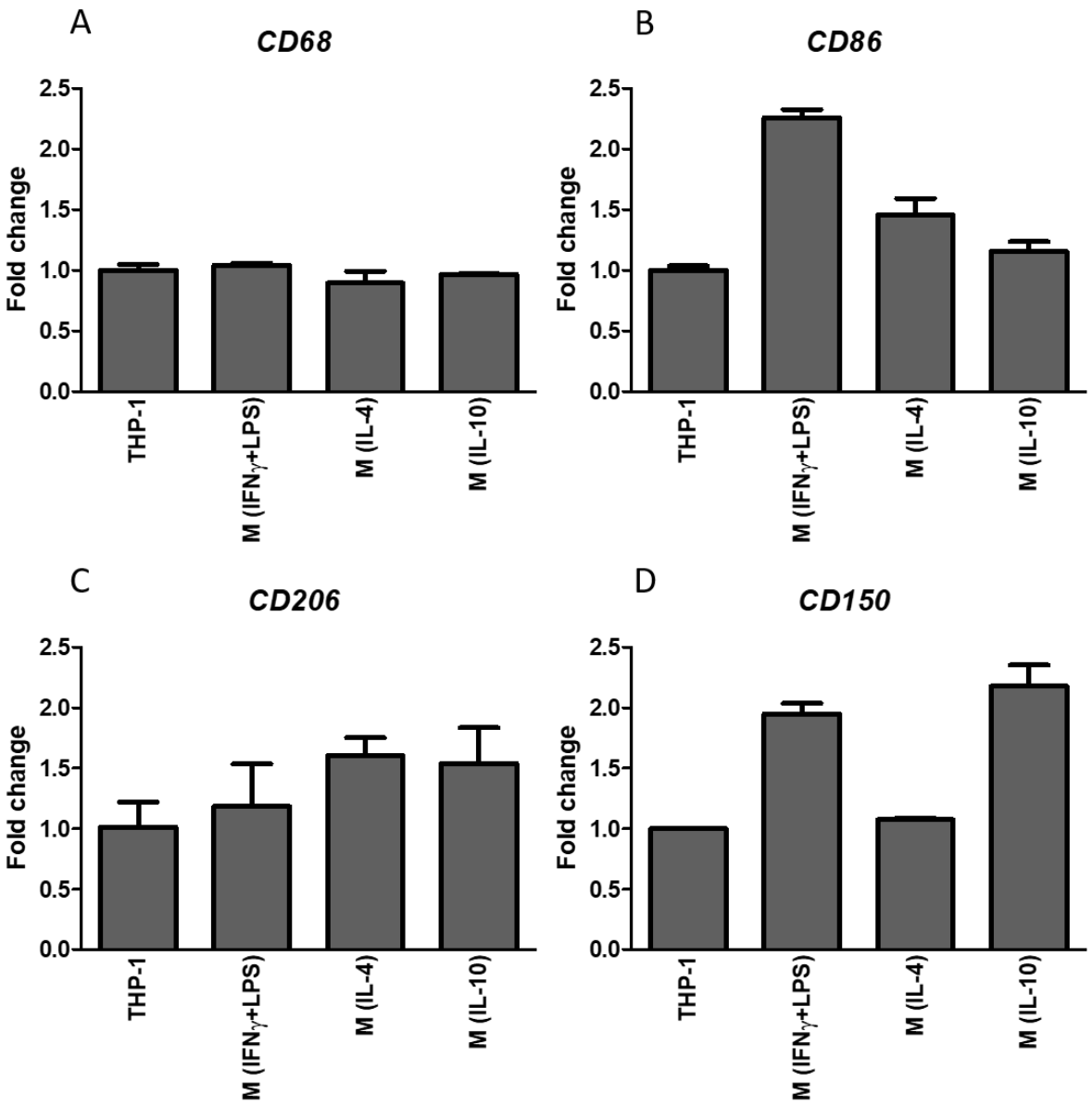

Figure 17: *First optimisation test*. $2^{-\Delta\Delta Ct}$ values from M (IFNγ + LPS), M (IL-4) and M (IL-10) cells, normalised to and compared with untreated THP-1 control. Markers of differentiation: *CD68*, pan-macrophage marker (A), *CD86*, M1 marker (B), *CD206*, mannose receptor, a pan-M2 marker (C) and *CD150*, also known as *SLAMF1*, an M2c macrophage marker (D). Data represented as mean fold change ±SD, *n*=2 technical replicates in a single experiment.

Results (Figure 17) showed all cells after culture, including undifferentiated cells, expressed comparable levels of pan-macrophage marker *CD68* (Figure 17A), whereas the M1 marker *CD86* (Figure 17B) was most highly expressed in M (IFNγ + LPS) cells (2.26±0.068 fold change). M2 marker *CD206* (Figure 17C), was most highly expressed in PMA treated cells (1.603±0.15 and 1.541±0.29-fold change for M (IL-4) and M (IL-10) cells respectively), but sample size (*n*=2) was too small to determine significance. M (IL-10) cells expressed *CD150* with a 2.18±0.175-fold increase (Figure 17D) from the control, but M (IFNγ + LPS) treated cells showed a 1.95±0.088-fold increase. Combined with *CD206* expression, Dr Pastel concluded that a differentiation can still be made between M2a-like and M2c-like cells, and that these data suggested an extended cell differentiation time may increase differentiation.

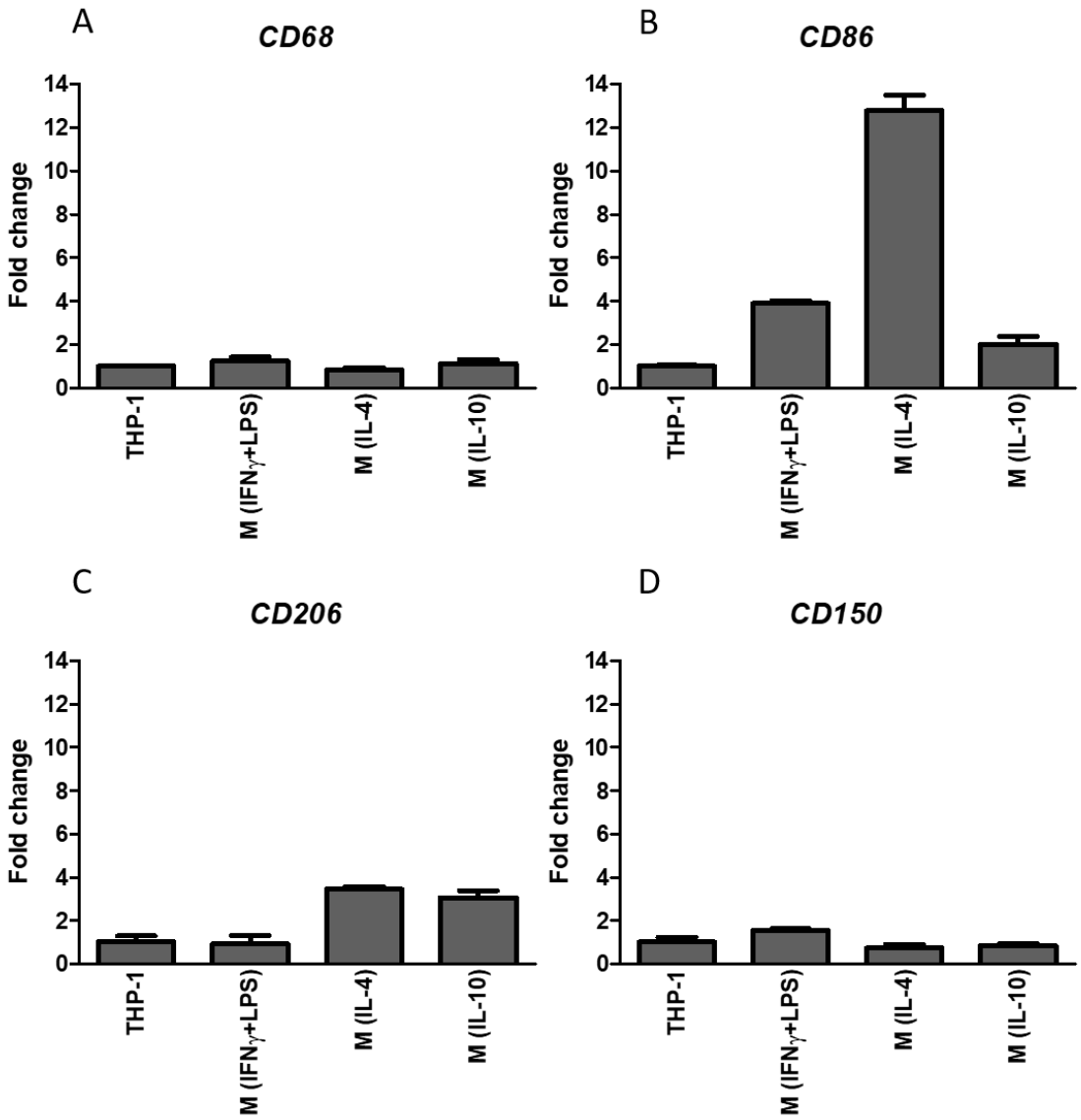

Figure 18: *Second optimisation test*. $2^{-\Delta\Delta Ct}$ values from M (IFNγ + LPS), M (IL-4) and M (IL-10) cells, normalised to and compared with the untreated THP-1 control. Markers of differentiation: *CD68*, pan-macrophage marker (A), *CD86* (B), *CD206* (C), and *CD150* (D). Data represented as mean fold change ±SD, *n*=2 technical replicates in a single experiment.

In the second round of optimisation, cells were seeded at $2x10^6$ cells/well (210,500 cells/cm^2), PMA incubation was carried out at 37°C, and cells were cultured for 48h (as opposed to 24h). This led to higher *CD86* expression (Figure

18B) from M (IFN-γ + LPS) cells (3.89±0.13 fold increase) and increased *CD206* expression (Figure 18C) in PMA-treated cells (mean 3.453±0.12 and 3.057±0.33 fold increases for M (IL-4) and M (IL-10) cells respectively), suggesting that a longer culture period and more physiologically-matched PMA incubation temperature helped increase differentiation.

7.1.1 *AT/THP-1 co-culture*

After optimisation of the differentiation protocol, Dr E Pastel performed a pilot co-culture experiment with human OMAT. The processed explant, (250±20mg per well) was cultured with differentiated THP-1 cells ($2x10^6$ cells/well) for 48 hours at 37°C, 5% CO_2, in media supplemented with insulin at various concentrations (vehicle, 1nM, 10nM, and 100nM). Supernatant and adherent macrophages were collected, along with all pieces of AT, and stored in Ambion TRI Reagent® Solution at -80°C. RNA was extracted from macrophages collected from control wells (without AT explants or insulin) to determine if dedifferentiation and taken place after an additional 48 hours with normal culture medium. THP-1, M (IFN-γ + LPS), M (IL-4) and M (IL-10) conditions were assessed in technical duplicates (one experiment), and RNA concentration was found to be low in all samples, i.e. <100ng/ml. For the THP-1 condition, RNA levels were particularly low – only one well yielded enough RNA to perform reverse transcription. Dr Pastel concluded that undifferentiated cells would be less adherent to the culture wells, and so fewer cells would have been collected. In response to this, cells would be seeded at $4x10^6$ cells/well in future experiments to increase RNA yield.

When qRT-PCR was performed on differentiated macrophages, all conditions showed elevated expression of *CD68* relative to the undifferentiated control (Figure 19A), suggesting a macrophage-like phenotype. M (IFNγ + LPS) cells upregulated *CD86* (Figure 19B) and showed a mean 9.229±1.56-fold increase relative to the control. M (IL-4) cells did not upregulate pan M2 marker *CD206* (Figure 19C), but M (IL-10) cells showed a 3.2±0.69-fold increase, and M2c marker *CD150* (Figure 19D) was decreased in M (IL-4) and M (IL-10) differentiated cells (0.485±0.002 and 0.42±0.09-fold change respectively). In light of this, a second TaqMan probe for *CD163*, reportedly another marker of M2c phenotype[233], was acquired to use in the main experiment.

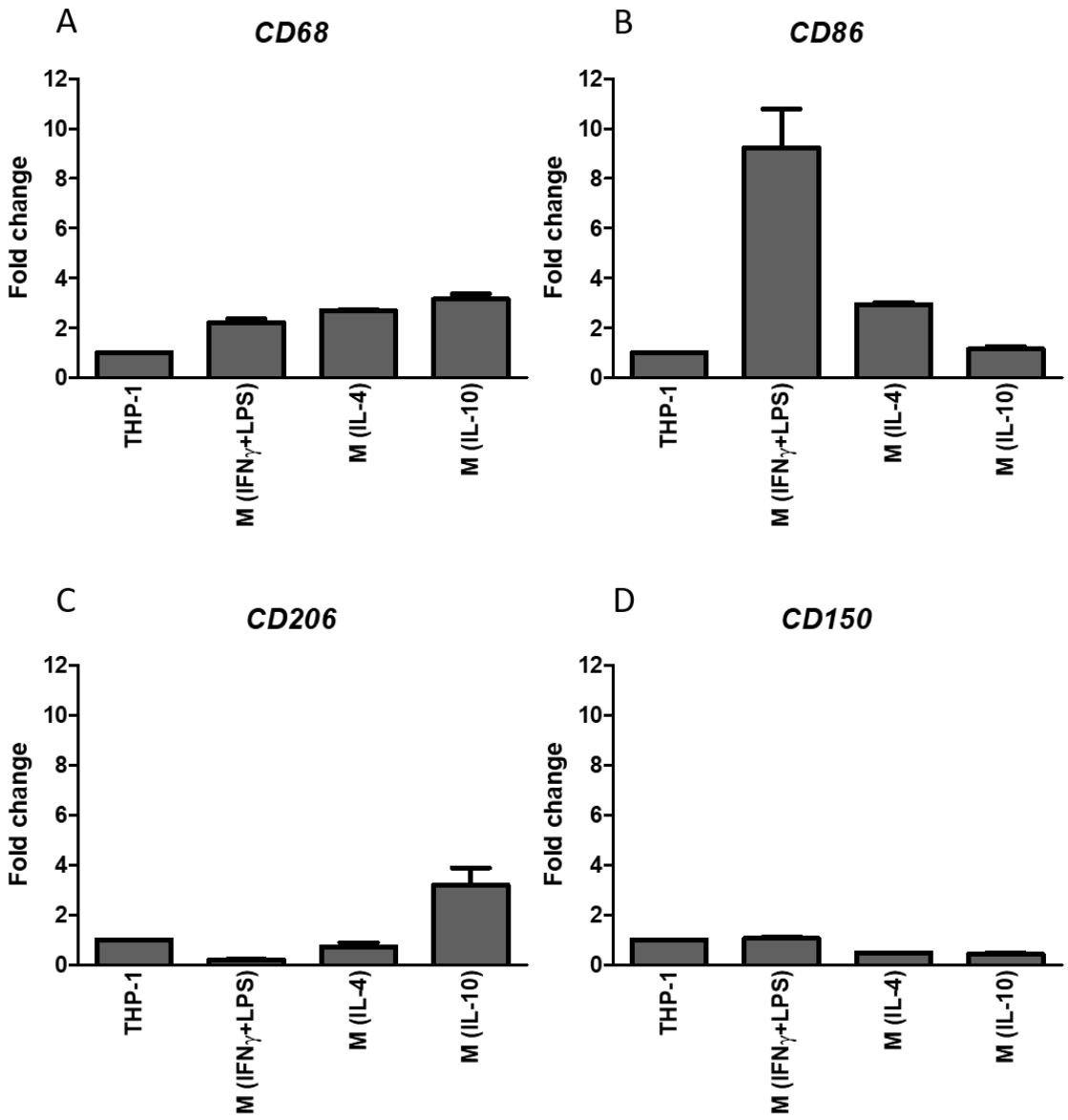

Figure 19: *Macrophage differentiation after pilot study.* $2^{-\Delta\Delta Ct}$ values from M (IFNγ + LPS), M (IL-4) and M (IL-10) cells, normalised to and compared with the untreated THP-1 control. Markers of differentiation: *CD68*, pan-macrophage marker (A), *CD86*, M1 marker (B), *CD206*, mannose receptor, a pan-M2 marker (C) and *CD150*, an M2c macrophage marker (D). Data represented as mean fold change ±SD, *n*=2 technical replicates in a single experiment.

7.1.1 *Housekeeping gene selection*

18S, PPIA and *TBP* were validated by Dr E Pastel as housekeeping genes for analysing THP-1 differentiation. All four genes were expressed consistently across control and treated cells (Figure 20), giving a stable baseline upon which to normalise all other data. *18S, PPIA* and *TBP* were selected for use when quantifying cell differentiation.

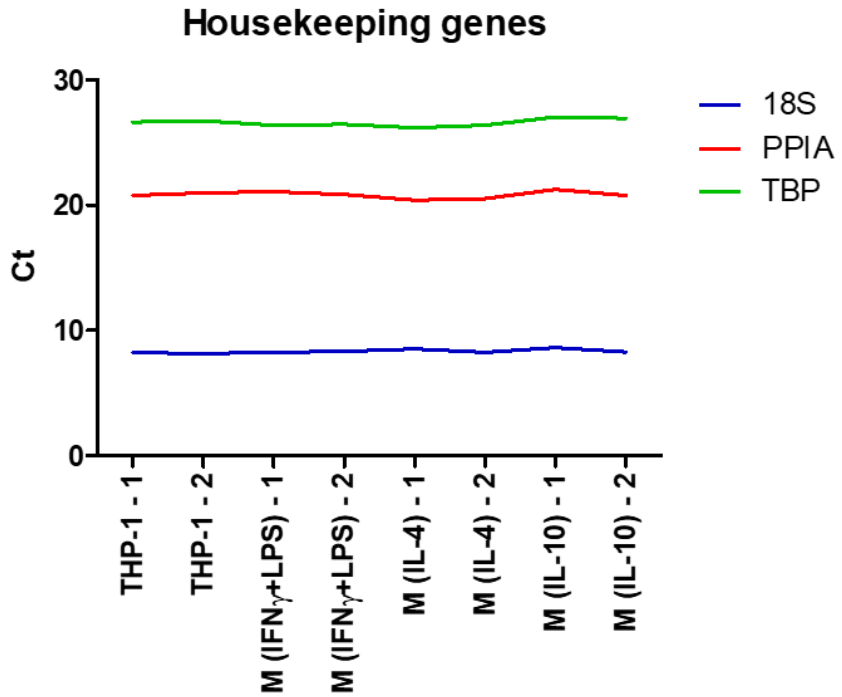

Figure 20: *Expression of housekeeping genes in differentiated macrophages.* Stability of housekeeping genes *18S*, *PPIA* and *TBP* was assessed across all four macrophage differentiation conditions. All three genes appear stable.

Appendix 2

7.2 RNA concentration and quality in AT samples

Patient	Macrophages	Insulin	Sample no.	Volume (µl)	Concentration (ng/µl)	260/280	260/230
2 - TB1779	ωM	N/A	1	35	274.9	1.92	1.54
			2	37	202.3	1.91	1.97
		1nM	3	40	270.9	1.91	1.52
			4	37	256.8	1.9	1.89
		10nM	5	33	257.5	1.87	1.89
			6	30	274.9	1.89	2.08
		100nM	7	40	238.7	1.9	1.78
			8	40	272.5	1.9	1.7
	M2c	N/A	3	30	195	1.93	0.94
			4	30	260.1	1.88	1.97
		1nM	5	30	143.5	1.82	2.03
			6	30	293.1	1.92	1.84
		10nM	7	30	205.5	1.91	1.66
			8	37	148.6	1.9	1.97
		100nM	9	34	224.3	1.93	1.1
			10	14	256.9	1.89	0.75
	M1	N/A	3	20	222	1.83	1.91
			4	30	264.3	1.9	1.88
		1nM	5	34	197	1.91	1.78
			6	31	216.1	1.9	1.92
		10nM	7	30	275.6	1.9	1.24
			8	30	213	1.86	1.94
		100nM	9	30	275.6	1.9	1.86
			10	30	238.6	1.9	1.8
	M2a	N/A	3	Sample contaminated			
			4	33	222	1.86	2.1
		1nM	5	20	251	1.85	1.97
			6	32	254.3	1.89	1.92
		10nM	7	30	214.3	1.84	2.19
			8	30	282.1	1.91	1.77
		100nM	9	30	187.3	1.89	1.09
			10	35	222.8	1.91	1.84
	M0	N/A	3	38	171.9	1.86	2.15
			4	36	280	1.9	1.71
		1nM	5	30	283.8	1.9	1.81
			6	30	279.5	1.89	1.78
		10nM	7	31	249.6	1.9	1.69
			8	31	277	1.91	0.74
		100nM	9	30	179.4	1.89	1.66
			10	32	299.4	1.92	1.78

Patient	Macrophages	Insulin	Sample no.	Volume (µl)	Concentration (ng/µl)	260/280	260/230
4 - TB1781	ϕM	N/A	1	21	170.7	1.85	2.09
			2	30	153.1	1.96	0.95
		1nM	3	30	228.2	1.91	1.11
			4	30	114.5	1.92	1
		10nM	5	30	171.2	1.81	1.95
			6	30	141.2	1.91	1.07
		100nM	7	30	250.6	1.9	2.15
			8	30	188.9	1.96	1.62
	M2c	N/A	3	30	190.2	1.93	1.11
			4	25	204.8	1.91	1.06
		1nM	5	30	135.9	1.83	1.9
			6	25	141.5	2	1.68
		10nM	7	30	198.1	1.9	2
			8	25	201.2	1.96	1.54
		100nM	9	30	260.3	1.92	1.61
			10	30	208.1	1.91	2.06
	M1	N/A	3	40	253.2	1.94	2.07
			4	41	293.5	1.88	1.81
		1nM	5	38	245.3	1.92	2.01
			6	35	203.4	1.94	1.8
		10nM	7	37	239.9	1.93	1.81
			8	30	291.8	1.92	2.02
		100nM	9	35	297.3	1.92	2.05
			10	37	299.2	1.95	1.87
	M2a	N/A	3	30	255.4	1.9	2.14
			4	30	269.1	1.92	2.26
		1nM	5	34	240.9	1.92	2.11
			6	30	257.9	1.95	1.81
		10nM	7	35	257.7	1.93	1.88
			8	30	254.2	1.92	1.85
		100nM	9	36	244.9	1.96	1.66
			10	38	262.6	1.88	1.93
	M0	N/A	3	35	246.2	1.95	1.88
			4	30	279.8	1.93	1.87
		1nM	5	30	245.8	1.9	1.96
			6	30	174.1	1.88	2.2
		10nM	7	34	210.5	1.94	1.58
			8	30	264.8	1.94	0.78
		100nM	9	30	297.8	1.92	2.13
			10	30	286.1	1.95	1.99

Patient	Macrophages	Insulin	Sample no.	Volume (µl)	Concentration (ng/µl)	260/280	260/230
5 - TB1782	ѡM	N/A	1	31	262.4	1.95	1.83
			2	37	255.4	1.95	1.32
		1nM	3	33	243.1	1.95	1.72
			4	34	254.2	1.95	1.63
		10nM	5	34	276	1.96	1.89
			6	34	263.6	1.95	1.62
		100nM	7	34	289.1	1.94	2.05
			8	31	246.9	1.92	1.84
	M2c	N/A	3	30	257.2	1.92	2.08
			4	30	279.7	2	1.24
		1nM	5	32	293.9	1.97	1.9
			6	30	280.5	1.97	1.82
		10nM	7	31	264.8	1.95	1.77
			8	35	235.2	1.94	1.82
		100nM	9	30	289.7	1.97	1.47
			10	35	233.8	1.92	2.09
	M1	N/A	3	20	274.9	1.95	1.94
			4	32	228.8	1.94	1.94
		1nM	5	30	292	1.95	1.94
			6	30	297	1.92	2.14
		10nM	7	34	236.6	1.96	1.88
			8	30	299.6	1.95	1.94
		100nM	9	35	245	1.97	1.87
			10	30	217.9	1.95	1.71
	M2a	N/A	3	34	269.4	1.95	1.83
			4	32	200.7	1.94	1.85
		1nM	5	34	246.6	1.94	2.08
			6	32	198.3	1.96	1.68
		10nM	7	31	271	1.95	1.94
			8	28	256.7	1.93	1.75
		100nM	9	30	270.4	2.02	2.1
			10	30	295.9	1.94	1.41
	M0	N/A	3	31	228.7	1.96	2.23
			4	31	295.8	1.94	1.84
		1nM	5	35	291.8	1.99	1.86
			6	35	291.3	1.93	1.83
		10nM	7	30	292.1	1.94	2.22
			8	30	287.9	1.97	1.25
		100nM	9	30	271.4	1.94	2.24
			10	12	58.58	1.93	1.08

Patient	Macrophages	Insulin	Sample no.	Volume (µl)	Concentration (ng/µl)	260/280	260/230
6 - TB1783	ϕM	N/A	1	130	272.6	1.96	2.1
			2	160	136.5	2	2.12
		1nM	3	130	241.7	1.98	2.16
			4	110	277.3	1.93	1.93
		10nM	5	110	296.8	2	2.17
			6	110	299.6	2	2.09
		100nM	7	160	263.1	2.07	2.12
			8	160	255.9	2.05	2.14
	M2c	N/A	3	120	240.7	1.97	2.16
			4	130	237.9	2	2.19
		1nM	5	130	292	1.95	2.14
			6	110	295.7	2	2.05
		10nM	7	140	268.3	1.99	2.15
			8	160	276.4	1.99	2.08
		100nM	9	170	232.6	1.99	2.11
			10	150	261.1	1.96	2.16
	M1	N/A	3	Sample lost			
			4	160	235.9	1.97	2.17
		1nM	5	160	272.6	2.02	2.25
			6	120	277.9	1.99	2.19
		10nM	7	120	271.4	2.01	2.04
			8	150	278.9	2.06	2.21
		100nM	9	140	270.7	1.99	2.1
			10	170	260.2	2.04	2.08
	M2a	N/A	3	190	191.2	1.98	2.1
			4	160	209.2	1.97	2.16
		1nM	5	160	223.5	2.02	2.11
			6	140	208.2	1.94	2.05
		10nM	7	140	258.8	2.02	2.17
			8	150	249.6	1.98	2.13
		100nM	9	160	239.8	2.05	2.13
			10	160	264	2.01	2.13
	M0	N/A	3	90	257.9	2.01	2.31
			4	80	259.9	1.92	2.07
		1nM	5	100	260.3	1.95	2.21
			6	80	285.2	1.99	2.18
		10nM	7	80	266.2	1.91	2.07
			8	90	268.3	1.97	2.21
		100nM	9	90	270.3	1.98	2.09
			10	100	279.1	1.88	2.18

Patient	Macrophages	Insulin	Sample no.	Volume (µl)	Concentration (ng/µl)	260/280	260/230
7 - TB1784	ѡM	N/A	1	140	183	2.02	2.05
			2	80	168.7	1.92	1.43
		1nM	3	90	266.7	193	2.18
			4	90	183.9	2.04	2.05
		10nM	5	90	265.4	1.96	2.17
			6	100	297.5	2.07	2.2
		100nM	7	170	151.2	2.02	2.18
			8	170	191.2	1.99	2.09
	M2c	N/A	3	90	245	1.96	2.07
			4	120	243.9	2	2.12
		1nM	5	100	284.1	2.03	2.15
			6	130	270.5	2.1	2.01
		10nM	7	160	177.1	2.01	2.2
			8	110	263.5	1.99	2.02
		100nM	9	100	249.3	1.93	2.07
			10	120	266.6	2.03	2.18
	M1	N/A	3	70	220.8	1.93	2.01
			4	130	290.7	2.08	2.1
		1nM	5	90	221.4	1.98	1.98
			6	160	253.2	1.98	2.06
		10nM	7	100	170.9	1.89	2.05
			8	100	249.3	2.01	2.22
		100nM	9	70	246.1	1.91	2.05
			10	100	268	2.06	2.18
	M2a	N/A	3	120	230.5	1.99	2.12
			4	100	234.1	1.98	2.13
		1nM	5	110	254.3	1.97	1.98
			6	100	280.3	2.02	2.07
		10nM	7	110	280.6	2.03	1.51
			8	80	286.6	2.12	2.18
		100nM	9	160	249	2.01	2.08
			10	140	207.6	1.99	2.18
	M0	N/A	3	120	265.8	2.02	2.09
			4	110	261.7	2.02	2.09
		1nM	5	120	276.7	2.04	1.98
			6	110	280.5	2.11	2.05
		10nM	7	140	297.1	2.03	2.14
			8	80	255.3	1.95	2.09
		100nM	9	130	244.8	1.83	1.72
			10	40	271.9	1.89	2.12

Patient	Macrophages	Insulin	Sample no.	Volume (µl)	Concentration (ng/µl)	260/280	260/230
9 - TB1786	ϕM	N/A	1	35	276.7	1.94	2.12
			2	30	279.1	2.06	0.79
		1nM	3	30	209.3	1.94	1.76
			4	30	288.3	2	1.63
		10nM	5	35	249.8	1.92	2.25
			6	30	234.1	1.97	1.8
		100nM	7	30	243.5	1.89	2.2
			8	30	292.5	1.94	2.12
	M2c	N/A	3	30	177.9	1.95	1.63
			4	30	118.9	1.85	2.45
		1nM	5	30	192.5	1.89	2.14
			6	30	177.2	1.86	2.41
		10nM	7	30	238.6	1.9	2.33
			8	45	279.5	1.93	2.26
		100nM	9	30	237.9	1.98	1.81
			10	30	199.3	1.98	1.81
	M1	N/A	3	44	191.7	1.91	2.39
			4	30	331	1.94	2.37
		1nM	5	38	241.5	1.91	2.22
			6	30	286.3	1.92	2.29
		10nM	7	30	285.3	1.91	2.34
			8	31	266.6	1.87	2.18
		100nM	9	30	283.9	1.92	2.31
			10	30	254.7	1.92	2.19
	M2a	N/A	3	38	201	1.95	1.93
			4	30	258.8	1.92	1.8
		1nM	5	30	289.2	1.9	2.3
			6	37	267.3	1.92	2.28
		10nM	7	33	268	1.9	2.18
			8	30	285.5	1.91	2.39
		100nM	9	60	233.6	1.88	2.21
			10	38	256.4	1.91	2.33
	M0	N/A	3	30	174.1	1.84	2.41
			4	30	194.8	1.88	2.02
		1nM	5	30	162.4	1.87	2.29
			6	30	133.9	1.83	2.07
		10nM	7	30	180.5	1.88	2.18
			8	30	147.2	1.86	2.59
		100nM	9	30	188.7	1.84	2.17
			10	30	177.9	1.88	2.44

References

1. Kershaw EE, Flier JS. Adipose tissue as an endocrine organ. *J Clin Endocrinol Metab*. 2004;89(6):2548-2556. doi:10.1210/jc.2004-0395

2. Stamenkovic I. Extracellular matrix remodelling: the role of matrix metalloproteinases. *J Pathol*. 2003;200(4):448-464. doi:10.1002/path.1400

3. Saely CH, Geiger K, Drexel H. Brown versus white adipose tissue: A mini-review. *Gerontology*. 2012;58(1):15-23. doi:10.1159/000321319

4. Coelho M, Oliveira T, Fernandes R. Biochemistry of adipose tissue: An endocrine organ. *Arch Med Sci*. 2013;9(2):191-200. doi:10.5114/aoms.2013.33181

5. Gray SL, Vidal-Puig AJ. Adipose Tissue Expandability in the Maintenance of Metabolic Homeostasis. *Nutr Rev*. 2007;65(SUPPL.1):7-12. doi:10.1111/j.1753-4887.2007.tb00331.x

6. Bjørndal B, Burri L, Staalesen V, Skorve J, Berge RK. Different adipose depots: Their role in the development of metabolic syndrome and mitochondrial response to hypolipidemic agents. *J Obes*. 2011;2011. doi:10.1155/2011/490650

7. Frühbeck G. Overview of Adipose Tissue and Its Role in Obesity and Metabolic Disorders. In: Yang K, ed. *Adipose Tissue Protocols*. Totowa, NJ: Humana Press; 2008:1-22. doi:10.1007/978-1-59745-245-8_1

8. Mott JD, Werb Z. Regulation of matrix biology by matrix metalloproteinases. *Curr Opin Cell Biol*. 2004;16(5):558-564. doi:10.1038/jid.2014.371

9. Frantz C, Stewart KM, Weaver VM. The extracellular matrix at a glance. *J Cell Sci*. 2010;123:4195-4200. doi:10.1242/jcs.023820

10. Iozzo R V, Murdoch AD. Proteoglycans of the extracellular environment: clues from the gene and protein side offer novel perspectives in molecular diversity and function. *FASEB J*. 1996;10(5):598-614. doi:10.1096/fasebj.10.5.8621059

11. Schaefer L, Schaefer RM. Proteoglycans: From structural compounds to signaling molecules. *Cell Tissue Res*. 2010;339(1):237-246. doi:10.1007/s00441-009-0821-y

12. Brinckmann J. Collagens at a glance. *Top Curr Chem*. 2005;247:1-6. doi:10.1007/b103817

13. Sillat T, Saat R, Pöllänen R, Hukkanen M, Takagi M, Konttinen YT. Basement membrane collagen type IV expression by human mesenchymal stem cells during adipogenic differentiation. *J Cell Mol Med*. 2012;16(7):1485-1495. doi:10.1111/j.1582-4934.2011.01442.x

14. Aratani Y, Kitagawa Y. Enhanced synthesis and secretion of type IV collagen and entactin during adipose conversion of 3T3-L1 cells and production of unorthodox laminin complex. *J Biol Chem*. 1988;263(31):16163-16169.

15. Reggio S, Rouault C, Poitou C, Bichet JC, Prifti E, Bouillot JL, Rizkalla S, Lacasa D, Tordjman J, Clément K. Increased basement membrane components in adipose tissue during obesity: Links with TGF- And metabolic phenotypes. *J Clin Endocrinol Metab*. 2016;101(6):2578-2587. doi:10.1210/jc.2015-4304

16. Cescon M, Gattazzo F, Chen P, Bonaldo P, Aigner T, Hambach L, Söder S, Schlötzer-Schrehardt U, Pöschl E, Alexeev V, Arita M, Donahue A, Bonaldo P, Chu M-L, Igoucheva O, Alexopoulos LG, Youn I, Bonaldo P, Guilak F, et al.

Collagen VI at a glance. *J Cell Sci*. 2015;128(19):3525-3531. doi:10.1242/jcs.169748

17. Ronald Kahn C. The Molecular Mechanism of Insulin Action. *Annu Rev Med*. 1985;36:429-451.

18. Koeslag JH, Saunders PT, Terblanche E. A Reappraisal of the Blood Glucose Homeostat which Comprehensively Explains the Type 2 Diabetes Mellitus-Syndrome X Complex. *J Physiol*. 2003;549(2):333-346. doi:10.1113/jphysiol.2002.037895

19. Saltiel AR, Kahn CR. Insulin signalling and the regulation of glucose and lipid metabolism. *Nature*. 2001;414(6865):799-806. doi:10.1038/414799a

20. Myers MG, Backer JM, Sun XJ, Shoelson S, Hu P, Schlessinger J, Yoakim M, Schaffhausen B, White MF. IRS-1 activates phosphatidylinositol 3'-kinase by associating with src homology 2 domains of p85. *Proc Natl Acad Sci*. 1992;89(21):10350-10354. doi:10.1073/pnas.89.21.10350

21. Pronk GJ, McGlade J, Pelicci G, Pawson T, Bos JL. Insulin-induced phosphorylation of the 46- and 52-kDa Shc proteins. *J Biol Chem*. 1993;268(8):5748-5753.

22. Boucher J, Kleinridders A, Kahn CR. Insulin Receptor Signaling in Normal and Insulin Resistant States. *Cold Spring Harb Perspect Biol 2014*. 2014;6:1-23.

23. Bost F, Aouadi M, Caron L, Binétruy B. The role of MAPKs in adipocyte differentiation and obesity. *Biochimie*. 2005;87(1):51-56. doi:10.1016/J.BIOCHI.2004.10.018

24. BOST F, CARON L, MARCHETTI I, DANI C, MARCHAND-BRUSTEL Y LE, BINÉTRUY B. Retinoic acid activation of the ERK pathway is required for embryonic stem cell commitment into the adipocyte lineage. *Biochem J*. 2002;361(3):621-627. doi:10.1042/bj3610621

25. C. Dani, A. G. Smith, S. Dessolin, P. Leroy, L. Staccini, P. Villageois, C. Darimont, G. Ailhaud1. Differentiation of embryonic stem cells into adipocytes in vitro. *J Cell Sci*. 1997;110:1279-1285. http://jcs.biologists.org/content/joces/110/11/1279.full.pdf.

26. Aubin D, Gagnon A, Sorisky A. Phosphoinositide 3-kinase is required for human adipocyte differentiation in culture. *Int J Obes*. 2005;29(8):1006-1009. doi:10.1038/sj.ijo.0802961

27. McCurdy CE, Klemm DJ. Adipose tissue insulin sensitivity and macrophage recruitment: Does PI3K pick the pathway? *Adipocyte*. 2013;2(3):135-142. doi:10.4161/adip.24645

28. Choi SM, Tucker DF, Gross DN, Easton RM, DiPilato LM, Dean AS, Monks BR, Birnbaum MJ. Insulin Regulates Adipocyte Lipolysis via an Akt-Independent Signaling Pathway. *Mol Cell Biol*. 2010;30(21):5009-5020. doi:10.1128/MCB.00797-10

29. Peraldi P, Van Obberghen E, Emanuelli B, Filloux C, Hilton D, Sawka-Verhelle D. SOCS-3 Is an Insulin-induced Negative Regulator of Insulin Signaling. *J Biol Chem*. 2002;275(21):15985-15991. doi:10.1074/jbc.275.21.15985

30. Emanuelli B, Peraldi P, Filloux C, Chavey C, Freidinger K, Hilton DJ, Hotamisligil GS, Van Obberghen E. SOCS-3 Inhibits Insulin Signaling and Is Up-regulated in Response to Tumor Necrosis Factor-α in the Adipose Tissue of Obese Mice. *J Biol Chem*. 2001;276(51):47944-47949. doi:10.1074/jbc.M104602200

31. Rui L, Yuan M, Frantz D, Shoelson S, White MF. SOCS-1 and SOCS-3 block insulin signaling by ubiquitin-mediated degradation of IRS1 and IRS2. *J Biol Chem*. 2002;277(44):42394-42398. doi:10.1074/jbc.C200444200

32. Mooney RA, Senn J, Cameron S, Inamdar N, Boivin LM, Shang Y, Furlanetto RW. Suppressors of Cytokine Signaling-1 and -6 Associate with and Inhibit the Insulin Receptor. *J Biol Chem*. 2002;276(28):25889-25893. doi:10.1074/jbc.m010579200

33. Venable CL, Frevert EU, Kim YB, Fischer BM, Kamatkar S, Neel BG, Kahn BB. Overexpression of protein-tyrosine phosphatase-1B in adipocytes inhibits insulin-stimulated phosphoinositide 3-kinase activity without altering glucose transport or Akt/protein kinase B activation. *J Biol Chem*. 2000;275(24):18318-18326. doi:10.1074/jbc.M908392199

34. Carpentier JL, Fehlmann M, Van Obberghen E, Gorden P, Orci L. Insulin receptor internalization and recycling: mechanism and significance. *Biochimie*. 1985;67(10-11):1143-1145. doi:10.1016/S0300-9084(85)80112-7

35. Di Guglielmo GM, Drake PG, Baass PC, Authier F, Posner BI, Bergeron JJM. Insulin receptor internalization and signalling. *Mol Cell Biochem*. 1998;182(1-2):59-63. doi:10.1023/A:1006883311233

36. Morcavallo A, Stefanello M, Iozzo R V., Belfiore A, Morrione A. Ligand-mediated endocytosis and trafficking of the insulin-like growth factor receptor I and insulin receptor modulate receptor function. *Front Endocrinol (Lausanne)*. 2014;5(DEC):1-7. doi:10.3389/fendo.2014.00220

37. Carpentier JL. Insulin receptor internalization: molecular mechanisms and physiopathological implications. *Diabetologia*. 1994;37(2 Supplement). doi:10.1007/BF00400835

38. Huang S, Czech MP. The GLUT4 Glucose Transporter. *Cell Metab*. 2007;5(4):237-252. doi:10.1016/j.cmet.2007.03.006

39. Frayn KN. Adipose tissue and the insulin resistance syndrome. *Proc Nutr Soc*. 2001;60(2001):375-380. doi:10.1079/PNS200195

40. Guo X, Li H, Xu H, Woo S, Dong H, Lu F, Lange AJ, Wu C. Glycolysis in the control of blood glucose homeostasis. *Acta Pharm Sin B*. 2012;2(4):358-367. doi:10.1016/j.apsb.2012.06.002

41. Ameer F, Scandiuzzi L, Hasnain S, Kalbacher H, Zaidi N. De novo lipogenesis in health and disease. *Metabolism*. 2014;63(7):895-902. doi:10.1016/j.metabol.2014.04.003

42. Coleman RA, Mashek DG. Mammalian triacylglycerol metabolism: synthesis, lipolysis and signaling. *Chem Rev*. 2011;1(3):233-245. doi:10.1016/j.dcn.2011.01.002.The

43. Li J, Cheng J-X. Direct visualization of de novo lipogenesis in single living cells. *Sci Rep*. 2014;4:6807. doi:10.1038/srep06807

44. Hanson RW, Reshef L. Glyceroneogenesis revisited. *Biochimie*. 2003;85(12):1199-1205. doi:10.1016/j.biochi.2003.10.022

45. Gathercole LL, Morgan SA, Bujalska IJ, Hauton D, Stewart PM, Tomlinson JW. Regulation of lipogenesis by glucocorticoids and insulin in human adipose tissue. *PLoS One*. 2011;6(10). doi:10.1371/journal.pone.0026223

46. Kersten S. Mechanisms of nutritional and hormonal regulation of lipogenesis. *EMBO Rep*. 2001;2(4):282-286. doi:10.1093/embo-reports/kve071

47. Girard J, Perdereau D, Foufelle F, Prip-Buus C, Ferré P. Regulation of lipogenic enzyme gene expression by nutrients and hormones. *FASEB J*. 1994;8(1):36-42. http://www.ncbi.nlm.nih.gov/pubmed/7905448. Accessed December 3, 2017.

48. Goldberg IJ, Eckel RH, Abumrad N a. Regulation of fatty acid uptake into tissues: lipoprotein lipase- and CD36-mediated pathways. *J Lipid Res*. 2009;50 Suppl:S86-90. doi:10.1194/jlr.R800085-JLR200

49. Gonzales AM, Orlando RA. Role of adipocyte-derived lipoprotein lipase in adipocyte hypertrophy. *Nutr Metab (Lond)*. 2007;4:22. doi:10.1186/1743-7075-4-22

50. Greenwood MR. The relationship of enzyme activity to feeding behavior in rats: lipoprotein lipase as the metabolic gatekeeper. *Int J Obes*. 1985;9 Suppl 1:67-70. http://www.ncbi.nlm.nih.gov/pubmed/4066124. Accessed November 11, 2016.

51. Lass A, Zimmermann R, Oberer M, Zechner R. Lipolysis - A highly regulated multi-enzyme complex mediates the catabolism of cellular fat stores. *Prog Lipid Res*. 2011;50(1):14-27. doi:10.1016/j.plipres.2010.10.004

52. Duncan RE, Ahmadian M, Jaworski K, Sarkadi-Nagy E, Sul HS. Regulation of lipolysis in adipocytes. *Annu Rev Nutr*. 2007;27:79-101. doi:10.1146/annurev.nutr.27.061406.093734

53. Ragolia L, Begum N. Protein phosphatase-1 and insulin action. 1998:49-58.

54. Wijkander J, Landström TR, Manganiello V, Belfrage P, Degerman E. Insulin-induced phosphorylation and activation of phosphodiesterase 3b in rat adipocytes: Possible role for protein kinase b but not mitogen-activated protein kinase or p70 s6 kinase. *Endocrinology*. 1998;139(1):219-227. doi:10.1210/endo.139.1.5693

55. Johnson J a, Fried SK, Pi-Sunyer FX, Albu JB. Impaired insulin action in subcutaneous adipocytes from women with visceral obesity. *Am J Physiol Endocrinol Metab*. 2001;280(1):E40-E49.

56. Frühbeck G, Aguado M, Martínez JA. In vitro lipolytic effect of leptin on mouse adipocytes: evidence for a possible autocrine/paracrine role of leptin. *Biochem Biophys Res Commun*. 1997;240(3):590-594. doi:10.1006/bbrc.1997.7716

57. Ahima RS. Revisiting leptin's role in obesity and weight loss. *J Clin Invest*. 2008;118(7):2380-2383. doi:10.1172/JCI36284.2380

58. Martin ML, Jensen MD. Effects of body fat distribution on regional lipolysis in obesity. *J Clin Invest*. 1991;88(2):609-613. doi:10.1172/JCI115345

59. Jensen MD. Role of Body Fat Distribution and the Metabolic Complications of Obesity. *J Clin Endocrinol Metab*. 2008;93(11_supplement_1):s57-s63. doi:10.1210/jc.2008-1585

60. Ronti T, Lupattelli G, Mannarino E. The endocrine function of adipose tissue: An update. *Clin Endocrinol (Oxf)*. 2006;64(4):355-365. doi:10.1111/j.1365-2265.2006.02474.x

61. Klok MD, Jakobsdottir S, Drent ML. The role of leptin and ghrelin in the regulation of food intake and body weight in humans: A review. *Obes Rev*. 2007;8(1):21-34. doi:10.1111/j.1467-789X.2006.00270.x

62. Schwartz MW, Peskind E, Raskind M, Boyko EJ, Porte D. Cerebrospinal fluid leptin levels: Relationship to plasma levels and to adiposity in humans. *Nat Med*. 1996;2(5):589-593. doi:10.1038/nm0596-589

63. Schwartz MW. Brain Pathways Controlling Food Intake and Body Weight. *Exp Biol Med*. 2001;226(11):978-981. doi:10.1177/153537020122601103

64. Matsubara M, Maruoka S, Katayose S. Inverse relationship between plasma adiponectin and leptin concentrations in normal-weight and obese women. *Eur J Endocrinol*. 2002;147(2):173-180. doi:10.1530/eje.0.1470173

65. Chandran M, Phillips SA, Ciaraldi T, Henry RR. Adiponectin: More than just another fat cell hormone? *Diabetes Care*. 2003;26(8):2442-2450. doi:10.2337/diacare.26.8.2442

66. Stefan N, Vozarov B, Funahashi T, Matsuzawa Y, Weyer C, Lindsay R s, Youngren JF, Havel PJ, Pratley RE, Bogardus C, Tataranni PA. Plasma adiponectin concentration is associated with skeletal muscle insulin receptor tyrosine phosphorylation, and low plasma concentration precedes a decrease in whole-body insulin sensitivity in humans. *Diabetes*. 2002;50(8):1884-1888.

67. Yamauchi T, Kamon J, Waki H, Terauchi Y, Kubota N, Hara K, Mori Y, Ide T, Murakami K, Tsuboyama-Kasaoka N, Ezaki O, Akanuma Y, Gavrilova O, Vinson C, Reitman ML, Kagechika H, Shudo K, Yoda M, Nakano Y, et al. The fat-derived hormone adiponectin reverses insulin resistance associated with both lipoatrophy and obesity. *Nat Med*. 2001;7(8):941-946. doi:10.1038/90984

68. Weyer C, Funahashi T, Tanaka S, Hotta K, Matsuzawa Y, Pratley RE, Tataranni P a. Hypoadiponectinemia in obesity and type 2 diabetes: close association with insulin resistance and hyperinsulinemia. *J Clin Endocrinol Metab*. 2001;86(5):1930-1935. doi:10.1210/jcem.86.5.7463

69. Fain JN, Madan AK, Hiler ML, Cheema P, Bahouth SW. Comparison of the release of adipokines by adipose tissue, adipose tissue matrix, and adipocytes from visceral and subcutaneous abdominal adipose tissues of obese humans. *Endocrinology*. 2004;145(5):2273-2282. doi:10.1210/en.2003-1336

70. Hotamisligil GS, Arner P, Caro JF, Atkinson RL, Spiegelman BM. Increased adipose tissue expression of tumour necrosis factor alpha in human obesity and insulin resistance. *J Clin Invest*. 1995;95(January):2409-2415.

71. Kern PA, Ranganathan S, Li C, Wood L, Ranganathan G. Adipose tissue tumor necrosis factor and interleukin-6 expression in human obesity and insulin resistance. *Am J Physiol Metab*. 2001;280(5):E745-E751. doi:10.1152/ajpendo.2001.280.5.e745

72. Xu H, Barnes G, Yang Q, Tan G, Yang D, Chou C, Sole J, Nichols A, Ross J, Tartaglia L, Chen H. Chronic inflammation in fat plays a crucial role in the development of obesity-related insulin resistance. *J Clin Invest*. 2003;112(12):1821-1830. doi:10.1172/JCI200319451.Introduction

73. Zinman B, Hanley AJG, Harris SB, Kwan J, Fantus IG. Circulating tumor necrosis factor-α concentrations in a native canadian population with high rates of type 2 diabetes mellitus. *J Clin Endocrinol Metab*. 1999;84(1):272-278. doi:10.1210/jc.84.1.272

74. Ruan H, Miles PDG, Ladd CM, Ross K, Golub TR, Olefsky JM, Lodish HF. Profiling gene transcription in vivo reveals adipose tissue as an immediate target of tumor necrosis factor-α: Implications for insulin resistance. *Diabetes*. 2002;51(11):3176-3188. doi:10.2337/diabetes.51.11.3176

75. White MF, Davis R, Uchida T, Yenush L, Aguirre V. The c-Jun NH 2 -terminal Kinase Promotes Insulin Resistance during Association with Insulin Receptor Substrate-1 and Phosphorylation of Ser 307 . *J Biol Chem*. 2002;275(12):9047-9054. doi:10.1074/jbc.275.12.9047

76. Kanety H, Hemi R, Papa MZ, Karasik A. Sphingomyelinase and ceramide suppress insulin-induced tyrosine phosphorylation of the insulin receptor substrate-1. *J Biol Chem*. 1996;271(17):9895-9897. doi:10.1074/jbc.271.17.9895

77. Hotamisligil GS. Inflammatory pathways and insulin action. *Int J Obes*. 2003;27:S53-S55. doi:10.1038/sj.ijo.0802502

78. Gasic S, Tian B, Green A. Tumor Necrosis Factor α Stimulates Lipolysis in Adipocytes by Decreasing G i Protein Concentrations. *J Biol Chem*. 1999;274(10):6770-6775.

79. Ruan H, Lodish HF. Insulin resistance in adipose tissue: Direct and indirect effects of tumor necrosis factor-α. *Cytokine Growth Factor Rev*. 2003;14(5):447-455. doi:10.1016/S1359-6101(03)00052-2

80. Fain JN, Madan AK, Hiler ML, Cheema P, Bahouth SW. Comparison of the release of adipokines by adipose tissue, adipose tissue matrix, and adipocytes from visceral and subcutaneous abdominal adipose tissues of obese humans. *Endocrinology*. 2004;145(5):2273-2282. doi:10.1210/en.2003-1336

81. De Benedetti F, Alonzi T, Moretta A, Lazzaro D, Costa P, Poli V, Martini A, Ciliberto G, Fattori E. Interleukin 6 causes growth impairment in transgenic mice through a decrease in insulin-like growth factor-I. A model for stunted growth in children with chronic inflammation. *J Clin Invest*. 1997;99(4):643-650. doi:10.1172/JCI119207

82. Fernández-Real JM, Ricart W. Insulin resistance and chronic cardiovascular inflammatory syndrome. *Endocr Rev*. 2003;24(3):278-301. doi:10.1210/er.2002-0010

83. Wang MY, Orci L, Ravazzola M, Unger RH. Fat storage in adipocytes requires inactivation of leptin's paracrine activity: implications for treatment of human obesity. *Proc Natl Acad Sci U S A*. 2005;102(50):18011-18016. doi:10.1073/pnas.0509001102

84. Siegrist-Kaiser C a, Pauli V, Juge-Aubry CE, Boss O, Pernin a, Chin WW, Cusin I, Rohner-Jeanrenaud F, Burger a G, Zapf J, Meier C a. Direct effects of leptin on brown and white adipose tissue. *J Clin Invest*. 1997;100(11):2858-2864. doi:10.1172/JCI119834

85. Frederich RC, Hamann A, Anderson S, Löllmann B, Lowell BB, Flier JS. Leptin levels reflect body lipid content in mice: Evidence for diet-induced resistance to leptin action. *Nat Med*. 1995;1(12):1311-1314. doi:10.1038/nm1295-1311

86. Santos-Alvarez J, Goberna R, Sánchez-Margalet V. Human leptin stimulates proliferation and activation of human circulating monocytes. *Cell Immunol*. 1999;194(1):6-11. doi:10.1006/cimm.1999.1490

87. Ouchi N, Parker JL, Lugus JJ, Walsh K. Adipokines in inflammation and metabolic disease. *Nat Publ Gr*. 2011;11(2):85-97. doi:10.1038/nri2921

88. Kwon H, Pessin JE. Adipokines mediate inflammation and insulin resistance. *Front Endocrinol (Lausanne)*. 2013;4(JUN):1-13. doi:10.3389/fendo.2013.00071

89. Weisberg SP, Hunter D, Huber R, Lemieux J, Slaymaker S, Vaddi K, Charo I, Leibel RL, Jr AWF. CCR2 modulates inflammatory and metabolic effects of high-fat feeding. *J Clin Invest*. 2006;116(1):115-124. doi:10.1172/JCI24335.or

90. Hotamisligil GS, Shargill NS, Spiegelman BM, Shargill S, Spiegelman BM. Adipose expression of tumor necrosis factor-alpha: direct role in obesity-linked insulin resistance. *Science*. 1993;259(5091):87-91. doi:10.1126/science.7678183

91. Zhang HH, Halbleib M, Ahmad F, Manganiello VC, Greenberg AS. Differentiated Human Adipocytes Through Activation of Extracellular Signal – Related Kinase and Elevation of. *Diabetes*. 2002;51:2929-2935. doi:10.2337/diabetes.51.10.2929

92. Takemura Y, Ouchi N, Shibata R, Aprahamian T, Kirber MT, Summer RS, Kihara S, Walsh K. Adiponectin modulates inflammatory reactions via calreticulin receptor - dependent clearance of ealy apoptotic bodies. *J Clin Invest*. 2007;117(2):375-386. doi:10.1172/JCI29709DS1

93. Wilk S, Jenke A, Stehr J, Yang C-A, Bauer S, Göldner K, Kotsch K, Volk H-D, Poller W, Schultheiss H-P, Skurk C, Scheibenbogen C. Adiponectin modulates NK-cell function. *Eur J Immunol*. 2013;43(4):1024-1033. doi:10.1002/eji.201242382

94. Mantovani A, Sica A, Sozzani S, Allavena P, Vecchi A, Locati M. The chemokine system in diverse forms of macrophage activation and polarization. *Trends Immunol*. 2004;25(12):677-686. doi:10.1016/j.it.2004.09.015

95. Mosser DM, Zhang X. Interleukin-10: New perspectives on an old cytokine. *Immunol Rev*. 2008;226(1):205-218. doi:10.1111/j.1600-065X.2008.00706.x

96. Tan JTM, Mclennan S V, Song WW, Lo LW, Bonner JG, Williams PF, Twigg SM. Connective tissue growth factor inhibits adipocyte differentiation. *Am J cell Physiol*. 2008:740-751.

97. Jo J, Gavrilova O, Pack S, Jou W, Mullen S, Sumner AE, Cushman SW, Periwal V. Hypertrophy and/or hyperplasia: Dynamics of adipose tissue growth. *PLoS Comput Biol*. 2009;5(3). doi:10.1371/journal.pcbi.1000324

98. Christodoulides C, Lagathu C, Sethi JK, Vidal-Puig A. Adipogenesis and WNT signalling. *Trends Endocrinol Metab*. 2009;20(1):16-24. doi:10.1016/j.tem.2008.09.002

99. Ali AT, Hochfeld WE, Myburgh R, Pepper MS. Adipocyte and adipogenesis. *Eur J Cell Biol*. 2013;92(6-7):229-236. doi:10.1016/j.ejcb.2013.06.001

100. Ross S, Hemati N, Longo K, Bennett C, Luca P, Erickson R, MacDougald O. Inhibition of adipogenesis by Wnt signaling. *Science (80-)*. 2000;289(5481):950-953. doi:10.1126/science.289.5481.950

101. Demeulemeester D, Collen D, Lijnen HR. Effect of matrix metalloproteinase inhibition on adipose tissue development. *Biochem Biophys Res Commun*. 2005;329(1):105-110. doi:10.1016/j.bbrc.2005.01.103

102. Brew K, Nagase H. The tissue inhibitors of metalloproteinases (TIMPs): An ancient family with structural and functional diversity. *Biochim Biophys Acta*. 2010;1803(1):55-71. doi:10.1038/jid.2014.371

103. Goossens GH, Blaak EE. Adipose Tissue Dysfunction and Impaired Metabolic Health in Human Obesity: A Matter of Oxygen? *Front Endocrinol (Lausanne)*. 2015;6(April):1-5. doi:10.3389/fendo.2015.00055

104. Di Cesare M, Bentham J, Stevens GA, Zhou B, Danaei G, Lu Y, Bixby H, Cowan MJ, Riley LM, Hajifathalian K, Fortunato L, Taddei C, Bennett JE, Ikeda N, Khang YH, Kyobutungi C, Laxmaiah A, Li Y, Lin HH, et al. Trends in adult body-mass index in 200 countries from 1975 to 2014: A pooled analysis of 1698 population-based measurement studies with 19.2 million participants. *Lancet*. 2016;387(10026):1377-1396. doi:10.1016/S0140-6736(16)30054-X

105. Craig R (eds), Mindell J (eds). *Health Survey for England: Summary of Key Findings*.; 2010.

106. Wright SM, Aronne LJ. Causes of obesity. *Abdom Imaging*. 2012;37(5):730-732. doi:10.1007/s00261-012-9862-x

107. Shaper AG, Wannamethee SG, Walker M. Body weight: implications for the prevention of coronary heart disease, stroke, and diabetes mellitus in a cohort study of middle aged men. *BMJ*. 1997;314(7090):1311. doi:10.1136/bmj.314.7090.1311

108. Whelton PK. Body Weight and Mortality Among Men and Women in China. 2012;295(7).

109. Vgontzas AN, Tan TL, Bixler EO, Martin LF, Shubert D, Kales A. Sleep Apnea and Sleep Disruption in Obese Patients. *JAMA Intern Med*. 1994;154(15):1705-1711. doi:10.1001/archinte.1994.00420150073007

110. Cicuttini F, Spector T. The association of obesity with osteoarthritis of the hand and knee in women: A twin study Genetic modifiers of fetal haemoglobin persistence View project. *Artic J Rheumatol*. 1996;(July 2014). https://www.researchgate.net/publication/14381057.

111. Russo A, Franceschi S, Vecchia C La, Maso LD, Montella M, Conti E, Giacosa A, Falcini F, Negri E. BODY SIZE AND COLORECTAL-CANCER RISK. *Int J Cancer*. 1998;165(March):161-165.

112. Khaodhiar L, McCowen KC, Blackburn GL. Obesity and its comorbid conditions. *Clin Cornerstone*. 1999;2(3):17-31. http://www.ncbi.nlm.nih.gov/pubmed/10696282. Accessed October 26, 2016.

113. Morgan L, Monica D. The economic burden of obesity. *NHS*. 2010;(October):1-13.

114. Hex N, Bartlett C, Wright D, Taylor M, Varley D. Estimating the current and future costs of Type 1 and Type 2 diabetes in the UK, including direct health costs and indirect societal and productivity costs. *Diabet Med*. 2012;29(7):855-862. doi:10.1111/j.1464-5491.2012.03698.x

115. Bjorntorp P, Sjostrom L. Number and size of adipose tissue fat cells in relation to metabolism in human obesity. *Metabolism*. 1971;20(7):703-713. doi:10.1016/0026-0495(71)90084-9

116. Lundgren M, Svensson M, Lindmark S, Renström F, Ruge T, Eriksson JW. Fat cell enlargement is an independent marker of insulin resistance and “hyperleptinaemia.” *Diabetologia*. 2007;50(3):625-633. doi:10.1007/s00125-006-0572-1

117. Monteiro R, De Castro PMST, Calhau C, Azevedo I. Adipocyte size and liability to cell death. *Obes Surg*. 2006;16(6):804-806. doi:10.1381/096089206777346600

118. Alkhouri N, Gornicka A, Berk MP, Thapaliya S, Dixon LJ, Kashyap S, Schauer PR, Feldstein AE. Adipocyte apoptosis, a link between obesity, insulin resistance, and hepatic steatosis. *J Biol Chem*. 2010;285(5):3428-3438. doi:10.1074/jbc.M109.074252

119. Monteiro R, Azevedo I. Chronic inflammation in obesity and the metabolic syndrome. *Mediators Inflamm*. 2010;2010(Atp Iii). doi:10.1155/2010/289645

120. Lovett M, Lee K, Edwards A, Kaplan DL. Vascularization Strategies for Tissue Engineering. *Tissue Eng Part B Rev*. 2009;15(3):353-370. doi:10.1089/ten.teb.2009.0085

121. Halberg N, Khan T, Trujillo ME, Wernstedt-Asterholm I, Attie AD, Sherwani S,

Wang Z V., Landskroner-Eiger S, Dineen S, Magalang UJ, Brekken RA, Scherer PE. Hypoxia-Inducible Factor 1 Induces Fibrosis and Insulin Resistance in White Adipose Tissue. *Mol Cell Biol*. 2009;29(16):4467-4483. doi:10.1128/MCB.00192-09

122. Cinti S, Mitchell G, Barbatelli G, Murano I, Ceresi E, Faloia E, Wang S, Fortier M, Greenberg AS, Obin MS. Adipocyte death defines macrophage localization and function in adipose tissue of obese mice and humans. *J Lipid Res*. 2005;46:2347-2355. doi:10.1194/jlr.M500294-JLR200

123. Ventura JJ, Cogswell P, Flavell RA, Baldwin AS, Davis RJ. JNK potentiates TNF-stimulated necrosis by increasing the production of cytotoxic reactive oxygen species. *Genes Dev*. 2004;18(23):2905-2915. doi:10.1101/gad.1223004

124. Surmi BK, Hasty AH. Macrophage infiltration into adipose tissue: initiation, propagation and remodeling. *Future Lipidol*. 2008;3(5):545-556. doi:10.2217/17460875.3.5.545.Macrophage

125. Alberts B, Johnson A, Lewis J. Programmed Cell Death (Apoptosis). In: *Molecular Biology of the Cell 4th Edition*. New York: Garland Science; 2002.

126. Cinti S, Mitchell G, Barbatelli G, Murano I, Ceresi E, Faloia E, Wang S, Fortier M, Greenberg AS, Obin MS. Adipocyte death defines macrophage localization and function in adipose tissue of obese mice and humans. *J Lipid Res*. 2005;46(11):2347-2355. doi:10.1194/jlr.M500294-JLR200

127. Murano I, Barbatelli G, Parisani V, Latini C, Muzzonigro G, Castellucci M, Cinti S. Dead adipocytes, detected as crown-like structures, are prevalent in visceral fat depots of genetically obese mice. *J Lipid Res*. 2008;49(7):1562-1568. doi:10.1194/jlr.m800019-jlr200

128. Strissel KJ, Stancheva Z, Miyoshi H, Perfield JW, DeFuria J, Jick Z, Greenberg AS, Obin MS. Adipocyte death, adipose tissue remodeling, and obesity complications. *Diabetes*. 2007;56(12):2910-2918. doi:10.2337/db07-0767

129. Cullberg KB, Larsen JØ, Pedersen SB, Richelsen B. Effects of LPS and dietary free fatty acids on MCP-1 in 3T3-L1 adipocytes and macrophages in vitro. *Nutr Diabetes*. 2014;4(February):e113. doi:10.1038/nutd.2014.10

130. Dalmas E, Clément K, Guerre-Millo M. Defining macrophage phenotype and function in adipose tissue. *Trends Immunol*. 2011;32(7):307-314. doi:10.1016/j.it.2011.04.008

131. Weisberg SP, McCann D, Desai M, Rosenbaum M, Leibel RL, Ferrante AW. Obesity is associated with macrophage accumulation in adipose tissue. *J Clin Invest*. 2003;112(12):1796-1808. doi:10.1172/JCI200319246

132. Kanda H, Tateya S, Tamori Y, Kotani K, Hiasa K, Kitazawa R, Kitazawa S, Miyachi H, Maeda S, Egashira K, Kasuga M. MCP-1 contributes to macrophage infiltration into adipose tissue , insulin resistance , and hepatic steatosis in obesity. *J Clin Invest*. 2006;116(6):1494-1505. doi:10.1172/JCI26498DS1

133. Curat CA, Miranville A, Sengenès C, Diehl M, Tonus C, Busse R, Bouloumié A. From Blood Monocytes to Adipose Tissue-Resident Macrophages: Induction of Diapedesis by Human Mature Adipocytes. *Diabetes*. 2004;53(5):1285-1292. doi:10.2337/diabetes.53.5.1285

134. Arner E, Mejhert N, Kulyté A, Balwierz PJ, Pachkov M, Cormont M, Lorente-Cebrián S, Ehrlund A, Laurencikiene J, Hedén P, Dahlman-Wright K, Tanti JF, Hayashizaki Y, Rydén M, Dahlman I, Van Nimwegen E, Daub CO, Arner P. Adipose tissue MicroRNAs as regulators of CCL2 production in human obesity.

Diabetes. 2012;61(8):1986-1993. doi:10.2337/db11-1508

135. Deshame SL, Kremlev S, Amini S, Sawaya BE. Monocyte Chemoattractant Protein-1 (MCP-1): An Overview. *J Interf cytokine Res*. 2009;29(6). doi:10.1089/jir.2008.0027

136. Morris DL, Singer K, Lumeng CN. Adipose tissue macrophages: phenotypic plasticity and diversity in lean and obese states. *Curr Opin Clin Nutr Metab Care*. 2011;14(4):341-346. doi:10.1097/MCO.0b013e328347970b.Adipose

137. Mantovani A, Sozzani S, Locati M, Allavena P, Sica A. Macrophage polarization: Tumor-associated macrophages as a paradigm for polarized M2 mononuclear phagocytes. *Trends Immunol*. 2002;23(11):549-555. doi:10.1016/S1471-4906(02)02302-5

138. Bosisio D, Polentarutti N, Sironi M, Bernasconi S, Miyake K, Webb GR, Martin MU, Mantovani A, Muzio M. Stimulation of toll-like receptor 4 expression in human mononuclear phagocytes by interferon-γ: A molecular basis for priming and synergism with bacterial lipopolysaccharide. *Blood*. 2002;99(9):3427-3431. doi:10.1182/blood.V99.9.3427

139. Zheng X, Hong Y, Feng G, Zhang G, Rogers H, Lewis MAO, Williams DW, Xia Z, Song B, Wei X. Lipopolysaccharide-Induced M2 to M1 Macrophage Transformation for IL-12p70 Production Is Blocked by Candida albicans Mediated Up-Regulation of EBI3 Expression. *PLoS One*. 2013;8(5):4-13. doi:10.1371/journal.pone.0063967

140. Shi H, Kokoeva M V, Inouye K, Tzameli I, Yin H, Flier JS. TLR4 links innate immunity and fatty acid – induced insulin resistance. *J Clin Invest*. 2006;116(11):3015-3025. doi:10.1172/JCI28898.TLRs

141. Jennings EG, Lander ES, Young RA, Richmond JFL, Nau GJ, Schlesinger A. Human macrophage activation programs induced by bacterial pathogens. *Proc Natl Acad Sci*. 2002;99(3):1503-1508. doi:10.1073/pnas.022649799

142. Martinez FO, Gordon S. The M1 and M2 paradigm of macrophage activation: time for reassessment. *F1000Prime Rep*. 2014;6(March):1-13. doi:10.12703/P6-13

143. Hu X, Ivashkiv LB. Cross-regulation of Signaling and Immune Responses by IFN-γ and STAT1. *Immunity*. 2009;31(4):539-550. doi:10.1016/j.immuni.2009.09.002.Cross-regulation

144. Spencer M, Yao-Borengasser A, Unal R, Rasouli N, Gurley CM, Zhu B, Peterson CA, Kern PA. Adipose tissue macrophages in insulin-resistant subjects are associated with collagen VI and fibrosis and demonstrate alternative activation. *Am J Physiol Endocrinol Metab*. 2010;299:1016-1027. doi:10.1152/ajpendo.00329.2010

145. Sun S, Ji Y, Kersten S, Qi L. Mechanisms of Inflammatory Responses in Obese Adipose Tissue. *Annu Rev Nutr*. 2012;100(2):130-134. doi:10.1016/j.pestbp.2011.02.012.Investigations

146. Finlin BS, Zhu B, Starnes CP, McGehee RE, Peterson CA, Kern PA. Regulation of thrombospondin-1 expression in alternatively activated macrophages and adipocytes: Role of cellular cross talk and omega-3 fatty acids. *J Nutr Biochem*. 2013;24(9):1571-1579. doi:10.1016/j.jnutbio.2013.01.007

147. McCulloch LJ, Rawling TJ, Sjöholm K, Franck N, Dankel SN, Price EJ, Knight B, Liversedge NH, Mellgren G, Nystrom F, Carlsson LM, Kos K. COL6A3 is regulated by leptin in human adipose tissue and reduced in obesity.

Endocrinology. 2015;156(1):134-146. doi:10.1210/en.2014-1042

148. Divoux A, Tordjman J, Lacasa D, Veyrie N, Hugol D, Aissat A, Basdevant A, Guerre-Millo M, Poitou C, Zucker J-D, Bedossa P, Clément K, Aissat A, Basdevant A, Zucker J-D, Bedossa P, Cle K. Fibrosis in Human Adipose Tissue: Composition , Distribution , and Link With Lipid Metabolism and Fat. *Diabetes*. 2010;59(November):2817-2825. doi:10.2337/db10-0585.A.D.

149. Stein M, Keshav S, Harris N, Gordon S. Interleukin 4 Potently Enhances Murine Macrophage Mannose Receptor Activity: A Marker of Alternative Immunologic Macrophage Activation By Michael Stein, Satish Keshav, Neil Harris,* and Siamon Gordon. *J Exp Med*. 1992;176(July):287-292.

150. Doyle AG, Herbein G, Montaner LJ, Minty AJ, Caput D, Ferrara P, Gordon S. Interleukin-13 alters the activation state of murine macrophages in vitro: Comparison with interleukin-4 and interferon-γ. *Eur J Immunol*. 1994;24(6):1441-1445. doi:10.1002/eji.1830240630

151. Mosser DM, Edwards JP. Exploring the full spectrum of macrophage activation. *Nat Rev Immunol*. 2009;8(12):958-969. doi:10.1038/nri2448.Exploring

152. Park-Min KH, Antoniv TT, Ivashkiv LB. Regulation of macrophage phenotype by long-term exposure to IL-10. *Immunobiology*. 2005;210(2-4):77-86. doi:10.1016/j.imbio.2005.05.002

153. Zurawski G, Vries JE De. Interleukin 13, an interleukin 4-like cytokine that acts on monocytes and B cells, but not on T cells. *Immunol Today*. 1994;15(1):19-26.

154. Das A, Sinha M, Datta S, Abas M, Chaffee S, Sen CK, Roy S. Monocyte and Macrophage Plasticity in Tissue Repair and Regeneration. *Am J Pathol*. 2015;185(10):2596-2606. doi:10.1016/j.ajpath.2015.06.001

155. Lumeng CN, Bodzin JL, Saltiel AR. Obesity induces a phenotypic switch in adipose tissue macrophage polarization. *J Clin Invest*. 2007;117(1):175-184. doi:10.1172/JCI29881.The

156. Odegaard JI, Chawla A. Alternative macrophage activation and metabolism. *Annu Rev Pathol*. 2011;6:275-297. doi:10.1146/annurev-pathol-011110-130138.Alternative

157. Zeyda M, Farmer D, Todoric J, Aszmann O, Speiser M, Gyori G, Zlabinger GJ, Stulnig TM. Human adipose tissue macrophages are of an anti-inflammatory phenotype but capable of excessive pro-inflammatory mediator production. *Int J Obes*. 2007;31:1420-1428. doi:10.1038/sj.ijo.0803632

158. Bourlier V, Miranville A, Barros S De, Maumus M, Sengenes C, Galitzky J, Lafontan M, Karpe F, Frayn KN, Bouloumié A. Remodeling Phenotype of Human Subcutaneous Adipose Tissue Macrophages. *Circulation*. 2008;117:806-816. doi:10.1161/CIRCULATIONAHA.107.724096

159. Fjeldborg K, Pedersen SB, Møller HJ, Christiansen T, Bennetzen M, Richelsen B. Human adipose tissue macrophages are enhanced but changed to an anti-inflammatory profile in obesity. *J Immunol Res*. 2014;2014. doi:10.1155/2014/309548

160. Buechler C, Krautbauer S, Eisinger K. Adipose tissue fibrosis. *World J Diabetes*. 2015;6(4):548-553. doi:10.4239/wjd.v6.i4.548

161. Mariman ECM, Wang P. Adipocyte extracellular matrix composition, dynamics and role in obesity. *Cell Mol Life Sci*. 2010;67(8):1277-1292. doi:10.1007/s00018-010-0263-4

162. Lodish H, Berk A, Zipursky S. Molecular Cell Biology: 4th Edition. In: *Molecular Cell Biology: 4th Edition*. 4th ed. New York: W.H. Freeman; 2000. https://www.ncbi.nlm.nih.gov/books/NBK21582/.

163. Kadler K, Holmes D, Trotter J, Chapman J. Collagen fibril formation. *Biochem J*. 1996;316:1-11.

164. Keophiphath M, Achard V, Henegar C, Rouault C, Clément K, Lacasa D. Macrophage-secreted factors promote a profibrotic phenotype in human preadipocytes. *Mol Endocrinol*. 2009;23(1):11-24. doi:10.1210/me.2008-0183

165. Gagnon A, Yarmo MN, Landry A, Sorisky A. Macrophages alter the differentiation-dependent decreases in fibronectin and collagen I/III protein levels in human preadipocytes. *Lipids*. 2012;47(9):873-880. doi:10.1007/s11745-012-3696-8

166. Wenstrup RJ, Florer JB, Brunskill EW, Bell SM, Chervoneva I, Birk DE. Type V collagen controls the initiation of collagen fibril assembly. *J Biol Chem*. 2004;279(51):53331-53337. doi:10.1074/jbc.M409622200

167. Spencer M, Unal R, Zhu B, Rasouli N, McGehee RE, Peterson C a, Kern P a. Adipose tissue extracellular matrix and vascular abnormalities in obesity and insulin resistance. *J Clin Endocrinol Metab*. 2011;96(12):E1990-8. doi:10.1210/jc.2011-1567

168. Yurchenco PD. Basement membranes: Cell scaffoldings and signaling platforms. *Cold Spring Harb Perspect Biol*. 2011;3(2):1-27. doi:10.1101/cshperspect.a004911

169. Khan T, Muise ES, Iyengar P, Wang Z V, Chandalia M, Abate N, Zhang BB, Bonaldo P, Chua S, Scherer PE. Metabolic dysregulation and adipose tissue fibrosis: role of collagen VI. *Mol Cell Biol*. 2009;29(6):1575-1591. doi:10.1128/MCB.01300-08

170. Pasarica M, Gowronska-Kozak B, Burk D, Remedios I, Hymel D, Gimble J, Ravussin E, Bray GA, Smith SR. Adipose tissue collagen VI in obesity. *J Clin Endocrinol Metab*. 2009;94(12):5155-5162. doi:10.1210/jc.2009-0947

171. DeMarsilis A, Walji T, Maedeker J, Stoka K, Kozel B, Mecham R, Wagenseil J, Craft C. Elastin insufficiency predisposes mice to impaired glucose metabolism. *J Mol Genet Med*. 2014;8(3):777-783. doi:10.1001/jamainternmed.2014.5466.Association

172. Martinez-Santibanez G, Singer K, Cho KW, DelProposto JL, Mergian T, Lumeng CN. Obesity-induced remodeling of the adipose tissue elastin network is independent of the metalloelastase MMP-12. *Adipocyte*. 2015;4(4):264-272. doi:10.1080/21623945.2015.1027848

173. Pankov R, Yamada KM. Fibronectin at a glance. *J Cell Sci*. 2002;115(Pt 20):3861-3863. doi:10.1242/jcs.00059

174. Lee SH, Park HS, Lee JA, Song YS, Jang YJ, Kim JH, Lee YJ, Heo Y. Fibronectin gene expression in human adipose tissue and its associations with obesity-related genes and metabolic parameters. *Obes Surg*. 2013;23(4):554-560. doi:10.1007/s11695-012-0801-2

175. Yan Q, Clark JI, Wight TN, Sage EH. Alterations in the lens capsule contribute to cataractogenesis in SPARC-null mice. *J Cell Sci*. 2002;115(Pt 13):2747-2756. http://www.ncbi.nlm.nih.gov/pubmed/12077365.

176. Michaud A, Tordjman J, Pelletier M, Liu Y, Laforest S, Noël S, Le Naour G, Bouchard C, Clément K, Tchernof A. Relevance of omental pericellular adipose

tissue collagen in the pathophysiology of human abdominal obesity and related cardiometabolic risk. *Int J Obes*. 2016;(October):1823-1831. doi:10.1038/ijo.2016.173

177. Kos K, Wong S, Tan B, Gummesson A, Jernas M, Franck N, Kerrigan D, Nystrom FH, Carlsson LMS, Randeva HS, Pinkney JH, Wilding JPH. Regulation of the Fibrosis and Angiogenesis Promoter SPARC / Osteonectin in Human Adipose Tissue by Weight. *Diabetes*. 2009;58(August):1780-1788. doi:10.2337/db09-0211.

178. Massagué J. TGFβ signalling in context. *Nat Rev Mol Cell Biol*. 2012;13(10):616-630. doi:10.1038/nrm3434

179. Kagan HM, Li W. Lysyl oxidase: Properties, specificity, and biological roles inside and outside of the cell. *J Cell Biochem*. 2003;88(4):660-672. doi:10.1002/jcb.10413

180. Pellegrinelli V, Heuvingh J, Du Roure O, Rouault C, Devulder A, Klein C, Lacasa M, Clément E, Lacasa D, Clément K. Human adipocyte function is impacted by mechanical cues. *J Pathol*. 2014;233(2):183-195. doi:10.1002/path.4347

181. Sun K, Tordjman J, Clement K, Scherer PE. Fibrosis and adipose tissue dysfunction. *Cell Metab*. 2013;18(4):470-477. doi:10.1016/j.cmet.2013.06.016

182. Hosogai N, Fukuhara A, Oshima K, Miyata Y, Tanaka S, Segawa K, Furukawa S, Tochino Y, Komuro R, Matsuda M, Shimomura I. Adipose tissue hypoxia in obesity and its impact on adipocytokine dysregulation. *Diabetes*. 2007;56(4):901-911. doi:10.2337/db06-0911

183. Wang B, Wood IS, Trayhurn P. Dysregulation of the expression and secretion of inflammation-related adipokines by hypoxia in human adipocytes. *Pflugers Arch Eur J Physiol*. 2007;455(3):479-492. doi:10.1007/s00424-007-0301-8

184. Wang P, Keijer J, Bunschoten A, Bouwman F, Renes J, Mariman E. Insulin modulates the secretion of proteins from mature 3T3-L1 adipocytes: A role for transcriptional regulation of processing. *Diabetologia*. 2006;49(10):2453-2462. doi:10.1007/s00125-006-0321-5

185. Kahn SE, Prigeon RL, McCulloch DK, Boyko EJ, Bergman RN, Schwartz MW, Neifing JL, Ward WK, Beard JC, Palmer JP. Quantification of the relationship between insulin sensitivity and beta-cell function in human subjects. *Diabetes*. 1993;42(11):1663-1672. doi:10.2337/diabetes.42.11.1663

186. Kim SH, Reaven GM. Insulin resistance and hyperinsulinemia. *Diabetes Care*. 2008;31(7):1433-1438. doi:10.2337/dc08-0045

187. Ferrannini E, Haffner SM, Mitchell BD, Stern MP. Hyperinsulinaemia: the key feature of a cardiovascular and metabolic syndrome. *Diabetologia*. 1991;34(6):416-422. doi:10.1007/BF00403180

188. Pedersen DJ, Guilherme A, Danai L V, Heyda L, Matevossian A, Cohen J, Nicoloro SM, Straubhaar J, Noh HL, Jung D, Kim JK, Czech MP. A major role of insulin in promoting obesity- associated adipose tissue inflammation. *Mol Metab*. 2015;4(7):507-518. doi:10.1016/j.molmet.2015.04.003

189. Dandona P, Aljada A, Mohanty P, Ghanim H, Hamouda W, Assian E, Ahmad S. Insulin inhibits intranuclear nuclear factor kappaB and stimulates IkappaB in mononuclear cells in obese subjects: evidence for an anti-inflammatory effect? *J Clin Endocrinol Metab*. 2001;86(7):3257-3265. doi:10.1210/jcem.86.7.7623

190. Boutens L, Stienstra R. Adipose tissue macrophages: going off track during obesity. *Diabetologia*. 2016;59:879-894. doi:10.1007/s00125-016-3904-9

191. Weyer C, Bogardus C, Mott DM, Pratley RE. The natural history of insulin secretory dysfunction and insulin resistance in the pathogenesis of type 2 diabetes mellitus. *J Clin Invest*. 1999;104(6).

192. Kahn SE, Hull RL, Utzschneider KM. Mechanisms linking obesity to insulin resistance and type 2 diabetes. *Nature*. 2006;444(7121):840-846. doi:10.1038/nature05482

193. Kahn SE. The Importance of β-Cell Failure in the Development and Progression of Type 2 Diabetes. *J Clin Endocrinol Metab*. 2001;86(9):4047-4058. doi:10.1210/jcem.86.9.7713

194. Robertson AP. Chronic oxidative stress as a central mechanism for glucose toxicity in pancreatic islet beta cells in diabetes. *J Biol Chem*. 2004;279(41):42351-42354. doi:10.1074/jbc.R400019200

195. Kahn SE. The relative contributions of insulin resistance and beta-cell dysfunction to the pathophysiology of Type 2 diabetes. *Diabetologia*. 2003;46:3-19. doi:10.1007/s00125-002-1009-0

196. Swinnen SG, Hoekstra JB, DeVries JH. Insulin therapy for type 2 diabetes. *Diabetes Care*. 2009;32 Suppl 2. doi:10.2337/dc09-S318

197. Garvey WT, Olefsky JM, Griffin J, Hamman RF, Kolterman OG. The effect of insulin treatment on insulin secretion and insulin action in type II diabetes mellitus. *Diabetes*. 1985;34(3):222-234. doi:10.2337/DIAB.34.3.222

198. Shoelson SE, Lee J, Goldfine AB. Inflammation and insulin resistance. *J Clin Invest*. 2006;116(7):1793-1801. doi:10.1172/JCI29069.and

199. Fantuzzi G. Adipose tissue, adipokines, and inflammation. *J Allergy Clin Immunol*. 2005;115(5):911-920. doi:10.1016/j.jaci.2005.02.023

200. Hotamisligil GS, Peraldi P, Budavari A, Ellis R, White MF, Spiegelman BM. IRS-1-mediated inhibition of insulin receptor tyrosine kinase activity in TNF-alpha- and obesity-induced insulin resistance. *Science*. 1996;271(5249):665-668. http://www.ncbi.nlm.nih.gov/pubmed/8571133.

201. Lumeng CN, DeYoung SM, Saltiel AR. Macrophages block insulin action in adipocytes by altering expression of signaling and glucose transport proteins. *Am J Physiol Endocrinol Metab*. 2007;292(1):E166-E174. doi:10.1152/ajpendo.00284.2006

202. Chanput W, Peters V, Wichers H. THP-1 and U937 Cells. In: *The Impact of Food Bioactives on Health*. ; 2015:147-159. doi:10.1007/978-3-319-16104-4

203. Traore K, Trush MA, George M, Wm E, Anderson W, Asseffa A. Signal transduction of phorbol 12-myristate 13-acetate (PMA) -induced growth inhibition of human monocytic leukemia THP-1 cells is reactive oxygen dependent. *Leuk Res*. 2005;29:863-879. doi:10.1016/j.leukres.2004.12.011

204. Life Technologies. *Real-Time PCR Handbook*.; 2012. http://find.lifetechnologies.com/Global/FileLib/qPCR/RealTimePCR_Handbook_Update_FLR.pdf.

205. Heid C, Livak K, Stevens J, Williams P. Real time quantitative PCR. *Genome Res*. 1996;6:986-994. doi:10.1101/gr.6.10.986

206. AppliedBiosystems. *TaqMan Universal PCR Master Mix, User Guide*.; 2010.

207. Eisenberg E, Levanon EY. Human housekeeping genes, revisited. *Trends Genet*. 2013;29(10):569-574. doi:10.1016/j.tig.2013.05.010

208. Ciechanover a, Schwartz a L. The ubiquitin-proteasome pathway: the complexity and myriad functions of proteins death. *Proc Natl Acad Sci U S A*. 1998;95(6):2727-2730. doi:10.1073/pnas.95.6.2727

209. Kuchipudi S V, Tellabati M, Nelli RK, White GA, Perez B, Sebastian S, Slomka MJ, Brookes SM, Brown IH, Dunham SP, Chang K-C. 18S rRNA is a reliable normalisation gene for real time PCR based on influenza virus infected cells. *Virol J*. 2012;9(1):230. doi:10.1186/1743-422X-9-230

210. Krummrei U, Bang R, Schmidtchen R, Brune K, Bang H. Cyclophilin-A is a zinc-dependent DNA binding protein in macrophages. *FEBS Lett*. 1995;371(1):47-51. doi:10.1016/0014-5793(95)00815-Q

211. NCBI. PPIA peptidylprolyl isomerase A [Homo sapiens (human)] - Gene. https://www.ncbi.nlm.nih.gov/gene/5478. Published 2016. Accessed November 22, 2016.

212. Vannini A, Cramer P. Conservation between the RNA Polymerase I, II, and III Transcription Initiation Machineries. *Mol Cell*. 2012;45(4):439-446. doi:10.1016/j.molcel.2012.01.023

213. Gabrielsson BG, Olofsson LE, Sjögren A, Jernås M, Elander A, Lönn M, Rudemo M, Carlsson LMS. Evaluation of reference genes for studies of gene expression in human adipose tissue. *Obes Res*. 2005;13(4):649-652. doi:10.1038/oby.2005.72

214. Taube M, Andersson-Assarsson JC, Lindberg K, Pereira MJ, Gäbel M, Svensson MK, Eriksson JW, Svensson P-A. Evaluation of reference genes for gene expression studies in human brown adipose tissue. *Adipocyte*. 2015;4(4):280-285. doi:10.1080/21623945.2015.1039884

215. Neville MJ, Collins JM, Gloyn AL, McCarthy MI, Karpe F. Comprehensive human adipose tissue mRNA and microRNA endogenous control selection for quantitative real-time-PCR normalization. *Obesity*. 2011;19(4):888-892. doi:10.1038/oby.2010.257

216. Bookout AL, Cummins CL, Kramer MF, Pesola JM, Mangelsdorf DJ. High-Throughput Real-Time Quantitative Reverse Transcription PCR. In: *Current Protocols in Molecular Biology*. Vol Supplement. ; 2006:15.8.1-15.8.28. doi:10.1002/0471142727.mb1508s73

217. Livak KJ, Schmittgen TD. Analysis of Relative Gene Expression Data Using Real-Time Quantitative PCR and the 2−ΔΔCT Method. *Methods*. 2001;25(4):402-408. doi:10.1006/meth.2001.1262

218. Porcheray F, Viaud S, Rimaniol A, Léone C, Samah B. Macrophage activation switching: an asset for the resolution of inflammation. *Clin Exp Immunol*. 2005;142:481-489. doi:10.1111/j.1365-2249.2005.02934.x

219. Gazi U, Martinez-pomares L. Influence of the mannose receptor in host immune responses. *Immunobiology*. 2009;214(7):554-561. doi:10.1016/j.imbio.2008.11.004

220. Lurier EB, Dalton D, Dampier W, Raman P, Nassiri S, Ferraro NM, Rajagopalan R, Sarmady M, Spiller KL. Transcriptome analysis of IL-10-stimulated (M2c) macrophages by next-generation sequencing. *Immunobiology*. 2017;222(7):847-856. doi:10.1016/j.imbio.2017.02.006

221. Yusuf I, Kageyama R, Monticelli L, Johnston RJ, Hansen K, Barnett B, Crotty S. Germinal center T follicular helper cell IL-4 production is dependent on signaling lymphocytic activation molecule receptor (CD150). *J Immunol*. 2011;185(1):190-

202. doi:10.4049/jimmunol.0903505.Germinal

222. Kzhyshkowska J, Gudima A, Moganti K, Gratchev A, Orekhov A. Perspectives for Monocyte/Macrophage-Based Diagnostics of Chronic Inflammation. *Transfus Med Hemotherapy*. 2016;43(2):66-77. doi:10.1159/000444943

223. KUME N, MORIWAKI H, KATAOKA H, MINAMI M, MURASE T, SAWAMURA T, MASAKI T, KITA T. Inducible Expression of LOX-1, a Novel Receptor for Oxidized LDL, in Macrophages and Vascular Smooth Muscle Cells. *Ann N Y Acad Sci*. 2006;902(1):323-327. doi:10.1111/j.1749-6632.2000.tb06332.x

224. Leanne Peiser, Subhankar Mukhopadhyay SG. Scavenger receptors in innate immunity Leanne Peiser , Subhankar Mukhopadhyay and Siamon Gordon. *Curr Opin Immunol*. 2002;14:123-128. http://www.pubfacts.com/fulltext_frame.php?PMID=11790542&title=Scavenger receptors in innate immunity.

225. Chanput W, Mes JJ, Savelkoul HFJ, Wichers H. Characterization of polarized THP-1 macrophages and polarizing ability of LPS and food compounds. *Food Funct*. 2013;4:266-276.

226. Zhao XQ, Zhang MW, Wang F, Zhao YX, Li JJ, Wang XP, Bu PL, Yang JM, Liu XL, Zhang MX, Gao F, Zhang C, Zhang Y. CRP enhances soluble LOX-1 release from macrophages by activating TNF-α converting enzyme. *J Lipid Res*. 2011;52(5):923-933. doi:10.1194/jlr.m015156

227. Ritter M, Buechler C, Langmann T, Orso E, Kluchen J, Schmitz G. The Scavenger Receptor CD163 : Regulation , Promoter Structure and Genomic Organization. *Pathobiology*. 1999;67:257-261.

228. Genin M, Clement F, Fattaccioli A, Raes M, Michiels C. M1 and M2 macrophages derived from THP-1 cells differentially modulate the response of cancer cells to etoposide. *BMC Cancer*. 2015;15(577):1-14. doi:10.1186/s12885-015-1546-9

229. Mia S, Warnecke A, Zhang X, Malmstr V, Harris RA. An optimized Protocol for Human M2 Macrophages using M-CSF and IL-4 / IL-10 / TGF- b Yields a Dominant Immunosuppressive Phenotype. *Scand J Immunol*. 2014;79:305-314. doi:10.1111/sji.12162

230. Fettelschoss A, Kistowska M, LeibundGut-Landmann S, Beer H-D, Johansen P, Senti G, Contassot E, Bachmann MF, French LE, Oxenius A, Kundig TM. Inflammasome activation and IL-1 target IL-1 for secretion as opposed to surface expression. *Proc Natl Acad Sci*. 2011;108(44):18055-18060. doi:10.1073/pnas.1109176108

231. Lolmede K, Campana L, Vezzoli M, Bosurgi L, Tonlorenzi R, Clementi E, Bianchi ME, Cossu G, Manfredi AA, Brunelli S, Rovere-Querini P. Inflammatory and alternatively activated human macrophages attract vessel-associated stem cells, relying on separate HMGB1- and MMP-9-dependent pathways. *J Leukoc Biol*. 2009;85(5):779-787. doi:10.1189/jlb.0908579

232. Redzic JS, Kendrick AA, Bahmed K, Dahl KD, Pearson CG, Robinson WA, Robinson SE, Graner MW, Eisenmesser EZ. Extracellular Vesicles Secreted from Cancer Cell Lines Stimulate Secretion of MMP-9, IL-6, TGF-β1 and EMMPRIN. *PLoS One*. 2013;8(8). doi:10.1371/journal.pone.0071225

233. Rőszer T. Understanding the Mysterious M2 Macrophage through Activation Markers and Effector Mechanisms. *Mediators Inflamm*. 2015;2015:1-16. doi:10.1155/2015/816460

234. Aron-Wisnewsky J, Tordjman J, Poitou C, Darakhshan F, Hugol D, Basdevant A, Aissat A, Guerre-Millo M, Clément K. Human adipose tissue macrophages: M1 and M2 cell surface markers in subcutaneous and omental depots and after weight loss. *J Clin Endocrinol Metab*. 2009;94(11):4619-4623. doi:10.1210/jc.2009-0925

235. Assoian RK, Fleurdelys BE, Stevenson HC, Miller PJ, Madtes DK, Raines EW, Ross R, Sporn MB. Expression and secretion of type beta transforming growth factor by activated human macrophages. *Proc Natl Acad Sci U S A*. 1987;84(17):6020-6024. doi:10.1073/pnas.84.17.6020

236. Aihara K-I, Ikeda Y, Yagi S, Akaike M, Matsumoto T. Transforming Growth Factor-β1 as a Common Target Molecule for Development of Cardiovascular Diseases, Renal Insufficiency and Metabolic Syndrome. *Cardiol Res Pract*. 2010;2011(Ang II):175381. doi:10.4061/2011/175381

237. Tan CK, Chong HC, Tan EHP, Tan NS. Getting 'Smad' about obesity and diabetes. *Nutr Diabetes*. 2012;2(3):e29. doi:10.1038/nutd.2012.1

238. Ignotz R a, Massagué J. Transforming growth factor-beta stimulates the expression of fibronectin and collagen and their incorporation into the extracellular matrix. *J Biol Chem*. 1986;261(9):4337-4345. http://www.ncbi.nlm.nih.gov/pubmed/3456347.

239. Galluzi L, Aaronson S, Abrams J, Alnemri E, Andrews D, Baaehrecke E, Bazan N, Blagosklonny M. Guidlines for the use and interpretation of assays for monitoring cell death in higher eukaryotes. *Cell death Differ*. 2009;16(8):394-398. doi:10.1038/cdd.2009.44.Guidelines

240. Juge-Aubry CE, Somm E, Pernin A, Alizadeh N, Giusti V, Dayer JM, Meier CA. Adipose tissue is a regulated source of interleukin-10. *Cytokine*. 2005;29(6):270-274. doi:10.1016/j.cyto.2004.10.017

241. Bourlier V, Sengenès C, Zakaroff-Girard A, Decaunes P, Wdziekonski B, Galitzky J, Villageois P, Esteve D, Chiotasso P, Dani C, Bouloumié A. TGFbeta family members are key mediators in the induction of myofibroblast phenotype of human adipose tissue progenitor cells by macrophages. *PLoS One*. 2012;7(2). doi:10.1371/journal.pone.0031274

242. Pastel E, Price E, Sjöholm K, McCulloch LJ, Rittig N, Liversedge N, Knight B, Møller N, Svensson PA, Kos K. Lysyl oxidase and adipose tissue dysfunction. *Metabolism*. 2018;78:118-127. doi:10.1016/j.metabol.2017.10.002

243. Borza DB, Bondar O, Ninomiya Y, Sado Y, Naito I, Todd P, Hudson BG. The NC1 domain of collagen IV encodes a novel network composed of the alpha 1, alpha 2, alpha 5, and alpha 6 chains in smooth muscle basement membranes. *J Biol Chem*. 2001;276(30):28532-28540. doi:10.1074/jbc.M103690200

244. Oono T, Specks U, Eckes B, Majewski S, Hunzelmann N, Timpl R, Krieg T. Expression of type VI collagen mRNA during wound healing. *J Invest Dermatol*. 1993;100(3):329-334. doi:10.1111/1523-1747.ep12470022

245. Bradshaw AD, Puolakkainen P, Dasgupta J, Davidson JM, Wight TN, Sage EH. SPARC-null mice display abnormalities in the dermis characterized by decreased collagen fibril diameter and reduced tensile strength. *J Invest Dermatol*. 2003;120(6):949-955. doi:10.1046/j.1523-1747.2003.12241.x

246. Nie J, Helene Sage E. SPARC inhibits adipogenesis By its enhancement of β-catenin signaling. *J Biol Chem*. 2009;284(2):1279-1290. doi:10.1074/jbc.M808285200

247. Smith-Mungo LI, Kagan HM. Lysyl oxidase: Properties, regulation and multiple functions in biology. *Matrix Biol*. 1998;16(7):387-398. doi:10.1016/S0945-053X(98)90012-9

248. Csiszar K, Jourdan-Le Saux C, Fong SFT, Fong KSK, Boyd CD. Lysyl oxidase: a family of multifunctional proteins K. Csiszar , C. Jourdan-Le Saux, S. F. T. Fong , K.S.K.Fong, C. D. Boyd. In: *Biochemistry and Molecular Biology of Vitamin B6 and PQQ-Dependent Proteins*. ; 2000:91-92.

249. Tartare-Deckert S, Chavey C, Monthouel MN, Gautier N, Van Obberghen E. The Matricellular Protein SPARC/Osteonectin as a Newly Identified Factor Up-regulated in Obesity. *J Biol Chem*. 2001;276(25):22231-22237. doi:10.1074/jbc.M010634200

250. Chavey C, Boucher J, Monthouel-Kartmann MN, Sage EH, Castan-Laurell I, Valet P, Tartare-Deckert S, Van Obberghen E. Regulation of secreted protein acidic and rich in cysteine during adipose conversion and adipose tissue hyperplasia. *Obes (Silver Spring)*. 2006;14(11):1890-1897. doi:14/11/1890 [pii]\n10.1038/oby.2006.220

251. Trombetta-eSilva J, Bradshaw AD. The Function of SPARC as a Mediator of Fibrosis. *Open Rheumatol J*. 2012;6(1):146-155. doi:10.2174/1874312901206010146

252. Wrana JL, Overall CM, Sodek J. Regulation of the expression of a secreted acidic protein rich in cysteine (SPARC) in human fibroblasts by transforming growth factor beta: Comparison of transcriptional and post-transcriptional control with fibronectin and type I collagen. *Eur J Biochem*. 1991;197(2):519-528. doi:10.1111/j.1432-1033.1991.tb15940.x

253. Shibata S, Ishiyama J. Secreted protein acidic and rich in cysteine (SPARC) is upregulated by transforming growth factor (TGF)-β and is required for TGF-β-induced hydrogen peroxide production in fibroblasts. *Fibrogenes Tissue Repair*. 2013;6(1):1-11. doi:10.1186/1755-1536-6-6

254. Alkhouli N, Mansfield J, Green E, Bell J, Knight B, Liversedge N, Tham JC, Welbourn R, Shore AC, Kos K, Winlove CP. The mechanical properties of human adipose tissues and their relationships to the structure and composition of the extracellular matrix. *Am J Physiol Endocrinol Metab*. 2013;305(12):E1427-35. doi:10.1152/ajpendo.00111.2013

255. Klionsky DJ. Blame it on Southern, but it's a western blot. *Autophagy*. 2017;13(1):1-2. doi:10.1080/15548627.2016.1255382

256. Shvartsman SY, Hagan MP, Yacoub A, Dent P, Wiley HS, Lauffenburger DA. Autocrine loops with positive feedback enable context-dependent cell signaling. *Am J Physiol Physiol*. 2001;282(3):C545-C559. doi:10.1152/ajpcell.00260.2001

257. Tada Iida K, Shimano H, Kawakami Y, Sone H, Toyoshima H, Suzuki S, Asano T, Okuda Y, Yamada N. Insulin Up-regulates Tumor Necrosis Factor-a Production in Macrophages through an Extracellular-regulated Kinase-dependent Pathway. *J Biol Chem*. 2001;276(35):32531-32537. doi:10.1074/jbc.M009894200

258. Chevenne D, Trivin F, Porquet D. Insulin assays and reference values. *Diabetes Metab*. 1999;25(6):459-476.

259. Yang G, Li C, Gong Y, Fang F, Tian H, Li J, Cheng X. Assessment of insulin resistance in subjects with normal glucose tolerance, hyperinsulinemia with normal blood glucose tolerance, impaired glucose tolerance, and newly diagnosed type 2 diabetes (prediabetes insulin resistance research). *J Diabetes*

Res. 2016;2016. doi:10.1155/2016/9270768

260. Sato T, Nagafuku M, Shimizu K, Taira T, Igarashi Y, Inokuchi J ichi. Physiological levels of insulin and IGF-1 synergistically enhance the differentiation of mesenteric adipocytes. *Cell Biol Int*. 2008;32(11):1397-1404. doi:10.1016/j.cellbi.2008.08.010

261. Tchobroutsky G, Kopf A, Eschwege E, Assan R. Serial Postprandial Plasma Insulin Levels in 117 Subjects With and Without Diabetes. *Diabetes*. 1973;22(11).

262. Marshall S, Olefsky JM. Characterization of insulin-induced receptor loss and evidence for internalization of the insulin receptor. *Diabetes*. 1981;30(9):746-753. doi:10.2337/diab.30.9.746

263. Koshy S, Alizadeh P, Timchenko LT, Beeton C. Quantitative Measurement of GLUT4 Translocation to the Plasma Membrane by Flow Cytometry. *J Vis Exp*. 2010;(45):8-10. doi:10.3791/2429

264. Matsui-Hirai H, Hayashi T, Yamamoto S, Ina K, Maeda M, Kotani H, Iguchi A, Ignarro LJ, Hattori Y. Dose-Dependent Modulatory Effects of Insulin on Glucose-Induced Endothelial Senescence In Vitro and In Vivo: A Relationship between Telomeres and Nitric Oxide. *J Pharmacol Exp Ther*. 2011;337(3):591-599. doi:10.1124/jpet.110.177584

265. Abu-Lebdeh HS, Barazzoni R, Meek SE, Bigelow ML, Persson X-MT, Nair KS. Effects of insulin deprivation and treatment on homocysteine metabolism in people with type 1 diabetes. *J Clin Endocrinol Metab*. 2006;91(9):3344-3348. doi:10.1210/jc.2006-0018

266. Klöting N, Koch L, Wunderlich T, Kern M, Ruschke K, Krone W, Brüning JC, Blüher M. Autocrine IGF-1 action in adipocytes controls systemic IGF-1 concentrations and growth. *Diabetes*. 2008;57(8):2074-2082. doi:10.2337/db07-1538

267. Doyle SL, Donohoe CL, Lysaght J, Reynolds J V. Visceral obesity, metabolic syndrome, insulin resistance and cancer. *Proc Nutr Soc*. 2012;71(01):181-189. doi:10.1017/S002966511100320X

268. Bar RS, Gorden P, Roth J, Kahn CR, De Meyts P. Fluctuations in the affinity and concentration of insulin receptors on circulating monocytes of obese patients: effects of starvation, refeeding, and dieting. *J Clin Invest*. 1976;58(5):1123-1135. doi:10.1172/JCI108565

269. Fu Y, Maianu L, Melbert BR, Garvey WT. Facilitative glucose transporter gene expression in human lymphocytes, monocytes, and macrophages: a role for GLUT isoforms 1, 3, and 5 in the immune response and foam cell formation. *Blood Cells, Mol Dis*. 2004;32(1):182-190. doi:10.1016/j.bcmd.2003.09.002

270. Liang CP, Han S, Senokuchi T, Tall AR. The macrophage at the crossroads of insulin resistance and atherosclerosis. *Circ Res*. 2007;100(11):1546-1555. doi:10.1161/CIRCRESAHA.107.152165

271. Eger M, Hussen J, Koy M, Dänicke S, Schuberth H-J, Breves G. Glucose transporter expression differs between bovine monocyte and macrophage subsets and is influenced by milk production. *J Dairy Sci*. 2016;99(3):2276-2287. doi:10.3168/jds.2015-10435

272. Ieronymaki E, Theodorakis EM, Lyroni K, Vergadi E, Lagoudaki E, Al-Qahtani A, Aznaourova M, Neofotistou-Themeli E, Eliopoulos AG, Vaporidi K, Tsatsanis C. Insulin Resistance in Macrophages Alters Their Metabolism and Promotes an

M2-Like Phenotype. *J Immunol*. 2019;202(6):1786-1797. doi:10.4049/jimmunol.1800065

273. Lo KA, Labadorf A, Kennedy NJ, Han MS, Sing Y, Matthews B, Xin X, Sun L, Davis RJ, Lodish HF, Fraenkel E. Analysis of in vitro insulin resistance models and their physiological relevance to in vivo diet-induced adipose insulin resistance. 2014;5(1):1-20. doi:10.1016/j.celrep.2013.08.039.Analysis

274. Zabolotny JM, Kim YB, Welsh LA, Kershaw EE, Neel BG, Kahn BB. Protein-tyrosine phosphatase 1B expression is induced by inflammation in vivo. *J Biol Chem*. 2008;283(21):14230-14241. doi:10.1074/jbc.M800061200

275. Heinonen KM, Dube N, Bourdeau A, Lapp WS, Tremblay ML. Protein tyrosine phosphatase 1B negatively regulates macrophage development through CSF-1 signaling. *Proc Natl Acad Sci*. 2006;103(8):2776-2781. doi:10.1073/pnas.0508563103

276. Ghanim H, Aljada A, Hofmeyer D, Syed T, Mohanty P, Dandona P. Circulating mononuclear cells in the obese are in a proinflammatory state. *Circulation*. 2004;110(12):1564-1571. doi:10.1161/01.CIR.0000142055.53122.FA

277. Iwasaki Y, Nishiyama M, Taguchi T, Asai M, Yoshida M, Kambayashi M, Terada Y, Hashimoto K. Insulin exhibits short-term anti-inflammatory but long-term proinflammatory effects in vitro. *Mol Cell Endocrinol*. 2009;298(1-2):25-32. doi:10.1016/j.mce.2008.09.030

278. Grunberger G, Iacopetta B, Carpentier JL, Gorden P. Diacylglycerol modulation of insulin receptor from cultured human mononuclear cells. Effects on binding and internalization. *Diabetes*. 1986;35(12):1364-1370. doi:10.2337/diab.35.12.1364

279. Kitamura T, Kahn CR, Accili D. Insulin receptor knockout mice. *Annu Rev Physiol*. 2003;65:313-332. doi:10.1146/annurev.physiol.65.092101.142540

280. Kutz SM, Hordines J, McKeown-Longo PJ, Higgins PJ. TGF-beta1-induced PAI-1 gene expression requires MEK activity and cell-to-substrate adhesion. *J Cell Sci*. 2001;114:3905-3914.

281. Pscherer S, Freude T, Forst T, Nussler AK, Braun KF, Ehnert S. Anti-diabetic treatment regulates pro-fibrotic TGF-beta serum levels in type 2 diabetics. *Diabetol Metab Syndr*. 2013;5(1):48. doi:10.1186/1758-5996-5-48

282. Luo T, Nocon A, Fry J, Sherban A, Rui X, Jiang B, Xu XJ, Han J, Yan Y, Yang Q, Li Q, Zang M. AMPK activation by metformin suppresses abnormal extracellular matrix remodeling in adipose tissue and ameliorates insulin resistance in obesity. *Diabetes*. 2016;65(8):2295-2310. doi:10.2337/db15-1122

283. Valencak TG, Osterrieder A, Schulz TJ. Sex matters: The effects of biological sex on adipose tissue biology and energy metabolism. *Redox Biol*. 2017;12(March):806-813. doi:10.1016/j.redox.2017.04.012

284. Ferrara CM, Lynch NA, Nicklas BJ, Ryan AS, Berman DM. Differences in adipose tissue metabolism between postmenopausal and perimenopausal women. *J Clin Endocrinol Metab*. 2002;87(9):4166-4170. doi:10.1210/jc.2001-012034

285. Tchernof A, Desmeules A, Richard C, Laberge P, Daris M, Mailloux J, Rhéaume C, Dupont P. Ovarian hormone status and abdominal visceral adipose tissue metabolism. *J Clin Endocrinol Metab*. 2004;89(7):3425-3430. doi:10.1210/jc.2003-031561

286. Jóźwiak P, Forma E, Bryś M, Krześlak A. O-GlcNAcylation and metabolic

reprograming in cancer. *Front Endocrinol (Lausanne)*. 2014;5(SEP). doi:10.3389/fendo.2014.00145

287. Shirai T, Nazarewicz RR, Wallis BB, Yanes RE, Watanabe R, Hilhorst M, Tian L, Harrison DG, Giacomini JC, Assimes TL, Goronzy JJ, Weyand CM. The glycolytic enzyme PKM2 bridges metabolic and inflammatory dysfunction in coronary artery disease. *J Exp Med*. 2016;213(3):337-354. doi:10.1084/jem.20150900

288. Groh L, Keating ST, Joosten LAB, Netea MG, Riksen NP. Monocyte and macrophage immunometabolism in atherosclerosis. *Semin Immunopathol*. 2018;40(2):203-214. doi:10.1007/s00281-017-0656-7

289. D.M. R, E. G, P. D, R.J. S, P.M. S, C.J. L. Comparative genotypic and phenotypic analysis of human peripheral blood monocytes and surrogate monocyte-like cell lines commonly used in metabolic disease research. *PLoS One*. 2018;13(5):1-19. doi:10.1371/journal.pone.0197177

290. Schildberger A, Rossmanith E, Eichhorn T, Strassl K, Weber V. Monocytes, Peripheral Blood Mononuclear Cells, and THP-1 Cells Exhibit Different Cytokine Expression Patterns following Stimulation with Lipopolysaccharide. *Mediators Inflamm*. 2013;2013.

291. Lovren F, Pan Y, Quan A, Szmitko PE, Singh KK, Shukla PC, Gupta M, Chan L, Al-Omran M, Teoh H, Verma S. Adiponectin primes human monocytes into alternative anti-inflammatory M2 macrophages. *Am J Physiol Heart Circ Physiol*. 2010;299(July):H656-H663. doi:10.1152/ajpheart.00115.2010

292. Ohashi K, Parker JL, Ouchi N, Higuchi A, Vita JA, Gokce N, Pedersen AA, Kalthoff C, Tullin S, Sams A, Summer R, Walsh K. Adiponectin promotes macrophage polarization toward an anti-inflammatory phenotype. *J Biol Chem*. 2010;285(9):6153-6160. doi:10.1074/jbc.M109.088708

293. Vogel C, Marcotte EM. Insights into the regulation of protein abundance from proteomic and transcriptomic analyses. *Nat Rev Genet*. 2012;13(4):227-232. doi:10.1038/nrg3185

294. Dubois, C M; Laprise, M-H; Blanchette, F; Gentry, L E; Leduc R. Processing of Transforming Growth Factor Beta1 Precursor by Human Furin Convertase. *J Biol Chem*. 1995.

295. Lech M, Anders H. Macrophages and fibrosis: How resident and in filtrating mononuclear phagocytes orchestrate all phases of tissue injury and repair. *BBA - Mol Basis Dis*. 2013;1832(7):989-997. doi:10.1016/j.bbadis.2012.12.001

296. Luzina IG, Keegan AD, Heller NM, Rook GAW, Shea-donohue T. Regulation of inflammation by interleukin-4: a review of “alternatives.” *J Leukoc Biol*. 2012;92(4):753-764. doi:10.1189/jlb.0412214

297. Bertani FR, Mozetic P, Fioramonti M, Iuliani M, Ribelli G, Pantano F, Santini D, Tonini G, Trombetta M, Businaro L, Selci S, Rainer A. Classification of M1/M2-polarized human macrophages by label-free hyperspectral reflectance confocal microscopy and multivariate analysis. *Sci Rep*. 2017;7(1):1-9. doi:10.1038/s41598-017-08121-8

298. Barros MHM, Hauck F, Dreyer JH, Kempkes B. Macrophage Polarisation : an Immunohistochemical Approach for Identifying M1 and M2 Macrophages. *PLoS One*. 2013;8(11):1-11. doi:10.1371/journal.pone.0080908

299. Lech M, Gr R, Weidenbusch M, Anders H. Tissues Use Resident Dendritic Cells and Macrophages to Maintain Homeostasis and to Regain Homeostasis upon

Tissue Injury: The Immunoregulatory Role of Changing Tissue Environments. *Mediators Inflamm*. 2012;2012. doi:10.1155/2012/951390

300. Murray PJ, Allen JE, Fisher EA, Lawrence T. Macrophage activation and polarization: nomenclature and experimental guidelines. *Immunity*. 2014;41(1):14-20. doi:10.1016/j.immuni.2014.06.008.Macrophage

301. Muir LA, Neeley CK, Meyer KA, Baker NA, Brosius AM, Washabaugh AR, Varban OA, Finks JF, Zamarron BF, Flesher CG, Chang JS, DelProposto JB, Geletka L, Martinez-Santibanez G, Kaciroti N, Lumeng CN, O'Rourke RW. Adipose tissue fibrosis, hypertrophy, and hyperplasia: Correlations with diabetes in human obesity. *Obesity*. 2016;24(3):597-605. doi:10.1002/oby.21377

302. Sweetwyne MT, Pallero M a, Lu A, Van Duyn Graham L, Murphy-Ullrich JE. The calreticulin-binding sequence of thrombospondin 1 regulates collagen expression and organization during tissue remodeling. *Am J Pathol*. 2010;177(4):1710-1724. doi:10.2353/ajpath.2010.090903

303. Varma V, Yao-Borengasser, Bodles AM, Rasouli N, Phanavanh B, Nolen G, Kern EM, Nagarajan R, Spencer HJ, Lee M, Fried SK, McGehee Jr RE, Peterson CA, Kern PA. Thrombospondin-1 is an adipokine associated with obesity, adipose inflammation and insulin resistance. *Diabetes*. 2008;57(2):432-439. doi:10.1038/nmeth.2177.Coupling

304. Schultz-Cherry S, Murphy-Ullrich JE. Thrombospondin causes activation of latent transforming growth factor-beta secreted by endothelial cells by a novel mechanism. *J Cell Biol*. 1993;122(4):923-932. doi:10.1083/jcb.122.4.923

305. Ghanim H, Mohanty P, Deopurkar R, Sia CL, Korzeniewski K, Abuaysheh S, Chaudhuri A, Dandona P. Acute modulation of toll-like receptors by insulin. *Diabetes Care*. 2008;31(9):1827-1831. doi:10.2337/dc08-0561

306. Brundage SI, Kirilcuk NN, Lam JC, Spain DA, Zautke NA. Insulin Increases the Release of Proinflammatory Mediators. *J Trauma Inj Infect Crit Care*. 2008;65(2):367-372. doi:10.1097/TA.0b013e3181801cc0

307. Godsland IF. Insulin resistance and hyperinsulinaemia in the development and progression of cancer. *Clin Sci*. 2009;118(5):315-332. doi:10.1042/cs20090399